國 立 交 通 大 學

電信工程學系

博 士 論 文

感知無線電媒體存取控制層之通訊協定設計及性能分析

Design and Analysis for Medium Access Control Protocols in Cognitive Radio Networks

研究生： 陳 銘 賓

指導教授： 王 蒞 君

中 華 民 國 九十六 年 十 月

感知無線電媒體存取控制層之通訊協定設計及性能分析

Design and Analysis for Medium Access Control Protocol in Cognitive Radio Networks

研究生：陳銘賓　　Student: Ming Bing Chen

指導教授：王蒞君　博士　　Advisor: Dr. Li-Chun Wang

國立交通大學

電信工程學系

博士論文

A Dissertation
Submitted to Institute of Communication Engineering
College of Electrical and Computer Engineering
National Chiao Tung University
in Partial Fulfillment of the Requirements
for the Degree of Doctor of Philosophy
in
Communication Engineering
Hsinchu, Taiwan

2007 年 10 月

感知無線電媒體存取控制層之
通訊協定設計及性能分析

研究生：陳銘賓　　指導教授：王蒞君　博士

國立交通大學

電信工程學系

摘要

近年來由於無線通訊技術的進步，使得能夠分配的頻譜逐漸稀少，主要的原因來自於各個無線通訊系統為了防止彼此之間相互干擾的問題，每個系統都各自操作在特定的頻帶，且對該頻帶均有專屬的使用權，讓其他系統無法重複使用頻帶。最近的研究結果顯示，此種固定式頻率的分配方式，使得頻帶的使用效率低於 35%以下，而在時間及空間上使用效率也出現極大的非對稱性，其在效率上的變化可以從 15%變化到 85%。為解決極低的頻譜使用效率以及改善使用效率上的對稱性，一種新的無線網路設備期待具有一定程度的智能，可以主動去感測週遭的環境，判斷可以使用的頻帶及地區，在空轉的頻帶中或在不影響該頻帶中主要使用者的前提下，動態地與他人建立連線，當該頻帶主要使用者需要傳輸時，又能及時的停止其傳輸並轉移到其他頻帶而不干擾該頻帶主要使用者，符合此種傳輸要求的設備我們命名為感知無線電。然而為了能夠動態地建立不干擾他人的連線，感知無線電有三項重要的課題需面對：(1) 頻譜偵測及識別；(2) 具有感知能力的通訊協定設計；以及(3) 頻譜換手機制。在本篇論文中，我們將逐一檢視此三種重要課題及其相對應的設計，同時，我們也發展一套跨層的分析模型，得以分析感知無線電網路中的系統效能及傳輸延遲。

在第一個課題中，由於現今的頻譜偵測及識別技術均需要較為複雜的訊號處理及統計分析，使得硬體複雜度提高且造成多餘的能量消耗，對此若能藉由節點的位置資訊事先判斷出其所在的位置是否容易造成主要使用者的干擾，如此一來，只有當節點進入到會造成干擾的區域時，才區要執行頻譜偵測及識別的動作，若否則可直接與接收端建立連線，在此我們驗證此種想法的可行性，在我們

的結果中顯示出，在一個主要使用者基地台的覆蓋範圍中，有高達 45%的區域可以滿足此種要求，讓感知無線電在不需偵測頻譜的前提下即可與其接收端建立連線，而同時又不影響原先主要使用者連線的品質，其頻譜的使用效率在此種網路架構下，更較原先系統提高到 145%。

針對第二個感知通訊協定設計的課題中，由於感知無線電使用者被允許使用的時間只有在通道處在空轉的情況下，才能與接收端建立連線，可預期的是空轉的時間相當有限，在此，最大的問題在於要如何讓感知無線電在不干擾主要使用者的前提下，又能快速的和接收端建立連線，同時又能滿足連線品質的要求。對此，我們提出一套藉由觀察使用者鄰居的傳輸狀況，搭配可以根據鄰居傳輸資料而動態調整的競爭解決機制，避免干擾主要使用者並降低通訊延遲及碰撞，再加上邀請式保留機制，來滿足通訊服務對於連線品質的要求。從我們的模擬結果來看，我們所設計出的通訊協定可以完整保證不造成主要使用者的干擾，且頻譜使用效率較傳統的載波偵測多重存取既干擾避免機制的通訊協定提高至少 50%以上，同時存取時間上的公平性也大幅降低五倍以上。

最後一個頻譜換手的課題，也是感知無線電最獨特且亟需解決的問題，此種換手機制與傳統水平或垂直換手機制最大的不同在於，使用者必須被迫在傳輸封包的過程中轉換到另外一個頻帶，而傳統的換手機制可以等待使用者傳輸完一個完整的封包後再行轉換。在此，我們針對三種感知無線電可能的傳輸劇本：無頻譜換手機制；事先定義通道的頻譜換手以及頻譜偵測後的頻譜換手機制作性能分析，從我們得到的數值分析來看，頻譜偵測後的頻譜換手機制由於可以得到較為正確的標的通道，使其有較好的平均傳輸速率，同時，我們也藉由分析，提供設計者在給定的連線維持機率與平均傳輸速率的要求下，在兩種頻譜換手機制中各項系統參數最大忍受的設定值。

在本論文中最後一部份，我們提出一套跨層分析模型，將實體層因多重路徑衰減，屏蔽效應所造成傳輸失敗，或因擷取效應，多重通道傳輸以及方向性天線對訊號品質改善，而間接對於媒體存取控制層中競爭窗口大小改變的影響，一同於模型中考慮，藉此，我們得以準確的估計感知無線電於實際無線通道中的性能，同時藉由此模型，可以給設計者要如何有效提升性能提供一個明確的方向。

Design and Analysis for Medium Access Control Protocols in Cognitive Radio Networks

A Dissertation

Presented to

The Academic Faculty

By

Ming Bing Chen

In Partial Fulfillment

of the Requirements for the Degree of

Doctor of Philosophy in Communication Engineering

Department of Communication Engineering

National Chiao-Tung University

October, 2007

Abstract

As the advance of wireless communication technology, the spectrum scarcity becomes a severe problem due to the designated frequency band for each legacy system to avoid the interference. However, current experiments have showed that the overall spectrum efficiency over the 0∼3 GHz frequency range is less than 35%. In addition, the temporal and geographical variations in the utilization of the assigned frequency band range from 15% to 85%. Thus, it is necessary to develop a smart device to have the flexibility to access in various frequency bands while not obstructing the licensed user's transmissions in the legacy system. Cognitive radio (CR) is designed to be such an intelligent device, which can sense its surrounding environment, dynamically access the idle channel(s) for a temporary data transmission and return the occupied channel(s) to the licensed user's transmissions. However, to set up a temporary connection without interfering the legacy system, three essential functions are required to be solved: (1) the spectrum sensing over a wide frequency range, (2) an intelligent cognitive medium access control (MAC) protocol, and (3) the link maintenance mechanism to restore the CR user's link. In this dissertation, we will inspect the above three functions to design the MAC protocol and evaluate the performances of the CR networks.

In the wideband spectrum sensing issue, CR devices have to recognize when and which channel(s) the licensed users occupy and to identify the opportunity of reusing the frequency of legacy systems. However, the wideband spectrum sensing is a time and energy consuming processes. In this part, we aim to alleviate the burden of spectrum scanning in a CR device by means of location awareness. We investigate to what extent a CR system with location awareness capability can establish a scanning-free region where an ad hoc connection of the CR users can coexist with an infrastructure-based connection of the primary user. It has been shown that the frequency band of the legacy system can be reused up to 45% by the overlaying cogni-

tive ad hoc network if certain positioning techniques help CR users to locate primary and other secondary users.

Then, we put our effort on the cognitive MAC protocol design, in which a CR device can quickly establish a temporary connection without interfering the licensed user. To establish an overlaying ad hoc network, the cognitive MAC protocol shall not only achieve high spectrum utilization as well as the QoS satisfactory, but also establish the link in a short time without introducing interference to primary users. To this end, we propose four enhanced mechanisms for the CSMA/CA MAC protocol: (1) a neighbor list establishment mechanism for recognizing spectrum usage opportunities, (2) a set of contention resolution methods to reduce collisions as well as the access delay and its variance, (3) an invited reservation procedure for meeting the delay requirements of real-time traffic, and (4) a distributed frame synchronization mechanism to coordinate transmission without central controllers. Compared to the legacy IEEE 802.11 WLAN, the enhanced CSMA/CA MAC protocol can improve the system throughput by 50% through analysis and NS-2 simulations, while keeping the dropping rate lower than 2% for delay-sensitive traffic. Furthermore, the standard deviation of the access delay is reduced by five times.

Next, we study three link maintenance mechanisms for CR devices when the licensed user returns to the occupied channel(s): (1) non-spectrum handoff method, (2) the pre-determined channel list spectrum handoff and (3) the spectrum handoff with radio sensing scheme. In the non-spectrum-handoff scenario, the CR device stays in the original channel and continues the transmission after the licensed user leaves the channel. In the pre-determined channel list spectrum handoff, the CR device lists the target channels before setting up the link. As for the spectrum handoff with radio sensing scheme, the CR device senses the spectrum and then chooses the target channel when the licensed user returns back. In this part, we study the link maintenance probability and the effective data rate in these three mechanisms. Our numerical results are shown that the erroneous channel selection probability, the

radio sensing time and the number of handoff trials are the three important system parameters for the two spectrum handoff schemes. We also provide the design guide of the system parameters for the given effective data rate and the link maintenance probability.

At last, we develop a physical(PHY)/MAC cross-layer analytical model to investigate the performances of the single and multiple channels CSMA/CA MAC protocols in a lossy wireless environment. From the physical layer perspective, the developed model incorporates the effects of capture and directional antennas, while from the MAC layer perspective, our approach takes into account of the contentions in single and multi-channel environments and the effect of the binary exponential backoff process. The proposed cross-layer analytical model not only provides insights into the physical layer impacts on the throughput of the CSMA/CA MAC protocol, but also indicates to how directional antennas can improve the CSMA/CA based system in terms of antenna beamwidth and the number of radio transceivers.

In summery, we have explored the three important issues for CR devices in this dissertation: (1) the wideband spectrum sensing, (2) the cognitive MAC protocol and (3) the link maintenance mechanism. Finally, we develop a PHY/MAC cross-layer analytical model to investigate the performances of the single and multiple channels CSMA/CA MAC protocols.

Acknowledgments

First of all, I would like to express my deeply gratitude to my advisor Dr. Li-Chun Wang. Not only the important insights to research problems, encouragement, and support, he also show me a way be optimistic to face difficulties. Without his advice, guidance, comments, and all that, this work could not have been done. He indeed opened a door to the future for me.

Special thanks to my mates of Wireless Network Lab in NCTU. They gave me kindly help in many aspects in my study years. Dr. Chih Wen Chang and Tom Lee encouraged me every time when I felt frustrated. Dr. Jen Hua Huang and Hyper Wang gave me many valuable suggestions and ideas in my research. I was so lucky to have all the lab mates.

Most importantly, I am deeply indebted to my great parents and brother whose love and understanding have been supporting me without any hesitate through these years. In the end, I would like to thank my friends, Jeannie Chen, Lamb Lee, Hui Chin Wu, Clement Yang, Bill Yang and Yen Xui Zheng. They always warmly back me up from their deeply inside mind.

Contents

Abstract i

Acknowledgements iii

List of Tables ix

List of Figures x

1 Introduction 1

1.1 Problem and Solution 3

1.1.1 Location-aware Concurrent Transmission 3

1.1.2 Neighbor-aware Cognitive MAC Protocol 4

1.1.3 Spectrum Handoff for Link Maintenance 5

1.1.4 Cross-layer Analysis for Single and Multiple Channels CSMA/CA MAC Protocol 7

1.2 Dissertation Outline 9

2 Literature Survey and System Model 11

2.1 Literature Survey 11

2.1.1 Wideband spectrum sensing 11

2.1.2 Cognitive MAC protocol 14

2.1.3 Spectrum handoff 16

2.1.4 Performance analysis of CSMA/CA MAC protocol 16

2.2 System Model 18

3 Location-aware Cognitive Spectrum Identification with Concurrent Transmission 21

3.1 Motivation . . . 22
3.2 Signal-to-Interference Ratio Analysis . . . 22
3.2.1 Uplink SIR Analysis . . . 22
3.2.2 Downlink SIR Analysis: . . . 23
3.2.3 Multiple Ad Hoc Connections Coexisting with One Infrastructure Link . . . 28
3.3 Shadowing Effects . . . 29
3.4 MAC Layer Throughput Analysis . . . 31
3.5 Numerical Results . . . 33
3.5.1 Uplink Concurrent Transmission Probability . . . 35
3.5.2 Downlink Concurrent Transmission Probability . . . 35
3.5.3 Effects of Shadowing on the Concurrent Transmission . . . 38
3.5.4 Total Throughput of Cognitive Ad Hoc Networks Overlaying Infrastructure-based System With Concurrent Transmission . 41
3.6 Conclusions . . . 45
4 Neighbor-aware Cognitive Spectrum Access with QoS Provisioning 46
4.1 Motivation . . . 46
4.2 Neighbor List Establishment in *Observe* Stage . . . 49
4.3 Contention Resolution in *Plan* Stage . . . 51
4.3.1 Gating Mechanism . . . 52
4.3.2 Linear Backoff Algorithm . . . 53
4.3.3 Stall Avoidance Scheme . . . 54
4.4 Invited Reservation Procedure in *Decide* Stage . . . 56
4.4.1 Invited Reservation Procedure . . . 56
4.4.2 Link Establishment with Invited Reservation Procedure . . . 58
4.5 Distributed Frame Synchronization Mechanism in *Act* Stage . . . 60
4.6 Throughput Analysis . . . 63
4.6.1 Mixed non-real-time and delay-sensitive traffic flows . . . 64

4.7 Simulation 66
4.7.1 Simulation Environment 68
4.7.2 Performance Measurements 70
4.7.3 Numerical Results 71
4.8 Conclusion 79
5 Traffic-aware Cognitive Spectrum Handoff with Preemptive Interruption 82
5.1 System Model 82
5.2 Analytical Model 85
5.2.1 Link maintenance probability 85
5.2.2 Effective data rate 88
5.3 Numerical Results 90
5.3.1 Performance of effective data rate for a reliable secondary user's link 91
5.3.2 Impacts of spectrum handoff trials 93
5.3.3 Design of system parameters for spectrum handoff schemes . . 96
5.4 Summary 98
6 Cross-layer Analysis for A Cognitive MAC: Single Channel CSMA/CA Case Study 99
6.1 Motivation 99
6.2 MAC Layer Throughput Performance: Previous Analysis 100
6.2.1 CSMA/CA Backoff Process without Capture Effect 100
6.2.2 CSMA/CA with Capture Effect 102
6.3 Physical Layer Effects 103
6.3.1 Radio Channel Characteristics 103
6.3.2 Outage Probability 104
6.3.3 Effect of Directional Antenna on Outage Probability 104
6.4 Cross-layer Throughput Analysis 105

6.4.1 System Model 107
6.4.2 Capture Effect 107
6.4.3 Probability of Packet Loss 113
6.4.4 PHY/MAC Cross-layer Throughput 114
6.5 Numerical Results 116
6.5.1 Effect of Large Number of Contenders on Capture Probability 117
6.5.2 Throughput Comparison for Different Approaches 119
6.5.3 Effect of Shadowing on the Throughput Performance 122
6.5.4 Effect of Direction Antennas on Capture Probability 122
6.5.5 Effect of Directional Antenna on Throughput Performance . . 125
6.6 Conclusions 127
7 Resource Partition for A Hybrid MAC Based on Contention-oriented Cognitive Multi-channel CSMA/CA and Connection-oriented OFDMA/TDD 128
7.1 Motivation 129
7.2 Background 129
7.2.1 Frame Structure and Link Establishment Procedures in the OFDMA-TDD Mode 129
7.2.2 Multi-channel Random Access Protocol with Collision Avoidance 131
7.3 Resources Partition Optimization 133
7.4 Analysis 135
7.4.1 Efficiency of Reserved Radio Resources 135
7.4.2 Average Access Latency 138
7.5 Numerical Results 139
7.5.1 Performances of Default Radio Resource Partition 139
7.5.2 Performances of Alternative Radio Resource Partitions 142
7.5.3 Performance of Optimum Radio Resources Partitions 147
7.6 Conclusions 151

8 Conclusion **155**

8.1 Location-aware Concurrent Transmission 156

8.2 Neighbor-aware Cognitive MAC Protocol 157

8.3 Spectrum Handoff for Link Maintenance 157

8.4 Cross-layer Analysis for Single Channel CSMA/CA 158

8.5 Cross-layer Analysis for Multiple Channels CSMA/CA 159

8.6 Suggestions for Future Research 160

Appendices **162**

A.1 Derivation of (3.4) 162

A.2 Derivation of (3.10) and (3.11) 163

A.3 Derivation of (3.13) 163

A.4 Derivation of (3.16) 166

Bibliography **171**

Vita **191**

List of Tables

3.1 System Parameters for Concurrent Transmission in an Overlaying Ad Hoc Cognitive Radio Network 34

4.1 System Parameter for the Simulation of Cognitive MAC Protocol . . 69

5.1 System Parameters of the Spectrum Handoff for Link Maintenance . 90

6.1 System Parameters of the Performance Evaluation for the Single Channel CSMA/CA MAC Protocol 118

6.2 Required SNR Threshold and Outage Probability for Different Packet Lengths 118

7.1 System Parameters of the Performance Evaluation for the Multi-channel Random Access with Truncated Binary Exponential Backoff 140

7.2 Optimal parameters values for bandwidth request transmissions (T_o=10 msec) 149

7.3 Optimal parameters values for initial ranging transmissions (T_o=200 msec) 150

List of Figures

1.1 The main functions of a cognition cycle for CR devices. 6

2.1 An illustrative example for the hidden node problem in the transmitter detection method. 13

2.2 An illustrative example for the coexistence of two CR devices establishing an overlaying cognitive ad hoc link and a primary user connecting to the infrastructure-based network, where all the devices (MS_1, MS_2, and MS_3) use the same spectrum simultaneously. 19

3.1 Physical representation of the coexistence probability for the concurrent transmission of overlaying CR-based ad hoc link and infrastructure uplink transmission. 24

3.2 The area of concurrent transmission region R_{CT} in downlink cases. . . 27

3.3 The concurrent transmission probability $P_{CT}^{(u)}$ versus the infrastructure uplink user's locations as the ad hoc receiver MS_2 is located at $(50, -\frac{\pi}{2})$, where r_3 is the distance between the base station and the primary user MS_3. 36

3.4 The concurrent transmission probability $P_{CT}^{(d)}$ versus the CR-based ad hoc receiver's location as the infrastructure uplink user MS_3 is located at $(50, \frac{\pi}{2})$, where r_2 is the distance between the base station and ad hoc link receiver MS_2. 37

3.5 Impact of primary user MS_3's location on the downlink concurrent transmission probability $P_{CT}^{(d)}$ as the ad hoc receiver MS_2 is located at $(50, -\frac{\pi}{2})$. 39
3.6 Impact of CR-based ad hoc receiver MS_2's location on the concurrent transmission probability $P_{CT}^{(d)}$ as the infrastructure downlink user MS_3 is located at $(50, \frac{\pi}{2})$. 40
3.7 Impacts of shadowing on the reliability of downlink $F_{CT}^{(d)}$ (solid line) and uplink $F_{CT}^{(u)}$ (dotted line) concurrent transmission against the locations of (a) the primary user MS_3 and (b) the ad hoc user MS_2 in the cases of $\sigma_\xi = 1$ and 6 dB, respectively. 42
3.8 Total throughput performance of the uplink concurrent transmission. 43
3.9 Total throughput performance of the downlink concurrent transmission. 44
4.1 Comparison of CW size between linear and binary exponential backoff algorithms. 55
4.2 An illustration of the invited reservation procedure. 57
4.3 The timing diagram for the invited reservation procedure. 59
4.4 The timing diagram for the new proposed distributed frame synchronization mechanism. 60
4.5 (a) Interrupted Poisson process model for delay-sensitive traffic. (b) Markov modulated Poisson process (MMPP) model for one type delay-sensitive traffic with M users. 65
4.6 Two-dimensional Markov chain for the analysis of two delay-sensitive traffic types. 67
4.7 The considered network topology for the simulation, in which nodes are distributed to three clusters in a string-type topology. 68
4.8 Dropping rate of the primary user's transmissions in the network topologies that all secondary users are located in one cluster. 72

4.9 Throughput comparison of the proposed cognitive MAC protocol with the traditional CSMA/CA MAC protocol. 73
4.10 Comparison of mean access delay between the proposed cognitive MAC protocol and the CSMA/CA MAC protocol. 74
4.11 Comparison of fairness among the proposed cognitive MAC protocol and the CSMA/CA MAC protocol. 75
4.12 Dropping rate of delay-sensitive traffic for secondary users. 76
4.13 Throughput of the proposed cognitive MAC protocol in the mixed voice and FTP data traffic. 77
4.14 Dropping rate of primary user transmissions in the network topology that secondary users are distributed in three separated clusters. . . . 78
4.15 Comparison of throughput performance between the proposed cognitive MAC protocol and the CSMA/CA MAC protocol in the network topology that secondary users are distributed in three separated clusters. 80
4.16 Comparison of dropping rate for secondary users between the proposed cognitive MAC protocol and the CSMA/CA MAC protocol in the network topology that secondary users are distributed in three separated clusters. 80
5.1 An illustration of the transmission scenario that the secondary user stays in the original channel when the primary user accesses on the channel. 83
5.2 An illustration of the spectrum handoff scenario that the secondary user determines the list of target channels before the link is established. 84
5.3 An illustration of the spectrum handoff scenario that the secondary user performs the wideband radio sensing and then determines the target channel after the primary user appears. 86
5.4 Impact of primary user's traffic load on the effective data rate if the secondary user's transmission is reliable. 92

5.5 Impact of the handoff execution time on the effective data rate if the secondary user's transmission is reliable. 94
5.6 Impact of spectrum handoff trials on the link maintenance probability of a secondary user's transmission. 95
5.7 Contour of the effective data rate for the system parameters (a) p_s and N in the pre-determined channel list spectrum handoff scheme and (b) T_s and N in the spectrum handoff with spectrum sensing scheme when $p_{PU} = 0.1$ and $T_o = 100$ μsec, respectively. 97
6.1 Examples of antenna gain pattern for 120^o and 60^o directional antennas. 106
6.2 The coverage pattern of a tri-sector cell with three 120^o directional antennas. 108
6.3 The relation between the frame capture probability and number of contending nodes under the 6 dB shadowing standard deviation with different SIR threshold. 120
6.4 Capture effect on the throughput of the CSMA/CA MAC protocol with an omni-directional antenna. 121
6.5 Shadowing effect on the throughput of the CSMA/CA protocol with various SIR thresholds. 123
6.6 Comparison of capture effect between omni-directional and directional antennas. 124
6.7 Effects of multiple directional antenna with single/multiple radio transceivers and channel effects on the throughput of the CSMA/CA protocol. . . 126
7.1 Frame structure and Link Establishment of TDD-OFDMA mode in IEEE 802.16. 130
7.2 Illustrations of the multi-channel random access for the initial ranging and bandwidth request in IEEE 802.16. 132

7.3 Efficiency of the reserved radio resources based on the multi-channel random access MAC protocol with three time slots per frame and one/six sub-channels to send bandwidth/ranging requests in an OFDMA system by simulation and analysis. 141
7.4 Average latency of the reserved radio resources based on the multi-channel random access MAC protocol with three time slots per frame and one/six sub-channels to send bandwidth/ranging requests in an OFDMA system by simulation and analysis. 143
7.5 Effects of various sub-channels and time slots on the efficiency of the reserved radio resources based on the multi-channel random access MAC protocol in an OFDMA system with 100 stations. 144
7.6 Effects of various reserved sub-channels and time slots on the collision probability of the multi-channel random access MAC protocol in the considered OFDMA system with 100 stations. 146
7.7 Effects of various reserved sub-channels and time slots on the average latency of the multi-channel random access MAC protocol in the considered OFDMA system with 100 stations. 148
7.8 Performance comparisons of the optimal radio resource partition scheme according to Table 7.2 and the default partition scheme $(r, m) = (6, 3)$ in terms of (a) efficiency and (b) access latency, where $T_o = 10$ msec. 152
7.9 Performance comparisons of the optimal radio resource partition scheme according to Table 7.3 and the default partition scheme $(r, m) = (6, 3)$ in terms of (a) efficiency and (b) access latency, where $T_o = 200$ msec. 153
A.1 Definition of parameters in the calculation of the area of region $R_{CT}^{(u)}$ in the infrastructure uplink case. 164
A.2 Definition of parameters in the calculation of the area of region $R_{CT}^{(d)}$ in the infrastructure downlink case when $max(r^+, r^-) \leq R$. 165

A.3 Definition of parameters in the calculation of the areas of sections A_1 and A_2 in (3.16) in the infrastructure downlink case when $max(r^+, r^-) > R$. 168

A.4 Definitions of parameters in the calculation of the area of section A_3 in (3.16) in the infrastructure downlink case when $max(r^+, r^-) > R$. . 169

Chapter 1

Introduction

Like the last word that William Wallace cried out before he was finally beheaded at the last scene in the film, Breaveheart, which won the 68th Academy Award for the Best Picture, "freedom" is always the life style that the human being seeks for since a long time ago. In recent years, the communication techniques gradually step into the wireless era from the wired age so that the dream that people can freely connect with each other anywhere anytime has finally comes true. However, as the rapid advance of wireless technologies, current wireless communication systems encounter the spectrum scarcity problem because each system is designated at a fixed non-overlapped frequency spectrum to avoid interferences. This constraint lets the communication device have no flexibility on the spectrum usage and results in large variations of frequency utilization as the fast growing demand on bandwidth [1]. Recent research results have shown that this stationary frequency allocation is lack of the efficiency on the spectrum usage and also induces large variation of the spectrum utilization [2, 3]. In addition, the allocation specified by the government authority usually differs from countries. This stationary spectrum regulation further forbids people using mobile devices in worldwide regions and confines the communication between people. To this end, cognitive radio (CR) is considered as a promise to release the spectrum regulation and improve the spectrum utilization. CR device is proposed to reuse the frequencies of the existing legacy system for other unlicensed users [4–7]. The device looks for the available idle channel(s) over a wide frequency range to dynamically set up a temporary connection without interfering to the other on-going transmissions in the legacy systems. By this way, people no longer have to find appropriate devices to connect with others when traveling around the world and finally come to the dream of communicating at any place and any time.

To achieve the objective of reusing the spectrum of legacy systems and dynamically establishing a temporary connection, there are three fundamental techniques required to be solved: (1) wideband spectrum sensing, (2) cognitive medium access control (MAC) protocol and (3) link maintenance mechanism to restore the CR user's link [7–9].

- **W**ideband spectrum sensing: provides the spectrum usage of the legacy systems over a huge frequency range to the CR device. To avoid causing the interference, the unlicensed user[1] has to recognize when and which channel[2] the primary user will use. It also needs to know how long the primary user's transmission will last in the channel. With these information, the secondary user is capable of accessing the idle channel(s) to temporarily establish connections and stopping them before the primary user appears on the occupied spectrum.

- **C**ognitive MAC protocol: enables the CR device to establish connections with others. To transmit data over the license and license-exempted frequencies, the secondary user first requires to determine which channel(s) it will use. Secondly, because the secondary user is only allowed to access the channel in the spare time of the primary user's transmission, the cognitive MAC protocol must set up a connection in the short period of time. Then, the MAC protocol shall dynamically suspend the CR user's connection for the primary user to access the channel(s). At last, like the traditional MAC protocols, the device must efficiently utilize the selected channel to transmit data as well as satisfy the quality-of-service (QoS) requirement for the real-time traffic. Furthermore, in some situations, the secondary user may stay in the network without any central

[1] In this dissertation, the primary user and the licensed user are exchangeable since it has the highest priority to use the specific spectrum. In addition, the unlicensed user is referred to the secondary user because it only has the lowest authority to access the spectrum.

[2] Hereafter, the channel specifies the center frequency and the bandwidth that a communication device requires for data transmission.

controller. The cognitive MAC must be somehow in a distributed manner so that the CR device can transmit data individually without causing unnecessary collisions.

- **L**ink maintenance mechanism: preserves the established connections of secondary users even if the primary user proceeds its transmission in the occupied channel. The secondary user first detects if the primary user is bound to send data. Then, the user may either stay on the original channel or change to another new channel(s)[3] to continue its transmissions. Obviously, with these two options, the secondary user has to determine which method is best for itself. After that, the user has to perform a set of handshaking procedure with its destination to inform which channel and when it will continue the transmission. In the end, a novel mechanism for data protection shall be developed to concatenate and restore the data transmitted in different periods of time or channels.

1.1 Problem and Solution

In this dissertation, we provide some alternative solutions to the three corresponding issues from different standing points. Also, we develop analytical models to investigate the performances of the CR network on the system capacity, effective user's data rate and access delay. At last, we give a design guide of system parameters for CR devices.

1.1.1 Location-aware Concurrent Transmission

In traditional way, the spectrum sensing over a wide frequency range involves the sophisticated time and energy-consuming signal processing [10]. Instead of developing another efficient spectrum sensing technique, in this part, we discuss a challenging but

[3] The change of secondary user's transmissions on another channel(s) is also called "spectrum handoff".

fundamental issue – Can CR devices effectively identify the available spectrum holes without wideband spectrum sensing? Intuitively, when the secondary CR users are far away from the primary user of the legacy system, both CR and the primary users can concurrently transmit their data without causing interference. If a CR device knows the region where it can concurrently transmit with the primary user, the user does not need to rely on the time- and energy-consuming wide-band spectrum scanning to detect the spectrum holes. In addition, it is clear that concurrent transmission can enhance the overall throughput. In this sense, identifying concurrent transmission opportunity shall be given a higher priority over spectrum sensing for a CR user.

The next important issue is how to identify the concurrent transmission region where CR users will not cause any interference to the legacy wireless systems. In this part, we propose to utilize the location awareness techniques to help CR users to identify the concurrent transmission opportunity. Our specific goal is to dimension the concurrent transmission region where CR devices can establish an overlaying ad hoc network on top of an infrastructure-based legacy system. The overlaying ad hoc network can be considered an important application for CR devices because it can reuse the underutilized spectrum and significantly improve the efficiency of the frequency band. It is assumed that the location information of other nodes can be obtained from the upper layer, like the method in [11]. We will also investigate the throughput improvement resulting from concurrent transmissions based on the carrier sense multiple access with collision avoidance (CSMA/CA) MAC protocol.

1.1.2 Neighbor-aware Cognitive MAC Protocol

In the second part of this dissertation, we propose an enhanced CSMA/CA cognitive MAC protocol. The CSMA/CA MAC is a well known MAC protocol for resolving contentions in many existing wireless networks, such as the IEEE 802.11 wireless local area network (WLAN) [12]. Since the CSMA/CA MAC protocol requests a station to sense the channel usage before transmissions, this kind of MAC protocol

has potential and is natural to become a strong candidate for the overlaying cognitive ad hoc networks. Thus, we are motivated to ask two fundamental questions: Can the CSMA/CA MAC protocol be directly adopted for the overlaying ad hoc networks without changes? If not, how should the CSMA/CA MAC protocol be modified to become an appropriate cognitive MAC protocol for the overlaying ad hoc networks in the presence of primary users?

To this end, we propose a MAC protocol with QoS provisioning for overlaying single-hop ad hoc networks on the legacy system, which is assumed to adopt the time-division multiple access (TDMA) MAC protocol for packet transmissions to guarantee QoS requirements, like GSM and WiMax. The proposed MAC protocol coincides with the four stages of the cognition cycle, as shown in Fig. 1.1 [7,8,13]. Corresponding to the cognition cycle, the neighbor list establishment mechanism maps to the ***observe*** stage, which can help a secondary user to recognize the spectrum usage around its neighborhood. In the ***plan*** stage, the improved contention resolution mechanism can enhance the overall performance in terms of throughput, access delay and fairness. In the ***decide*** stage, the newly proposed reservation scheme ensures the established ad hoc link with satisfactory QoS requirements. The distributed frame synchronization mechanism then coordinates the transmissions among stations in the ***act*** stage. With the helps of these QoS enhanced techniques, an ad hoc network based on the proposed improved CSMA/CA MAC protocol can coexist with a legacy TDMA system.

1.1.3 Spectrum Handoff for Link Maintenance

After establishing an unharmful connection, the secondary user requires to dynamically suspend and resume its transmission when the primary user returns. Intuitively, the secondary user can either stay in the original channel or handover to another one to continue its data transmission. To stay in the original channel, the user has to stop sending data to wait until the primary user completes its connection. On the other hand, to handover to another channel(s), the device may need to determine whether

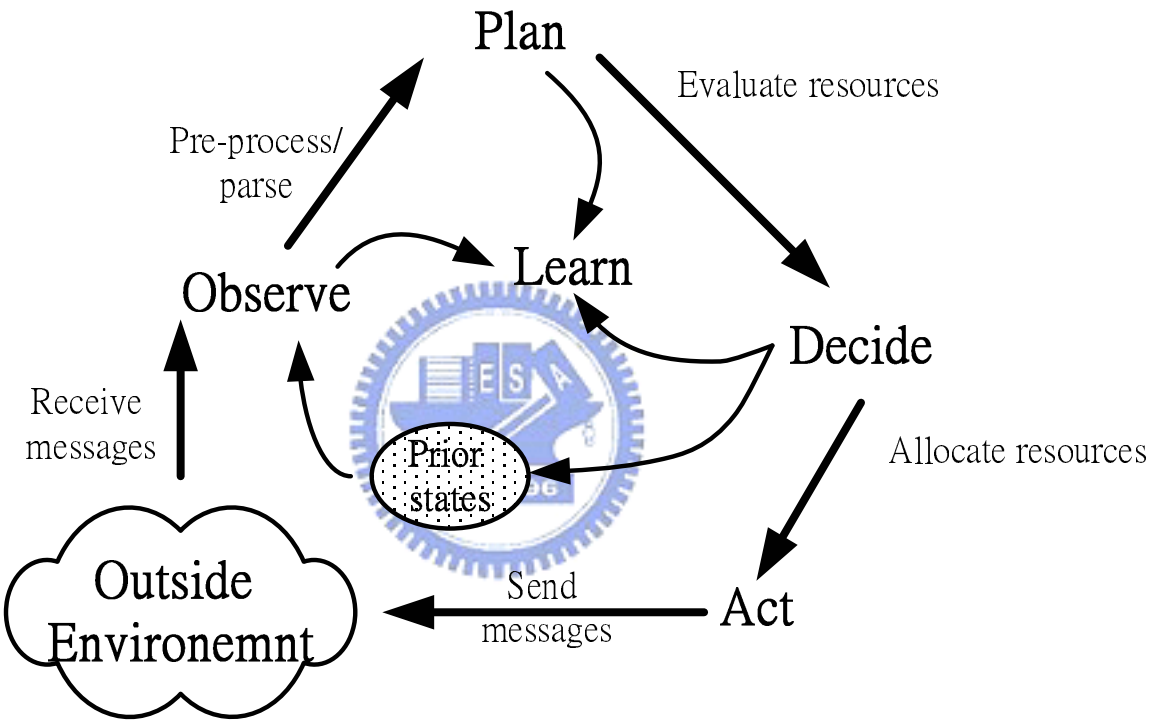

Fig. 1.1: The main functions of a cognition cycle for CR devices.

it should prepare the list of target channels before its link is established or it only senses and selects a target channel when the primary user appears. The transmission time in the former case is subject to the erroneous channel selection, which leads the user to continuously change channels for the transmission. Similarly, the later scheme also wastes time on the spectrum sensing to determine the target channel. Therefore, for secondary user, neither staying in the original channel nor changing to another one to continue the transmission requires an extra period of time and lowers the effective data rate. Thus, a fundamental question for the link maintenance to the secondary use is raised: whether a secondary user should stay or change channel to proceed its data transmission when the primary user appears in the occupied spectrum? Furthermore, if the spectrum handoff is necessary, then which scheme is appropriate for secondary users?

To answer this question, we are motivated to develop an analytical model to investigate the performances of these three transmission scenarios. Specifically, we investigate the link maintenance probability that the secondary user can thoroughly transmit a packet within a given number of handoff trials. Furthermore, the effective data rate that considers the impact of the primary user's transmission is also examined. With the developed model, we can determine the upper limits of the error probability for channel selection and the radio sensing time as well as the number of handoff trials for a given link maintenance probability and effective data rate.

1.1.4 Cross-layer Analysis for Single and Multiple Channels CSMA/CA MAC Protocol

As discussed before, since the CSMA/CA MAC protocol is a strong candidate for the cognitive MAC protocol, it is necessary to investigate the performance of this MAC protocol. However, current collision models for the CSMA/CA MAC protocol are both pessimistic and optimistic. From the pessimistic standpoint, frame transmissions in the wireless channel may fail due to signal outage even having only one user. From

the optimistic standpoint, although multiple frames are simultaneously transmitted from many different users, one of the transmitted frames may be successfully received if the signal-to-interference noise ratio (SINR) requirement can be satisfied. According to the so-called capture effect, a MAC protocol can be designed to allow multiple simultaneous transmissions to enhance throughput. Hence, it is of importance to investigate the performance of the CSMA/CA MAC protocol from a physical/MAC (PHY/MAC) cross-layer perspective.

In this part, we first develop such a cross-layer analytical model, taking into account of the effects of a practical directional antenna pattern, capture, log-normal shadowing, multipath Rayleigh fading and the number of radio transceivers, to accurately evaluate the throughput of the CSMA/CA MAC protocol. Here, we provide the complete derivation of the PHY/MAC cross-layer analytical model and the more detailed simulation results. Furthermore, we discuss the impacts of SINR requirement, shadowing parameters, directional antenna gain patterns and the number of radio transceivers for both the uplink and downlink transmissions.

In addition, CR devices can access in various channels at the same time once the channels are available for secondary users. Thus, we then extend the previously developed model to explore the performances of the random access among multiple channels. With additional channels, the transmission of CR devices can be allocated in either the time or frequency domain. Here, we assume that both the connection-oriented and contention-based MAC protocols, like the IEEE 802.16 WiMax OFDMA system, are adopted for allocating radio resources. The purpose for the connection-oriented MAC protocol is to allow users to transmit data in a reserved chunk of time slots and sub-channels. However, before transmitting data, stations must send requests for the access permission from the base station. The access permissions are granted based on a certain contention procedure in a reserved chunk of time slots and sub-channels. Intuitively, increasing the reserved resources for contention can shorten the access latency since there are fewer collisions, but it also decreases the

overall spectrum efficiency. Therefore, determining how long and how many sub-channels an OFDMA system should reserve for the contention-based random access scheme is an important issue.

The last part of this dissertation presents an analytical approach to determine the optimal number of reserved sub-channels and time slots for the random access scheme in the the mixed connection-oriented and contention-based OFDMA system. We formulate an optimization problem to maximize the efficiency of the reserved radio resources while meeting the delay requirement for supporting real-time applications. It is noteworthy that the multi-channel random access scheme can allow multiple users to access the sub-channels concurrently. The performance must be much different than the conventional single channel CSMA/CA MAC due to the reduced collisions. Based on the proposed approach, performance enhancement can be achieved without changing the specifications of the current OFDMA system.

1.2 Dissertation Outline

This dissertation is partitioned into four parts. First, we examine whether a CR device can coexist with the legacy system in an overlapped area. The region that a secondary user can establish concurrent connection with the primary user is also evaluated. Next, we discuss the possibility if the well-known CSMA/CA MAC protocol with a few modifications is appropriate as a cognitive MAC protocol for CR devices. An enhanced CSMA/CA MAC protocol with QoS provisioning is designed to establish an ad hoc link in the presence of the legacy system without any coordinator. Then, a fundamental issue of the spectrum handoff is studied to explore the link maintenance probability and the effective data rate of the secondary user's transmission. The system parameter values involving the spectrum handoff for the CR device is suggested based on the developed analytical model. At last, a cross-layer analysis jointly taking the frame capture and outage impacts of the physical (PHY)

layer into the contention resolution mechanism of the MAC layer is developed. The model is further extended to the multi-channel random access scheme, which is more realistic for the CR network.

The remaining chapters of this dissertation are organized as follows. In Chapter 2, we first give a literature survey of the state-of-the-art techniques in the field of the three essential functions for CR devices: (1) wideband spectrum sensing, (2) cognitive MAC protocol and (3) link maintenance mechanism. Chapter 3 studies the probability and dimensions the region where a secondary user can concurrently establish connection with other primary users. Next, Chapter 4 demonstrates an enhanced CSMA/CA MAC protocol with QoS provisioning as a cognitive MAC for CR devices. After that, in Chapter 5, the performance of the three transmission scenarios for lasting the secondary user's link is investigated, and the system parameters for the two spectrum handoff schemes are also designed. Next, Chapter 6 provides a cross-layer analytical model to accurately evaluate the throughput performance of the single channel CSMA/CA MAC protocol. Before the conclusion, in Chapter 7, an extended analytical model for the multi-channel CSMA/CA MAC protocol is developed based on the concept in Chapter 6. Finally, the concluding remarks and some suggestions for future research topics are given in Chapter 8.

Chapter 2

Literature Survey and System Model

In this chapter, we first give the literature survey of the state-of-the-art techniques for the three enabling functions of the CR devices: (1) wideband spectrum sensing, (2) cognitive MAC protocol, and (3) spectrum handoff for link maintenance. We also review some analytical models for the performance evaluation of the single and multiple channels CSMA/CA MAC protocol. The CSMA/CA MAC protocol can be considered a strong candidate for the MAC protocol in CR devices due to the capability of avoiding interference to the primary users. At last, we will provide the generic system model and the network architecture considered in this dissertation.

2.1 Literature Survey

2.1.1 Wideband spectrum sensing

The spectrum sensing is the essential function for CR devices since it enables the CR devices to adapt the transmissions according to the surrounding environment by detecting the spectrum holds. The difficult parts of spectrum sensing are that it has to deal with signals in a multi-giga hertz frequency range and more $20 \sim 40$ dB sensitivity than the conventional receivers [14, 15]. Furthermore, the secondary user has no direct measurement of the channel between the primary receiver and itself [2, 7, 9]. In general, the current techniques for the spectrum sensing can be classified into three categories based on the measurement target: (1) transmitter detection, (2) network detection and (3) interference-based detection.

- **Transmitter detection:** measures the signal power over the channels to enable the CR devices to acquire the spectrum usage of the primary users in its

surrounding environment. Since only the primary transmitter dissipates electromagnetic wave, the secondary user using this method has no knowledge of its induced interference to the primary receiver. According to its detecting process, the transmitter detection can be further divided into three types as follows [2, 9, 14, 15].

- Energy detection - scans and measures the energy appeared on every channel. This method is the optimal detector if the device has no information about the primary user's signal in the AWGN channel [9]. However, it is subject to the changing noise level and wireless channel impacts, e.g., shadowing and multipath fading effects [9, 14]. To expedite the scanning process over a wide frequency rang, the multi-resolution spectrum sensing technique using wavelet transform is proposed to detect the signal in the spectrum with various frequency resolution [16–18].
- Waveform detection - applies a matched filter to maximize the received signal-to-noise ratio (SNR) [19]. However, it requires the CR device to have a priori knowledge of the transmitted signal of the primary user.
- Statistic detection - utilizes the cyclostationary featured detector to examine the periodicity of the signals in the channel [2, 20–23]. Unlike the power spectral density (PSD) in the energy detection method, the statistic scheme uses the spectral correlation function (SCF) to preserve and differentiate the phase and frequency information from signals. However, it requires sophisticated computation and long observation time to perform the spectral correlation [9].

- **Network/cooperative detection:** gathers the information of primary users from other CR devices to avoid the hidden node problem [3, 24–29]. As shown in Fig. 2.1, the hidden node problem reveal that the CR device using the transmitter detection method may be incapable of detecting signals from the primary

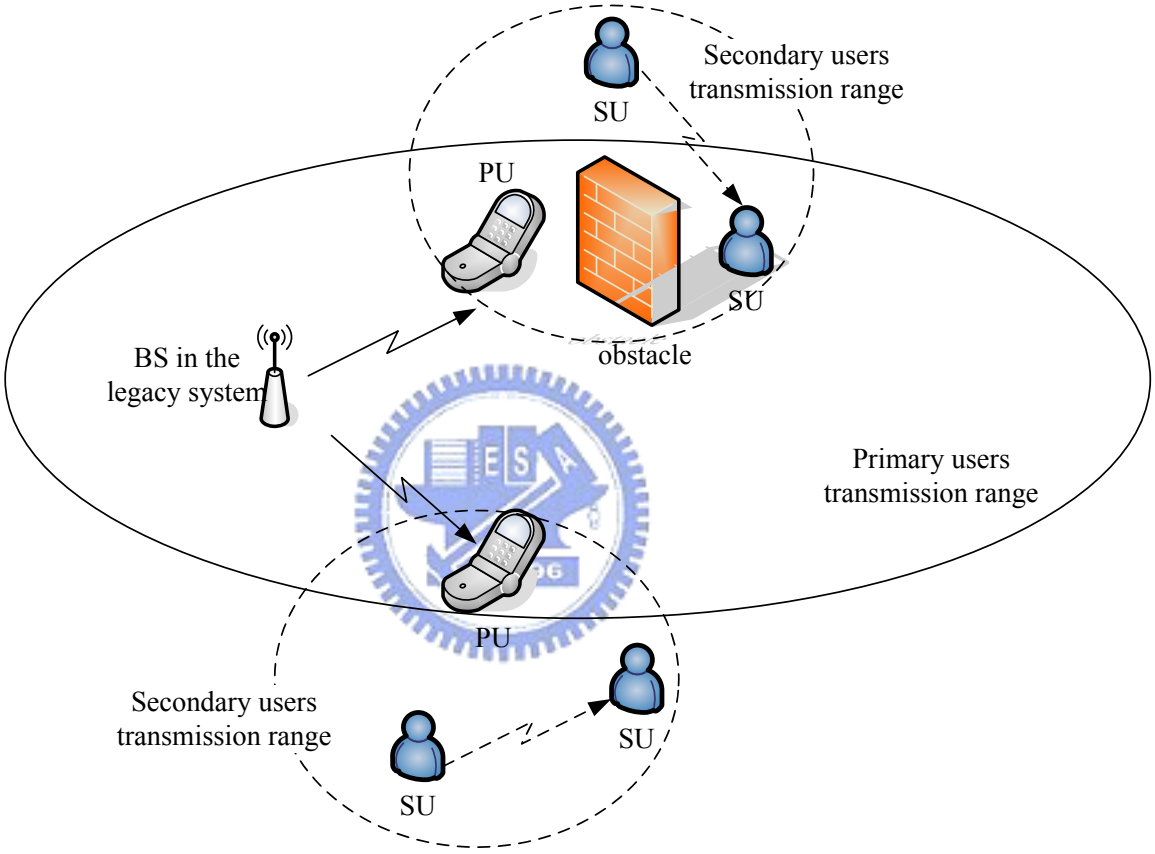

Fig. 2.1: An illustrative example for the hidden node problem in the transmitter detection method.

transmitter due to the path loss of long propagation or the shadowing of obstacles [2, 9, 14]. The network/cooperative detection is proposed that secondary users report the observed channel status and spread this information to other users in a distributed or centralized manner. The cooperation with other users can effectively lower the detection uncertainty by double checking the observations from other users. Intuitively, the more the users in the network, the less the detection uncertainty. However, because this mechanism involves the message exchange among users, the additional handshaking and traffic overhead are required to be studied [30]. Furthermore, the security issue that secondary users may emulate the primary user to occupy the channel is still needed to be investigated [31].

- **Interference-based detection:** accounts for the cumulative energy at the primary receiver [32–35]. A new model, referred as *interference temperature*, is introduced to show the increased interference power level to the primary user as a noise floor. As the interfering signals appears, the equivalent interference floor increases to indicate the peaks above the original noise floor. With the maximum tolerable interference limit, the secondary user can precisely evaluate whether its transmission causes the interference to the primary receiver. However, this mechanism requires the location of the primary user, which has to cooperate with other layers, for the interference calculation.

2.1.2 Cognitive MAC protocol

After sensing a wide frequency range, the CR device performs the cognitive MAC protocol to send data to its destination in the unoccupied channel(s). To establish a temporary connection in the presence of legacy system, the cognitive MAC protocol has to proceed the following three steps after the spectrum sensing. First, the secondary user requires to build up the spectrum usage model of the primary users. Then, select appropriate channel(s) for the data transmission. Finally, it executes the

predefined handshaking procedure with and sends packets to its destination.

- **Spectrum usage model:** characterizes when and how long the primary user uses the spectrum [36–41]. This step helps the secondary user to select the channel(s), in which the user can reside long enough for its data transmissions. Obviously, the more accurate the model the less times the primary user appears during the secondary user's transmissions. However, it is a challenging issue because the model not only describes the primary user's behavior but also has to take the wireless channel effects into account.

- **Channel allocation:** is the policy for secondary users to determine when and which channel(s) it can send data to the destination. The key issue for the spectrum allocation is the multi-dimension resource allocation, such as frequency, time and spreading codes. Various techniques have been developed to optimize the performances of spectrum utilization, system throughput and fairness among users. The strategies based on the game and graph theories are proposed in [42–45] and [46, 47], respectively. Another methods using the statistical model are developed to determine the channel for the secondary user's transmission [48–51]. The others gather the information of the global network topology to select the channel [11, 52–54].

- **Spectrum access:** is responsible of resolving the contentions among multiple secondary users in the presence of the legacy system [55–62]. Different from the legacy MAC protocol, the connections of the CR device in the channel must be established in a short period of time because of the limited available transmission time in the channel. The challenging issue is how to reduce the access latency while achieving high channel utilization as well as the QoS satisfactory. Furthermore, the fairness issue from the aspect of access latency is another distinct viewpoint from the conventional MAC protocol design.

2.1.3 Spectrum handoff

The last but the most unique issue for the CR device is the "*spectrum mobility*", which gives rise to a new kind of handoff between the idle channels [6, 9]. The need of this technique arises when the primary user appears or the occupied channel condition become worse. In these situations, the secondary user has to suspend its data transmission and to evacuate the occupied channel when the primary user returns. The CR device may resume its transmission in the original channel after the end of the primary user's transmission. On the other hand, it can also change to another channel to continue the transmission. Apparently, the probability that the secondary user's link can be maintained and the average transmission time are the two important performance metrics for the spectrum handoff. In the literature, most of research works focus on the physical layer impacts without regarding the procedures in the MAC layer. In [63, 64], the authors discuss the impacts of the number of the redundant channels on the link maintenance probability. As for the issue of the average transmission time, the authors in [65, 66] consider the goodput performance of the secondary user's transmission for the spectrum-exchanged OFDMA system. At last, the preliminary MAC protocol for the spectrum handoff is designed and implemented in [67, 68]without the performance analysis and system parameters design.

2.1.4 Performance analysis of CSMA/CA MAC protocol

In the following, we discuss the performance analysis of the CSMA/CA MAC protocol, in which the carrier sensing prior to any data transmission can satisfy the degree of the primary user avoidance. The analytical models for evaluating throughput of the CSMA/CA MAC protocol have been proposed in [69–79]. Under an error-free channel, the saturation throughput performance, delay and frame dropping probability of the CSMA/CA MAC protocol including the backoff process and finite retransmission limit were analyzed in [69–72]; whereas the performance in non-saturated condition

was inspected in [73, 74]. The effect of backoff freezing, i.e., a station freezing its backoff counter when the channel turns to busy, was considered in [75]. In [76,77,80], the throughput and delay performance of the CSMA/CA MAC protocol were investigated in the presence of Rayleigh fading, shadowing and finite retransmission limit, but the impact of frame capture on the backoff process was not considered. The authors of [81] considered the cross-layer interaction between the physical and MAC layers on the per-user throughput performance in multi-hop ad hoc networks. Recently, the impacts of various incoming traffic load, packet size, data transmission rate in imperfect channels were studied in [78,79]. However, the evaluation method of the physical layer effects of frame outage and capture probabilities was not explicitly expressed in [78, 79, 81]. Furthermore, the impact of the directional antenna with a more practical gain pattern on the throughput of the CSMA/CA MAC protocol is not considered in [69–71, 73–79].

Next, we discuss the performance analysis of multi-channel MAC protocol. Until now, the IEEE 802.16 WiMax system is the most well-know system allowing multiple mobile users to transmit data in different channel at the same time. Some analytical techniques have been reported to investigate the MAC performance of the IEEE 802.16e WiMax system. The throughput of the connection-oriented MAC protocol of the IEEE 802.16e WiMax system was investigated by considering the overhead of the control channels [82, 83]. In addition, the frame access delay in the contention and polling process of the IEEE 802.16e networks have been studied in [84,85]. Nevertheless, in [84, 85], it was assumed that the slotted ALOHA is used to resolve the contentions in the channel access. To our knowledge, the access latency analysis of a joint contention- and connection-oriented multi-channel access scheme combined with the binary backoff algorithm used in the IEEE 802.16e WiMax system is an open issue.

2.2 System Model

In this section, we define the generic system model discussed in this dissertation. Figure 2.2 illustrates a hybrid ad hoc/infrastructure-based network consisting of two CR devices (MS_1 and MS_2) and a primary user MS_3. Assume that the secondary CR users MS_1 and MS_2 try to make a peer-to-peer connection, and the primary user MS_3 has been connected to the base station (BS) or access point (AP) of the legacy infrastructure-based system. In the figure, MS_1, MS_2 and MS_3 are located at (r_1, θ_1), (r_2, θ_2) and (r_3, θ_3), respectively; the coverage area of the base station is πR^2. All the primary and secondary users stay fixed or hardly move.

We assume the CR devices can perform the positioning technique to acquire their relative or absolute position by using GPS or detecting the signal strength from the BSs of legacy systems [86–91]. The location information is broadcasted by using the geographical routing protocols [92–94]. Although both the positioning and geographical routing may waste time and consume the energy, they have no need to be processed for every data transmission. They are only performed when a new node joins or the node changes its position. Furthermore, with the help of upper layer, the location information is already stored in the device. Therefore, compared to the spectrum sensing at every transmission, we believe the additional energy consumption and memory space due to the positioning and location update is relatively small. The overhead and optimal reserved resources for acquiring the location information are beyond the scope of this paper and have been studied in some research works [95,96].

Based on the CSMA/CA MAC protocol, multiple users contend the channel, and only one mobile station within the coverage of the base station can establish an infrastructure-based communication link at any instant. To set up an extra peer-to-peer ad hoc connection in the same frequency band of the primary user, two secondary CR users have to ensure that the current infrastructure-based link quality cannot be degraded. Here, we consider that both primary and secondary users have

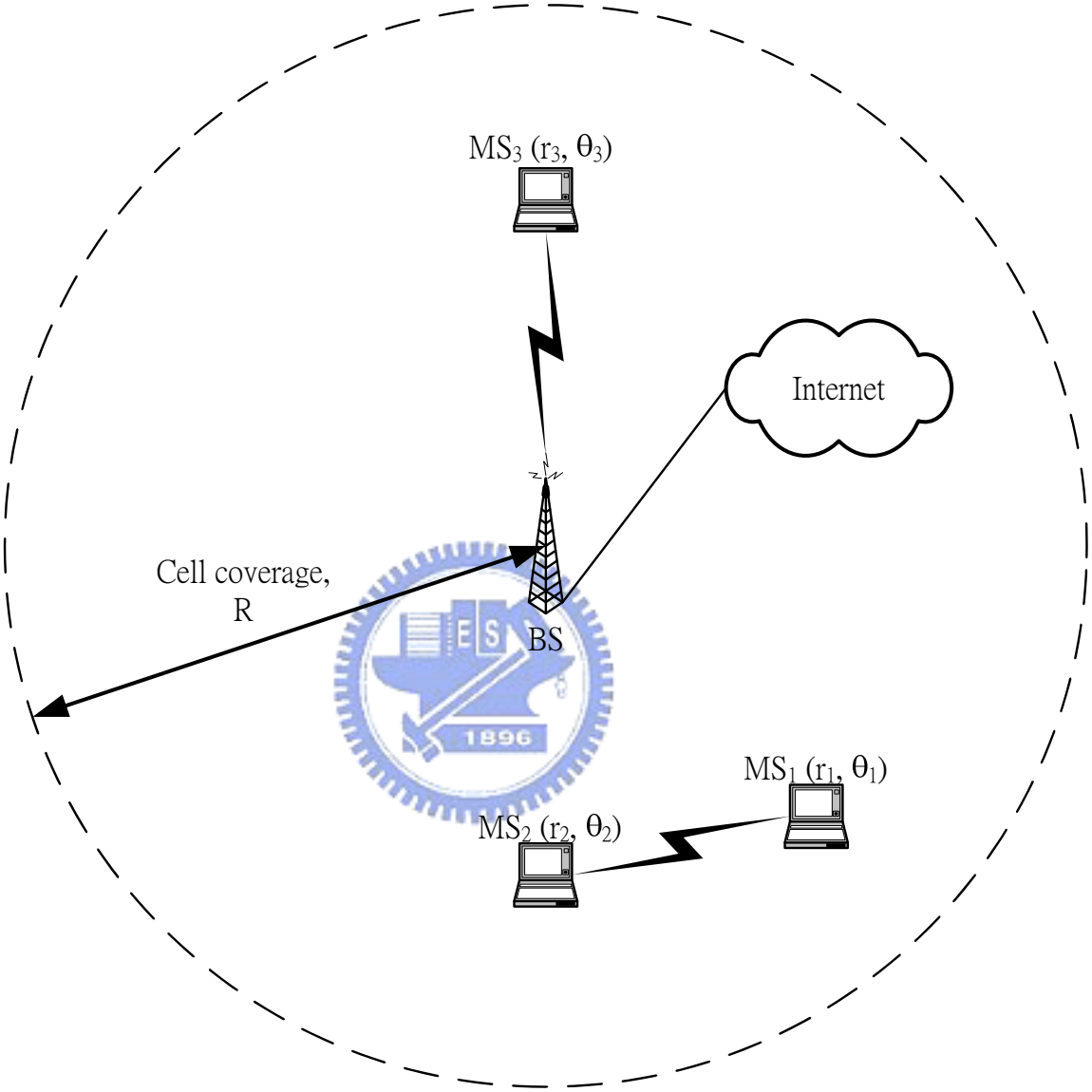

Fig. 2.2: An illustrative example for the coexistence of two CR devices establishing an overlaying cognitive ad hoc link and a primary user connecting to the infrastructure-based network, where all the devices (MS_1, MS_2, and MS_3) use the same spectrum simultaneously.

identical transmit power. It is reasonable to assume only one secondary user can be established a link after the contention at one instance due to the similar interference range. Denote SIR_i and SIR_a as the received signal-to-interference ratios (SIRs) of the infrastructure-based and ad hoc links, respectively. Then we can define the coexistence (or concurrent transmission) probability (P_{CT}) of the infrastructure-based link and CR-based ad hoc link in an overlapped area as follows:

$$P_{CT} = P\{(SIR_i > z_i) \cap (SIR_a > z_a)\}, \tag{2.1}$$

where z_i and z_a are the required SIR thresholds for the infrastructure-based and ad hoc links, respectively. To obtain the concurrent transmission region, it is crucial to calculate the coexistence probability of both the infrastructure and ad hoc links. If the link quality of the primary user cannot be guaranteed, CR devices have to sense and change to other frequency bands.

We consider the following propagation model [97]:

$$P_r = \frac{P_t h_{bs}^2 h_{ms}^2 G_{bs} G_{ms} 10^{\frac{\xi}{10}}}{r^{\alpha}}, \tag{2.2}$$

where P_r and P_t are the received and transmitted power levels at a mobile station, respectively; h_{bs} and h_{ms} represent the antenna heights of the base station and the mobile station, respectively; G_{bs} and G_{ms} stand for the antenna gains of the base station and the mobile station, respectively; r is the distance between the transmitter and receiver; α is the path loss exponent; $10^{\frac{\xi}{10}}$ is the log-normally distributed shadowing component.

Chapter 3

Location-aware Cognitive Spectrum Identification with Concurrent Transmission

Our main contribution of this chapter is to provide the idea of utilizing location awareness to facilitate frequency sharing in a concurrent transmission manner. Specific achievements are summarized in the following.

- We show that a CR device having location information of other nodes can concurrently transmit a peer-to-peer data in the presence of an infrastructure-based connection in some region. We also dimension the concurrent transmission (or the scanning-free) region for CR users. Note that a concurrent transmission region of a CR system is equivalent to a scanning-free region. Nevertheless, the wide-band spectrum sensing procedure is still needed but is initiated only when the CR user is outside the concurrent transmission region. Therefore, the energy consumption of CR systems with location awareness capability can be reduced significantly.

- Based on the CSMA/CA MAC protocol, a physical/MAC cross-layer analytical model is developed to compute the coexistence probability of a peer-to-peer connection and an infrastructure-based connection. Based on this analytical model, we find that concurrent transmission of the secondary CR users and the primary users in the legacy system can significantly enhance the total throughput over the pure legacy system.

3.1 Motivation

In the literature, the coexistence issue of the hybrid infrastructure-based and overlaying ad hoc networks has been addressed but in different scenarios. In [98–101], the idea of combining ad hoc link and infrastructure-based link was proposed mainly to extend the coverage area of the infrastructure-based network. That is, the coverage area of ad hoc networks is not overlapped with that of the infrastructure-based network. In the present hybrid ad hoc/infrastructure-based network, as shown in Fig. 2.2, the peer-to-peer CR users are located within the coverage area of the existing legacy wireless network. In [102], to further improve the throughput of a wireless local area network (WLAN), it was suggested that an access point (AP) could dynamically switch between the infrastructure mode and the ad hoc mode. In our considered scenario, the decision of establishing ad hoc connections is made by the CR users in a distributed manner.

3.2 Signal-to-Interference Ratio Analysis

3.2.1 Uplink SIR Analysis

In the *uplink case* when the primary user MS_3 transmits data to the base station, denote $SIR_i^{(u)}$ as the uplink SIR of MS_3 and let P_{30} and P_{10} be the received power from MS_3 and MS_1 at the base station, respectively. Then from (2.2), we have

$$SIR_i^{(u)} = (\frac{r_1}{r_3})^{\alpha} = \frac{P_{30}}{P_{10}} \ , \tag{3.1}$$

where r_1 and r_3 are the distances between MS_1 and MS_3 to the base station, respectively. Similarly, the SIR of a peer-to-peer ad hoc link from MS_1 to MS_2 can be written as

$$SIR_a = \frac{P_{12}}{P_{32}} = (\frac{d_{23}}{d_{12}})^{\alpha} \ , \tag{3.2}$$

where P_{12} is the received power at MS_2 from MS_1 and P_{32} is the interference power from MS_3; d_{12} and d_{23} are the distances from MS_1 and MS_3 to MS_2, respectively. Substituting (3.1) and (3.2) into (2.1), the concurrent transmission probability $P_{CT}^{(u)}$ in the *uplink case* can be written as

$$P_{CT}^{(u)} = P\{(r_3 z_i^{1/\alpha} < r_1 < R) \cap (d_{12} < \frac{d_{23}}{z_a{}^{1/\alpha}})\} \triangleq \frac{R_{CT}^{(u)}}{\pi R^2} \ . \tag{3.3}$$

Note that $R_{CT}^{(u)}$ denotes the concurrent transmission region where MS_1 can connect to MS_2 without interfering the uplink signal of MS_3 to the base station. As shown in Fig. 3.1, the condition $(r_3 z_i^{1/\alpha} < r_1 < R)$ leads to a donut-shaped area consisting of two circles centered at the base station with the radii of $r_3 z_i^{1/\alpha}$ and R, respectively. Meanwhile, the condition $(d_{12} < d_{23}/z_a^{1/\alpha})$ yields the circular area centering at MS_2 with a radius of $d_{23}/z_a^{1/\alpha}$. From the figure, the region $R_{CT}^{(u)}$ can be computed as

$$R_{CT}^{(u)} = \pi(\frac{d_{23}}{z_a^{1/\alpha}})^2 - A_1 - A_2 \ , \tag{3.4}$$

where

$$A_1 = (\frac{d_{23}}{z_a^{1/\alpha}})^2(\pi - \theta') - R^2\theta + 2\Delta \tag{3.5}$$

and

$$A_2 = (\frac{d_{23}}{z_a^{1/\alpha}})^2\phi - (r_3 z_i^{1/\alpha})^2\phi' - 2\Delta' \ . \tag{3.6}$$

The definitions of parameters θ, θ', ϕ, ϕ', Δ, and Δ' and the detailed derivation of (3.4), (3.5) and (3.6) are discussed in Appendix A.1.

3.2.2 Downlink SIR Analysis:

Now we consider the *downlink case* when the base station sends data to the primary user MS_3. Denote $SIR_i^{(d)}$ as the infrastructure link's SIR in the downlink direction. Then from (2.2), we have

$$SIR_i^{(d)} = \frac{P_{03}}{P_{13}} = (\frac{h_{bs}}{h_{ms}})^2(\frac{d_{13}}{r_3})^\alpha \ , \tag{3.7}$$

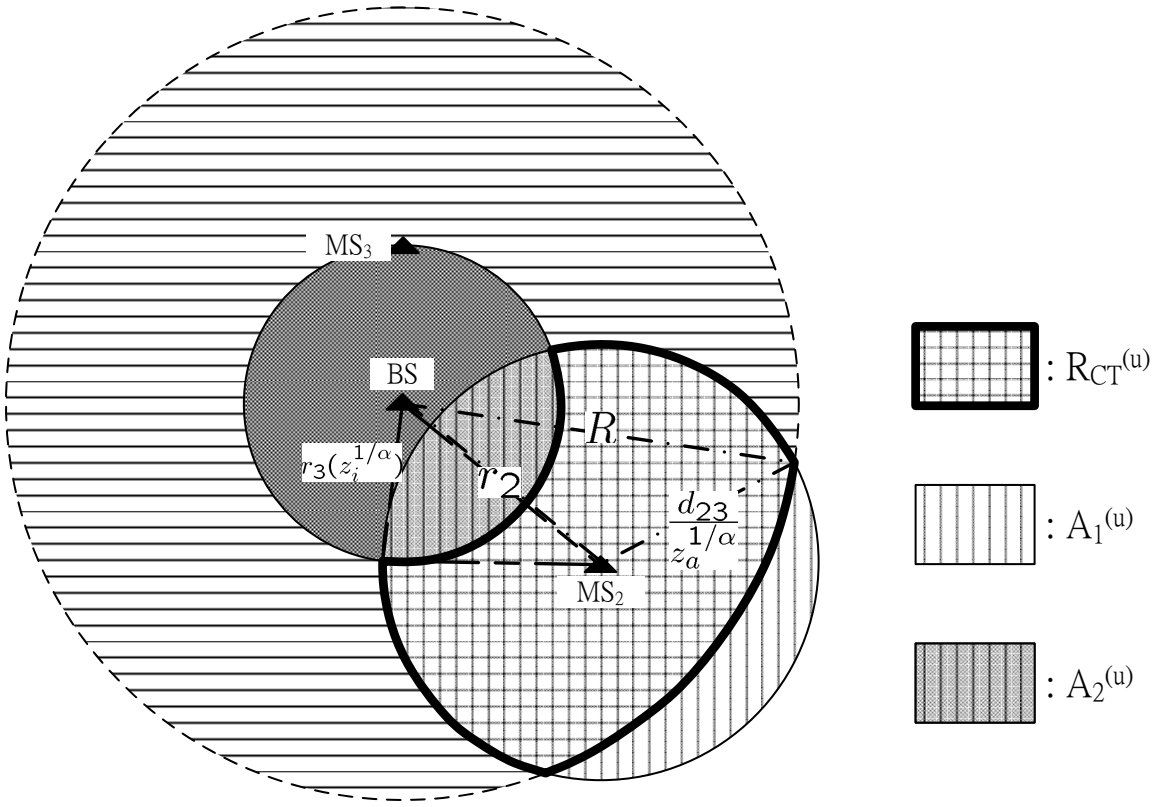

Fig. 3.1: Physical representation of the coexistence probability for the concurrent transmission of overlaying CR-based ad hoc link and infrastructure uplink transmission.

where P_{03} and P_{13} are the MS_3's received powers from the base station and MS_1, respectively; d_{13} stands for the distance from MS_1 to MS_3; h_{bs}, h_{ms} and r_3 are given in (2.2) and (3.1). Similarly, the ad hoc link's SIR from MS_1 to MS_2 can be expressed as

$$SIR_a = \frac{P_{12}}{P_{02}} = (\frac{h_{ms}}{h_{bs}})^2(\frac{r_2}{d_{12}})^{\alpha} \ , \tag{3.8}$$

where P_{12} and P_{02} are the received powers at MS_2 from MS_1 and the base station, respectively; r_2 represents the distance between MS_2 and the base station; d_{12}, h_{bs} and h_{ms} are defined in (3.2) and (2.2).

Substituting (3.7) and (3.8) into (2.1), we can obtain the concurrent transmission probability $P_{CT}^{(d)}$ of a CR-based peer-to-peer ad hoc link and an infrastructure-based downlink transmission as follows:

$$P_{CT}^{(d)} = P\{(d_{13} > r_3 z_i'^{1/\alpha}) \cap (d_{12} < r_2 z_a'^{1/\alpha}) \cap (r_1 < R)\} \triangleq \frac{R_{CT}^{(d)}}{\pi R^2} \ , \tag{3.9}$$

where $z_i' = z_i h_{ms}^2/h_{bs}^2$ and $z_a' = 1/z_a \cdot h_{ms}^2/h_{bs}^2$. From (3.9), the concurrent transmission region $R_{CT}^{(d)}$ in the *downlink case* is shown in Fig. 3.2. The criterion $(d_{13} > r_3 z_i'^{1/\alpha})$ results in the region outside the circle centered at MS_3 with a radius of $r_3 z_i'^{1/\alpha}$, while the criterion $(d_{12} < r_2 z_a'^{1/\alpha})$ yields the region inside the circle centered at MS_2 with radius $r_2 z_a'^{1/\alpha}$. At last, $r_1 < R$ because MS_1 is assumed to be uniformly distributed within a cell of radius R.

The coexistence probability of the CR-based ad hoc link and the infrastructure-based downlink can be obtained by calculating the area of $R_{CT}^{(d)}$. The distances from the AP to the intersections of the two circles with radii of $r_3 z_i'^{1/\alpha}$ and $r_2 z_a'^{1/\alpha}$ are denoted by r^+ and r^- as shown in Fig. 3.2. In Appendix A.2, we have shown that

$$\begin{aligned} r^+ \ = \ & \frac{1}{d_{23}^2}\{r_2 r_3[r_2 r_3(z_a'^{\frac{2}{\alpha}} + z_i'^{\frac{2}{\alpha}}) + \cos(\theta_2 - \theta_3)(d_{23}^2 - r_2^2 z_a'^{\frac{2}{\alpha}} - r_3^2 z_i'^{\frac{2}{\alpha}})] + \\ & \sin(\theta_2 - \theta_3)\delta\} \end{aligned} \tag{3.10}$$

and

$$\begin{aligned} r^- \ = \ & \frac{1}{d_{23}^2}\{r_2 r_3[r_2 r_3(z_a'^{\frac{2}{\alpha}} + z_i'^{\frac{2}{\alpha}}) + \cos(\theta_2 - \theta_3)(d_{23}^2 - r_2^2 z_a'^{\frac{2}{\alpha}} - r_3^2 z_i'^{\frac{2}{\alpha}})] - \\ & \sin(\theta_2 - \theta_3)\delta\} \ , \end{aligned} \tag{3.11}$$

where

$$\delta = \sqrt{2r_3^2 z_i'^{\frac{2}{\alpha}}(d_{23}^2 + r_2^2 z_a'^{\frac{2}{\alpha}}) - (d_{23}^2 - r_2^2 z_a'^{\frac{2}{\alpha}})^2 - r_3^4 z_i'^{\frac{4}{\alpha}}} \ . \tag{3.12}$$

With the values of r^+ and r^-, $R_{CT}^{(d)}$ can be calculated in the following two cases:

1. $max(r^+, r^-) \leq R$: In this case, referring to Fig. 3.2(a), the area of $R_{CT}^{(d)}$ can be expressed as

$$R_{CT}^{(d)} = \pi(d_{23} z_a'^{1/\alpha})^2 - A_1 - A_2 \ , \tag{3.13}$$

where

$$A_1 = (r_2 z_a'^{1/\alpha})^2(\pi - \theta') - R^2\theta + 2\Delta \ ; \tag{3.14}$$

$$A_2 = (r_2 z_a'^{1/\alpha})^2\phi - (r_3 z_i'^{1/\alpha})^2\phi' - 2\Delta' \ . \tag{3.15}$$

2. $max(r^+, r^-) > R$: As shown in Fig. 3.2(b), the area of $R_{CT}^{(d)}$ can be expressed as

$$R_{CT}^{(d)} = \pi(d_{23} z_a'^{1/\alpha})^2 - A_1 - A_2 + A_3 \ , \tag{3.16}$$

where

$$A_1 = (r_2 z_a'^{1/\alpha})^2(\pi - \theta') - R^2\theta + 2\Delta \ ; \tag{3.17}$$

$$A_2 = (r_2 z_a'^{1/\alpha})^2\phi - (r_3 z_i'^{1/\alpha})^2\phi' - 2\Delta' \ ; \tag{3.18}$$

$$\begin{aligned} A_3 \ = \ & \Delta'' + [(r_3 z_i'^{1/\alpha})^2\psi_2 - \frac{1}{2}(r_3 z_i'^{1/\alpha})^2 \sin\psi_2] + \\ & [(r_2 z_a'^{1/\alpha})^2\psi_3 - \frac{1}{2}(r_2 z_a'^{1/\alpha})^2 \sin\psi_3] - \\ & [R^2\psi_1 - \frac{1}{2}R^2 \sin\psi_1] \ . \end{aligned} \tag{3.19}$$

The detailed derivations of (3.13) and (3.16) and the definitions of the parameters θ, θ', ϕ, ϕ', ψ_1, ψ_2, ψ_3, Δ, Δ', and Δ'' are given in Appendices A.3 and A.4, respectively.

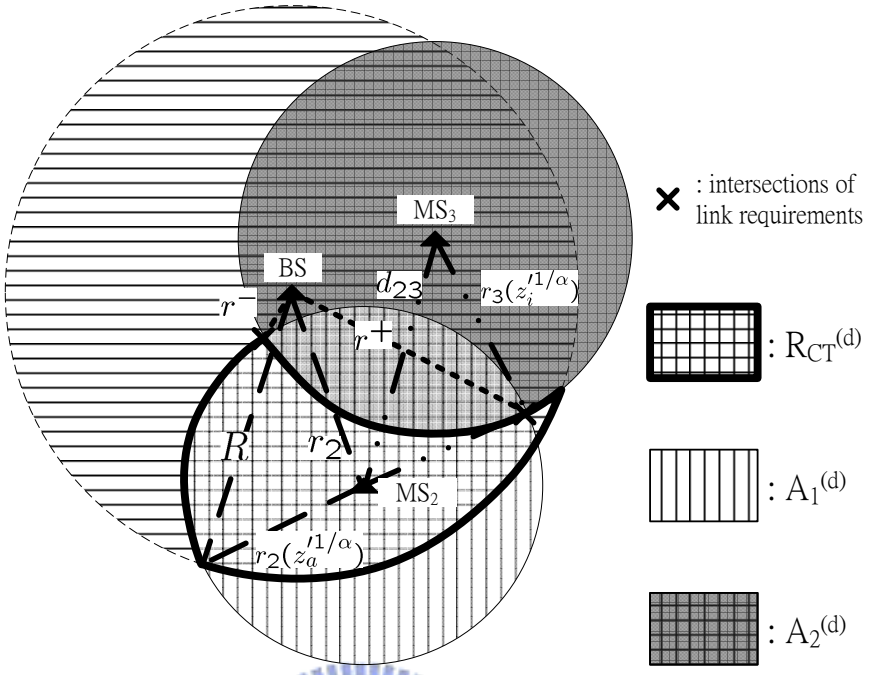

(a) The case when $max(r^+, r^-) \leq R$.

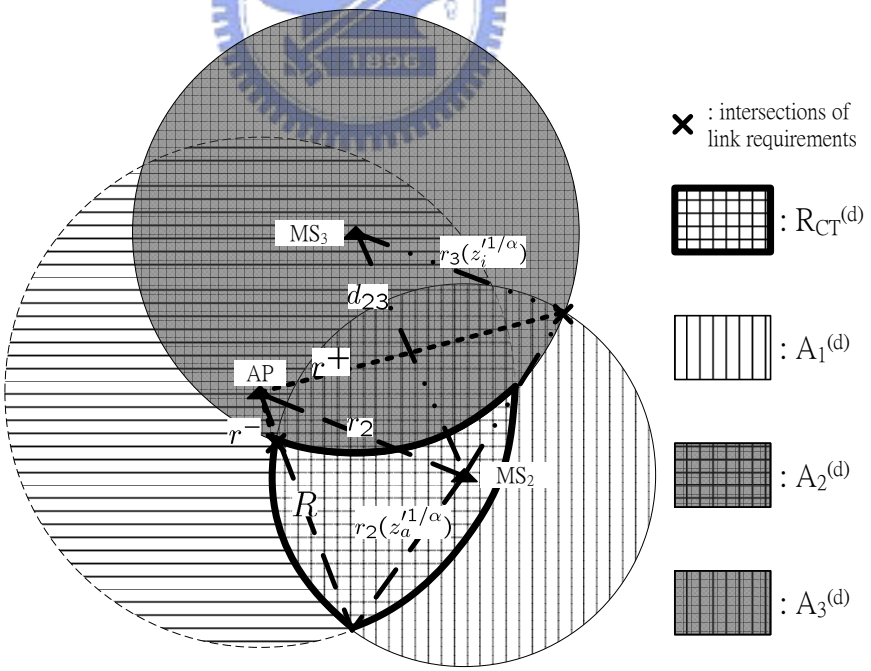

(b) The case when $max(r^+, r^-) > R$.

Fig. 3.2: The area of concurrent transmission region R_{CT} in downlink cases.

3.2.3 Multiple Ad Hoc Connections Coexisting with One Infrastructure Link

After evaluating the concurrent transmission probability of the infrastructure link and the one overlaying CR-based ad hoc link, one may be interested in knowing how many secondary users can concurrently establish ad hoc links together with the primary user. This question is non-trivial since it needs to consider the interference from a set of ad hoc links to the infrastructure link, and vice versa. Besides, different from the pure infrastructure network, both the locations of the transmitter and receiver in an ad hoc link are random.

Instead of calculating the maximum number of ad hoc links, we suggest constructive procedures enabling CR devices to establish ad hoc links in the presence of an infrastructure transmission. The detailed procedures are summarized as follows:

1. Consider a network in which all the primary and secondary users are fixed, and the CR device can learn the locations of its receiver and neighbors by the routing mechanism [11]. Here, we assume that l ad hoc links have been established and coexisted with the infrastructure link at the same time. Before establishing a new ad hoc connection, the CR device has to overhear the channel and memorizes the locations of all the existing transmitters.

2. With the location information, the new CR device starts evaluating the concurrent transmission region R_{CT}. The device should consider the interference from the infrastructure link as well as other existing ad hoc links, and vice versa. Denote the indices $\{p, m, n, k\}$ as the primary user, the transmitter and receiver of the new ad hoc link, and the transmitter of other existing ad hoc link, respectively. Using similar procedures in deriving (3.3), the three conditions in the infrastructure uplink case can be written by

$$r_m \geq \left(\frac{1}{\frac{1}{z_i}\left(\frac{1}{r_p}\right)^{\alpha} - \sum_k \left(\frac{1}{r_k}\right)^{\alpha}}\right)^{\frac{1}{\alpha}} ; \tag{3.20}$$

$$d_{mn} \leq \left(\frac{1}{z_a((\frac{1}{d_{pn}})^\alpha + \sum_k (\frac{1}{d_{kn}})^\alpha)}\right)^{\frac{1}{\alpha}} ; \tag{3.21}$$

$$r_m \leq R , \tag{3.22}$$

where r_i and d_{ij} are the distances between the base station and CR device j to i, respectively. Similarly, from (3.9), the three criteria in the downlink case are

$$d_{mp} \geq \left(\frac{1}{\frac{1}{z_i}(\frac{1}{r_p})^\alpha - \sum_k (\frac{1}{d_{kp}})^\alpha}\right)^{\frac{1}{\alpha}} ; \tag{3.23}$$

$$d_{mj} \leq \left(\frac{1}{z_a((\frac{1}{r_n})^\alpha + \sum_k (\frac{1}{d_{kn}})^\alpha)}\right)^{\frac{1}{\alpha}} ; \tag{3.24}$$

$$r_m \leq R . \tag{3.25}$$

3. Since the concurrent transmission regions $R_{CT}^{(u)}$ and $R_{CT}^{(d)}$ are known, the CR device can determine whether it can concurrently transmit data together with the infrastructure link and other ad hoc connections by the primary user and other secondary CR users.

3.3 Shadowing Effects

In the previous section, we only consider the impact of path loss on the concurrent transmission probability of CR-based network overlaying the infrastructure-based system. However, even though the CR device is located inside the concurrent transmission region R_{CT}, a peer-to-peer ad hoc connection may not be able to coexist together with the primary user's infrastructure link due to shadowing. Thus, it is important to investigate the reliability of concurrent transmissions of the hybrid infrastructure and CR-base ad hoc network when shadowing is taken into account.

Shadowing can be modeled by a log-normally distributed random variable [103]. Represent $10^{\frac{\xi_{ij}}{10}}$ as the shadowing component in the propagation path from users i to j, where ξ_{ij} is a Gaussian random variable with zero mean and standard deviation of σ_ξ. Thus, the uplink and downlink SIRs in both the infrastructure-based connection and CR-based ad hoc link are modified as:

- *uplink case:*

$$SIR_i^{(u)}(\xi_{30},\xi_{10}) = \frac{10^{\frac{\xi_{30}}{10}}/r_3^{\alpha}}{10^{\frac{\xi_{10}}{10}}/r_1^{\alpha}} \ ; \tag{3.26}$$

$$SIR_a^{(u)}(\xi_{12},\xi_{32}) = \frac{10^{\frac{\xi_{12}}{10}}/d_{12}^{\alpha}}{10^{\frac{\xi_{32}}{10}}/d_{23}^{\alpha}} \ ; \tag{3.27}$$

- *downlink case:*

$$SIR_i^{(d)}(\xi_{03},\xi_{13}) = \frac{10^{\frac{\xi_{03}}{10}}/r_3^{\alpha}}{10^{\frac{\xi_{13}}{10}}/d_{13}^{\alpha}} \ ; \tag{3.28}$$

$$SIR_a^{(d)}(\xi_{12},\xi_{02}) = \frac{10^{\frac{\xi_{12}}{10}}/d_{12}^{\alpha}}{10^{\frac{\xi_{02}}{10}}/r_2^{\alpha}} \ . \tag{3.29}$$

Note that the index 0 represents the base station and ξ_{30} of (3.27) in the uplink case is equivalent to ξ_{03} of (3.29) in the downlink case. Let $\boldsymbol{\xi} = (\xi_{10},\xi_{30},\xi_{12},\xi_{32})$ and $\boldsymbol{\xi'} = (\xi_{13},\xi_{03},\xi_{12},\xi_{02})$ and assume that these shadowing components are identical and independently distributed. Taking shadowing into account, the concurrent transmission probability P_{CT} can be represented by

- *uplink case:*

$$P_{CT}^{(u)}(\boldsymbol{\xi}) = P\{(r_3(z_i 10^{\frac{\xi_{10}-\xi_{30}}{10}})^{1/\alpha} < r_1 < R) \cap (d_{12} < d_{23}(z_a 10^{\frac{\xi_{12}-\xi_{32}}{10}})^{1/\alpha})\} \ ; \tag{3.30}$$

- *downlink case:*

$$\begin{aligned} P_{CT}^{(d)}(\boldsymbol{\xi'}) \ &= \ P\{(d_{13} > r_3(z_i 10^{\frac{\xi_{13}-\xi_{03}}{10}})^{1/\alpha}) \cap (d_{12} < r_2(z_a 10^{\frac{\xi_{12}-\xi_{02}}{10}})^{1/\alpha}) \\ &\quad \cap (r_1 < R)\} \ . \end{aligned} \tag{3.31}$$

We define the reliability of uplink concurrent transmission $F_{CT}^{(u)}(\xi)$ as the probability that, in the region R_{CT}, a CR device can successfully establish an ad hoc link in the presence of the primary user's uplink transmission subject to the shadowing effect. That is,

$$F_{CT}^{(u)}(\boldsymbol{\xi}) = P\{(SIR_i^{(u}(\xi_{30},\xi_{10}) > z_i) \cap (SIR_a^{(u)}(\xi_{12},\xi_{32}) > z) | MS_1 \in R_{CT}^{(u)}\} \ . \tag{3.32}$$

Note that $F_{CT}^{(u)}(\boldsymbol{\xi}) = 1$ when shadowing is not considered. Substituting (3.26) and (3.27) into (3.32), we can obtain

$$\begin{aligned} F_{CT}^{(u)}(\boldsymbol{\xi}) &= P\{(\xi_{30}-\xi_{10} > 10\log_{10}(z_i(\frac{r_3}{r_1})^{\alpha})) \cap (\xi_{12}-\xi_{32} > 10\log_{10}(z_a(\frac{d_{12}}{d_{23}})^{\alpha})) \\ &\quad |MS_1 \in R_{CT}^{(u)}\} \ . \end{aligned} \tag{3.33}$$

Assume that ξ_{ij} have the same standard deviation for all i and j and let $\xi_i^{(u)} = \xi_{30}-\xi_{10}$, $\xi_a^{(u)} = \xi_{12} - \xi_{32}$. Then, $\xi_i^{(u)}$ and $\xi_a^{(u)}$ becomes a Gaussian random variable with $\mathsf{N}(0, 2\sigma_\xi)$. Hence, it is followed that

$$\begin{aligned} F_{CT}^{(u)}(\boldsymbol{\xi}) &= P\{\xi_i^{(u)} \geq 10\log_{10}(z_i(\frac{r_3}{r_1})^{\alpha}) | MS_1 \in R_{CT}^{(u)}\} \cdot \\ &\quad P\{\xi_a^{(u)} \geq 10\log_{10}(z_a(\frac{d_{12}}{d_{23}})^{\alpha}) | MS_1 \in R_{CT}^{(u)}\} \\ &= Q(\frac{10\log_{10}(z_i(\frac{r_3}{r_1})^{\alpha})}{2\sqrt{2}\sigma}) \cdot Q(\frac{10\log_{10}(z_a(\frac{d_{12}}{d_{23}})^{\alpha})}{2\sqrt{2}\sigma}) \ , \end{aligned} \tag{3.34}$$

where $Q(x) = \frac{1}{\pi}\int_x^{\infty} \exp^{-x^2}\, dx$.

Following similar procedures in the uplink case, we can also obtain the reliability of downlink concurrent transmission:

$$\begin{aligned} F_{CT}^{(d)}(\boldsymbol{\xi'}) &= P\{(SIR_i^{(d)}(\xi_{03}, \xi_{13}) > z_i) \cap (SIR_a^{(d)}(\xi_{12}, \xi_{02}) > z) | MS_1 \in R_{CT}^{(d)}\} \\ &= Q(\frac{10\log_{10}(z_i(\frac{r_3}{d_{13}})^{\alpha})}{2\sqrt{2}\sigma}) \cdot Q(\frac{10\log_{10}(z_a(\frac{d_{12}}{r_2})^{\alpha})}{2\sqrt{2}\sigma}) \ . \end{aligned} \tag{3.35}$$

3.4 MAC Layer Throughput Analysis

In this section, the MAC layer throughput performance of the considered hybrid infrastructure and overlaying CR-based ad hoc network is evaluated from a PHY/MAC cross-layer perspective. The main task here is to incorporate the interference from both the infrastructure and ad hoc links into the throughput evaluation model in the MAC layer.

In this paper, the CSMA/CA MAC protocol with the binary exponential backoff algorithm is considered because it is widely deployed in many license-exempt frequency bands. However, the CSMA/CA MAC protocol may not be used to establish

the CR-based ad hoc link since the clear channel assessment (CCA) by measuring the received signal strength (RSS) may forbid the transmissions in the presence of infrastructure link. To remove this constraint, we use the location and channel station information to replace the RSS measurement for CCA in the traditional CSMA/CA MAC protocol. Therefore, the CR device can establish the ad hoc connection once the new connection does not injure the existing primary infrastructure link.

Next, we first summarize the throughput calculation in the traditional CSMA/CA MAC protocol [69, 104]. Assume N stations always transmit data packets in the network, and let W and 2^bW be the minimum and maximum backoff window sizes, respectively. Given the stationary transmission probability τ that a station transmits packet in a given slot and the successful transmission probability $p_s(N)$, the throughput $S(N)$ of the CSMA/CA MAC protocol can be expressed as

$$S(N) = \frac{p_{tr}p_s(N)\mathrm{E}[P]}{(1-p_{tr})\sigma + p_{tr}(1-p_s(N))T_c + p_{tr}p_s(N)T_c} , \tag{3.36}$$

where $p_{tr} = 1-(1-\tau)^N$; E[P], T_s, T_c, and σ are the average payload size, the average successful transmission duration, the average collision duration, and the slot duration. The stationary transmission probability τ is a function of the packet loss probability p_L, that is

$$\tau(p_L) = \frac{2}{1+W+p_LW\sum_{i=0}^{b-1}(2p_L)^i} . \tag{3.37}$$

Note that both the packet loss probability p_L and the successful transmission probability $p_s(N)$ are influenced by the radio channel effect and the multiuser capture effect in the physical layer [104].

Then, we evaluate the total throughput performance of the concurrent transmission in the hybrid infrastructure and overlaying CR-based ad hoc network. Here, we assume N_{CR} CR devices and N non-CR devices using the same frequency band in the coverage of a base station. Since the CR device can establish an ad hoc connection without interfering the existing infrastructure link, the total throughput of such a

hybrid network S_{CT} is independently contributed by the two links. The throughput of the infrastructure link and the CR-based ad hoc connection are denoted by S_i and S_a, respectively. The total throughput S_{CT} then can be expressed as

$$S_{CT} = S_i(N) + S_a(N_{CR}P_{CT}) \ . \tag{3.38}$$

Since N non-CR devices contend for data transmission to the base station, the throughput of infrastructure-based link S_i is the same as (3.36). However, because only $N_{CR}P_{CT}$ CR devices have the opportunity to establish the connection, the throughput of a CR-based ad hoc link S_a is similar to S_i, but the number of contending stations changes to $N_{CR}P_{CT}$.

3.5 Numerical Results

In this section, we first investigate the concurrent transmission probability of the infrastructure and overlaying CR-based ad hoc network. Then we apply the proposed cross-layer analytical model to evaluate the total throughput performance in this hybrid network. Figure 2.2 illustrates the considered network topology, where MS_1, MS_2 and MS_3 are the CR-based ad hoc transmitter, receiver and infrastructure primary user, respectively. The stations MS_2 and MS_3 are, respectively, located at $(r_2, -\frac{\pi}{2})$ and $(r_3, \frac{\pi}{2})$, where r_2 and r_3 are the distances between the base station to MS_2 and MS_3; whereas MS_1 is uniformly distributed in the cell with radius $R = 100$ meters. In addition, we also perform the simulation to verify the proposed analytical model for the concurrent transmission probability P_{CT}. In the simulation, 10^4 points, which are uniformly distributed in the region πR^2, represent the possible locations of the ad hoc transmitter MS_1. The probability P_{CT} is calculated by counting the number of points where MS_1 can successfully establish an ad hoc link to MS_2 in the presence of the infrastructure link (base station to MS_3). As shown in the following figures, the results in the analytical model agrees well with that in the simulation. The other system parameters are listed in Table I.

Tab. 3.1: System Parameters for Concurrent Transmission in an Overlaying Ad Hoc Cognitive Radio Network

MAC/PHY header	224/192 bits
ACK/RTS/CTS	304/352/304 bits
DATA payload	16000 bits
Bit rate	1 Mbps
Slot time	20μs
SIFS/DIFS	10/50μs
Min contention window	32
Maximum backoff stage	5
Transmission power, P_t	20 dBm
Noise power, N_0	-90 dBm

3.5.1 Uplink Concurrent Transmission Probability

Figure 3.3 shows the impact of the primary user's location on the uplink concurrent transmission probability $P_{CT}^{(u)}$, where the transmission power $P_t = 20$ dBm and noise power $N_0 = -90$ dBm, respectively; the required link SIR threshold is 0 dB or 3 dB. First, one can see that the analytical results match the simulation results well. Second and more importantly, there exists an optimal concurrent transmission probability $P_{CT}^{(u)}$ against the distance r_3 from the primary user MS_3 to the base station. Note that for $z_i = 0$ dB, the maximal $P_{CT}^{(u)} = 0.45$ at $r_3 = 40$ meters; and for $z_i = 3$ dB the maximal $P_{CT}^{(u)} = 0.22$ at $r_3 = 26$ meters. This phenomenon can be explained as follows. On the one hand, when MS_3 approaches to the base station, it is also closer to the CR-based ad hoc receiver, thereby causing higher interference and decreasing the concurrent transmission probability. On the other hand, when MS_3 moves away from the base station, its uplink SIR decreases due to the weaker signal strength and thus yields a lower $P_{CT}^{(u)}$. Hence, an optimal primary user's location can be found in the sense of maximizing the uplink concurrent transmission probability $P_{CT}^{(u)}$.

Figure 3.4 shows the impact of MS_2's locations on the uplink concurrent transmission probability $P_{CT}^{(u)}$. As shown in the figure, as the CR-based ad hoc user moves away from the base station, the concurrent transmission probability monotonically increases from 10% to 50% because the interference from the infrastructure-based link to the ad hoc connection decreases.

3.5.2 Downlink Concurrent Transmission Probability

Figure 3.5 shows the downlink concurrent transmission probability $P_{CT}^{(d)}$ versus the distance r_3 of the primary user MS_3 to the base station when user MS_2 is located at $(50, -\frac{\pi}{2})$. For the SIR requirement $z_i = z_a = 0$ dB, $P_{CT}^{(d)} = 25\%$ is a constant in the range of $r_3 \leq 100$ meters. This is because the interference transmitted from the base station to the ad hoc users is independent of the locations of the primary user,

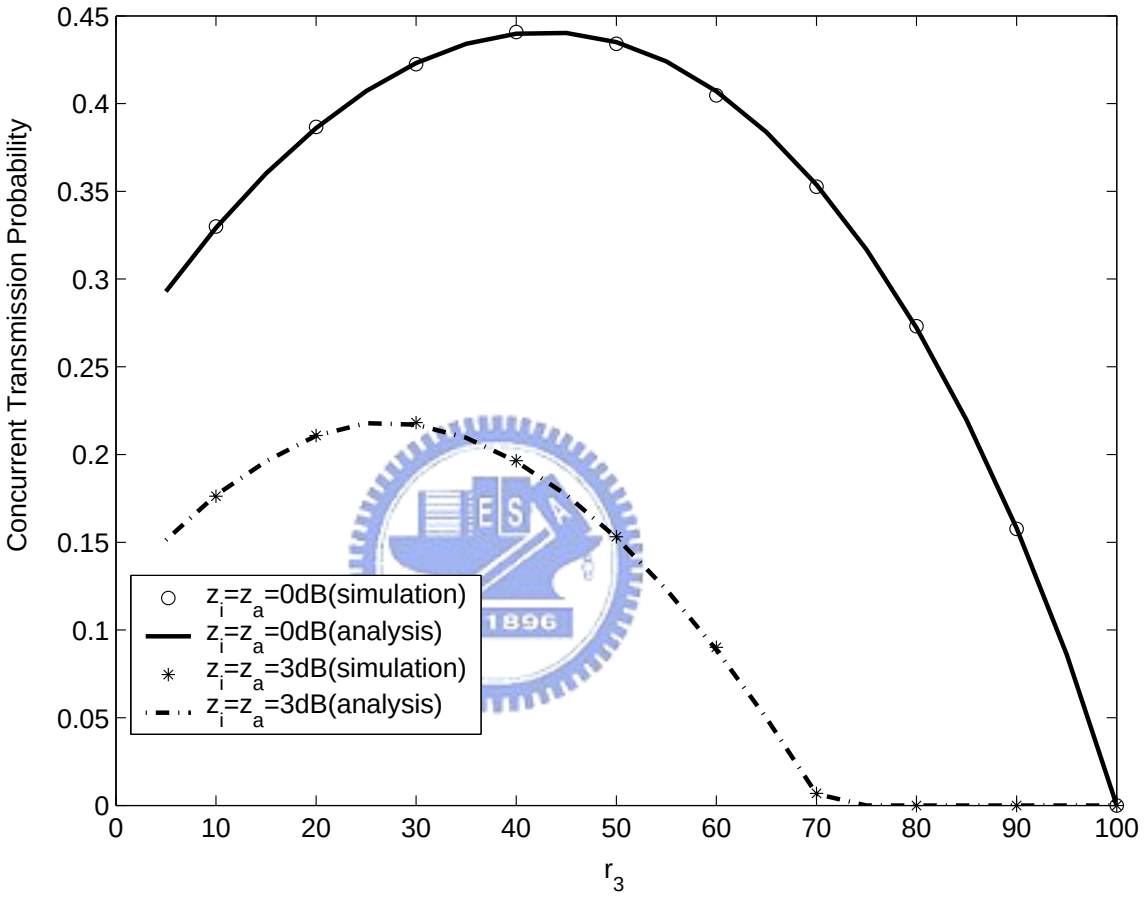

Fig. 3.3: The concurrent transmission probability $P_{CT}^{(u)}$ versus the infrastructure uplink user's locations as the ad hoc receiver MS_2 is located at $(50, -\frac{\pi}{2})$, where r_3 is the distance between the base station and the primary user MS_3.

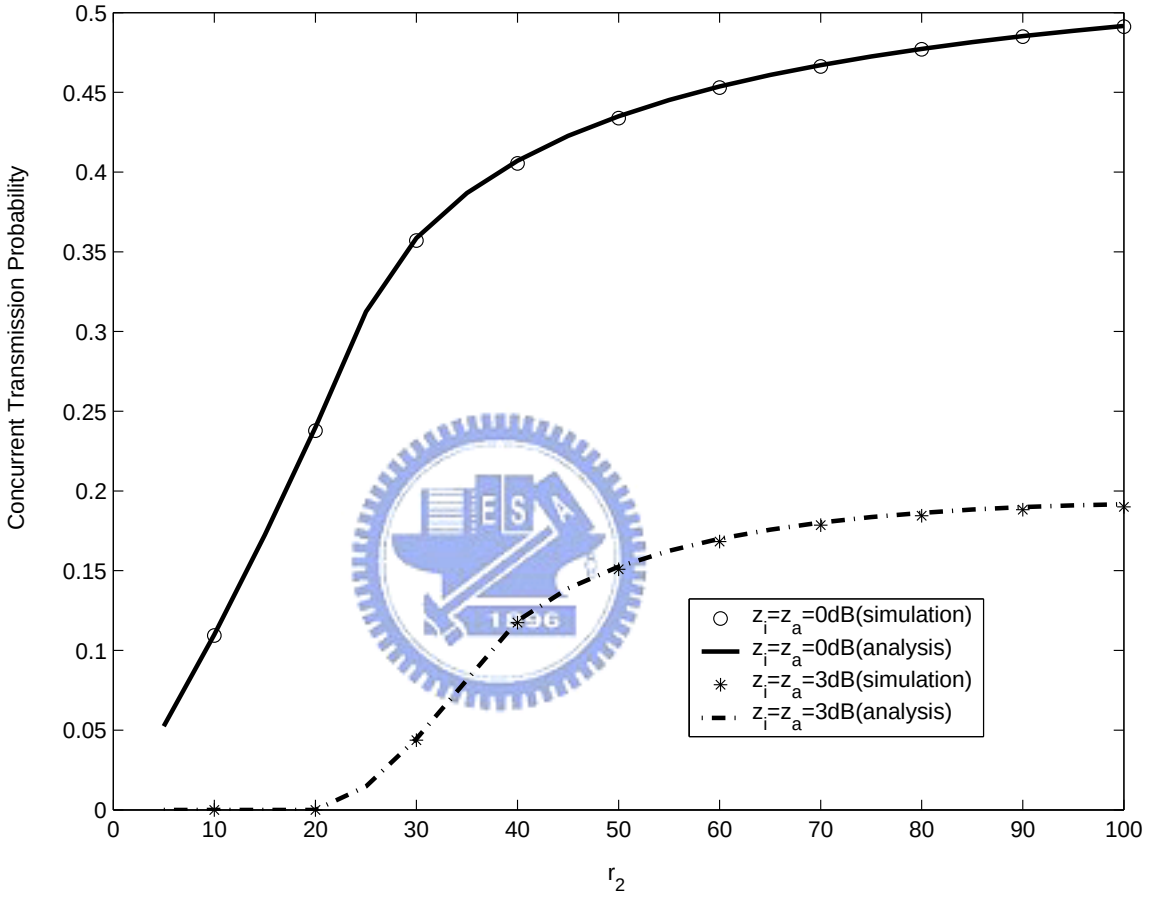

Fig. 3.4: The concurrent transmission probability $P_{CT}^{(d)}$ versus the CR-based ad hoc receiver's location as the infrastructure uplink user MS_3 is located at $(50, \frac{\pi}{2})$, where r_2 is the distance between the base station and ad hoc link receiver MS_2.

MS_3. However, a more stringent SIR requirement $z_i = z_a = 3$ dB yields a lower and decreasing downlink concurrent transmission probability when r_3 increases.

Figure 3.6 shows the impact of CR user MS_2's locations on the downlink concurrent transmission probability. Similar to Fig. 3.4, $P_{CT}^{(d)}$ also monotonically increases when CR user MS_2 moves away from the base station. However, comparing Figs. 3.4 and 3.6, the uplink's concurrent transmission probability is higher than that of the downlink's. For $z_i = z_a = 0$ dB and $r_2 = 100$ meters, $P_{CT}^{(u)} = 49\%$ and $P_{CT}^{(d)} = 39\%$, respectively. This is because in the considered scenario the interference to the ad hoc user from the infrastructure-based uplink transmission is weaker than that from the downlink transmission.

3.5.3 Effects of Shadowing on the Concurrent Transmission

Figures 3.7(a) and (b) illustrate the reliability of the concurrent transmissions with various shadowing standard deviations versus r_3 and r_2, respectively. In general, comparing $\sigma_\xi = 6$ dB and $\sigma_\xi = 1$ dB, one can find that the larger shadowing variance leads to a lower reliability for both uplink and downlink concurrent transmissions. For example, in Fig. 3.7(a), when the primary user's distance to the base station r_3 in the range of $0 \sim 100$ meters, $F_{CT}^{(d)}$ is larger than 0.9 for $\sigma_\xi = 1$ dB, whereas it decreases to $0.6 \sim 0.7$ for $\sigma_\xi = 6$ dB. However, when the primary user moves to the cell edge, the reliability of uplink and downlink concurrent transmissions decreases due to shadowing and weaker received signal strength. As shown in Fig. 3.7(a), for $\sigma_\xi = 6$ dB, $F_{CT}^{(d)}$ and $F_{CT}^{(u)}$ decrease from 0.7 to 0.5 and 0.4, respectively. Since the uplink signal strength is weaker than the downlink signal, the reliability of uplink concurrent transmission is usually more sensitive to shadowing effects than downlink concurrent transmission, especially when the primary user is at the cell edge. In Fig. 3.7(b), it is shown that, subject to the influence of shadowing, the reliability of uplink and downlink concurrent transmissions increases when the receiver MS_2 of the ad hoc link approaches to the cell edge. For $\sigma_\xi = 1$ dB, $F_{CT}^{(u)}$ and $F_{CT}^{(d)}$ increase from 0.4 and

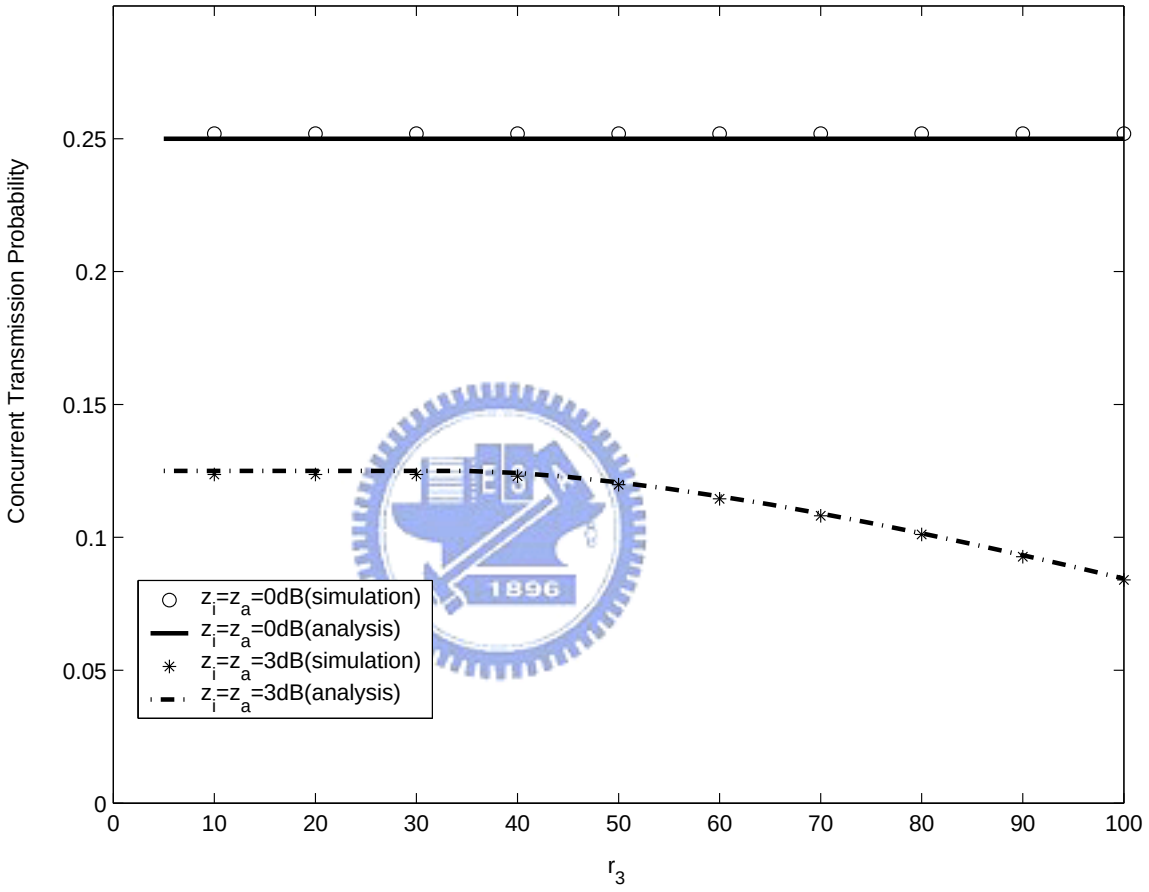

Fig. 3.5: Impact of primary user MS_3's location on the downlink concurrent transmission probability $P_{CT}^{(d)}$ as the ad hoc receiver MS_2 is located at $(50, -\frac{\pi}{2})$.

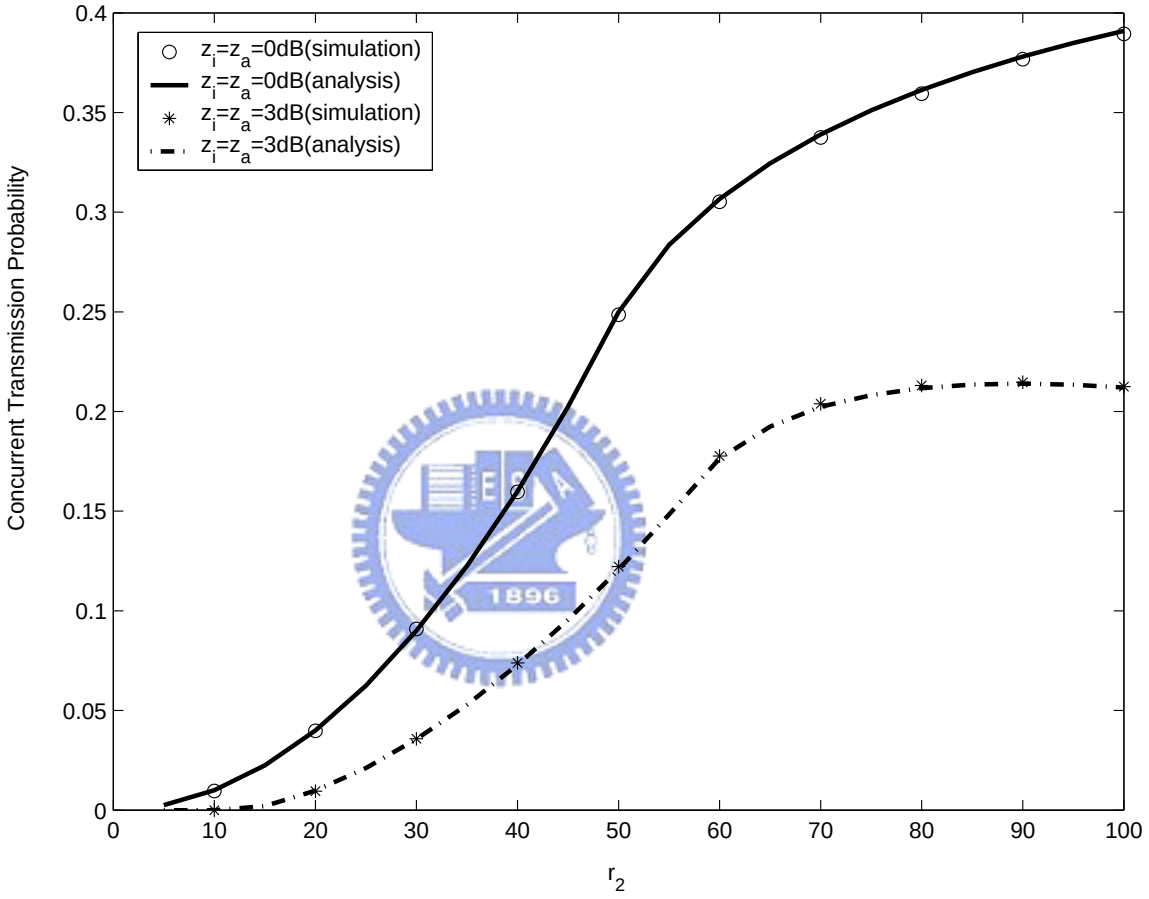

Fig. 3.6: Impact of CR-based ad hoc receiver MS_2's location on the concurrent transmission probability $P_{CT}^{(d)}$ as the infrastructure downlink user MS_3 is located at $(50, \frac{\pi}{2})$.

0.63 to 0.89 and 0.92 as r_2 increases to 100 meters; for $\sigma_\xi = 6$ dB $F_{CT}^{(u)}$ and $F_{CT}^{(d)}$ also increase from 0.29 and 0.4 to 0.54 and 0.62. Clearly, the interference from the primary user to the ad hoc user becomes weaker when ad hoc users moves away from the base station. As a result, the reliability of concurrent transmission increases and the shadowing effect on the reliability remains constant as $r_2 > 30$ meters for $\sigma_\xi = 1$ dB and $r_2 > 60$ meters for $\sigma_\xi = 6$ dB.

3.5.4 Total Throughput of Cognitive Ad Hoc Networks Overlaying Infrastructure-based System With Concurrent Transmission

Figure 3.8 demonstrates the total throughput of the CR-based ad hoc link and the infrastructure-based uplink transmissions for various numbers of ad hoc users and different locations of primary users. The total throughput is normalized to the infrastructure-based uplink capacity. As shown in the figure, in the worst case at $r_3 = 50$ meters the total throughput with the concurrent transmission is still 145% higher than the pure infrastructure-based uplink, and the total throughput reaches a maximum of 173% at $r_3 = 10$ meters.

Figure 3.9 shows the total throughput performance of the concurrent transmission of infrastructure-based downlink and ad hoc link. In this case, the concurrent transmission probability is constant for various locations of primary users as shown in Fig. 3.5. Thus the throughput is mainly affected by the number of ad hoc users. For $N_{CR} = 50$, the total throughput is 157% when $10 < r_3 < 100$ meters. However, when $r_3 = 50$ meters, the total throughput improves from 148% to 173% as N_{CR} is changed from 100 to 10.

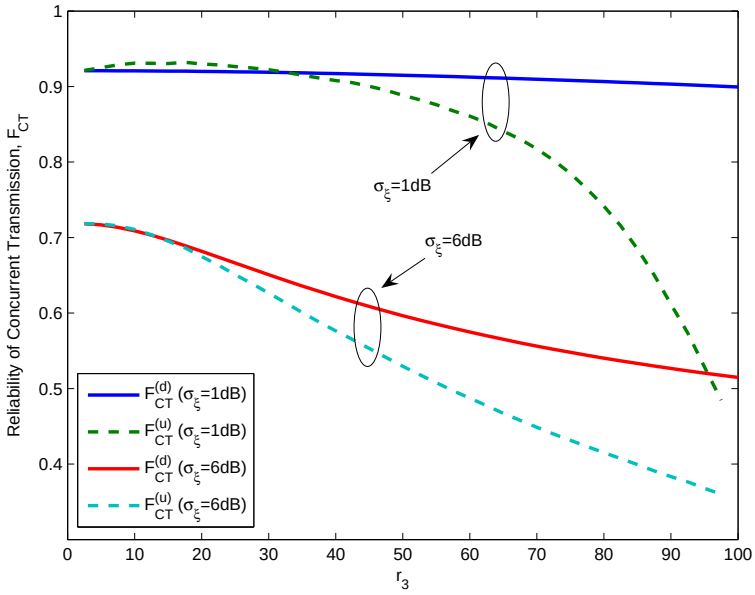

(a)

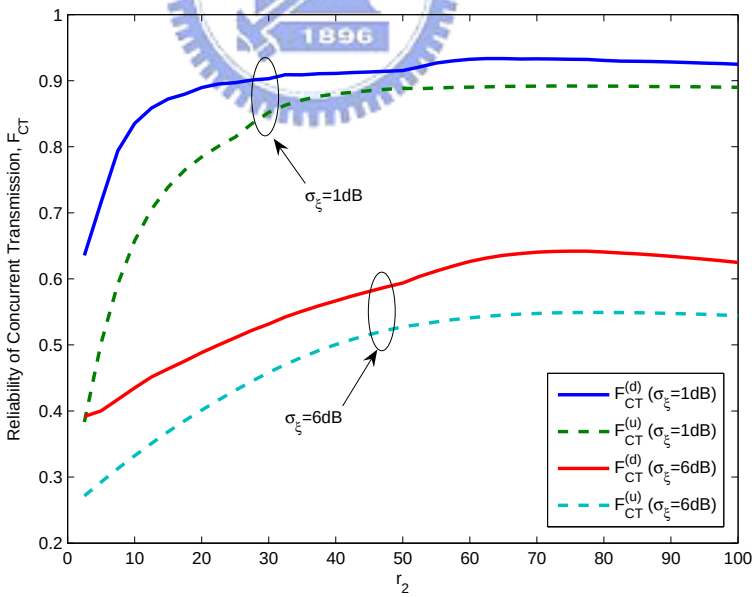

(b)

Fig. 3.7: Impacts of shadowing on the reliability of downlink $F_{CT}^{(d)}$ (solid line) and uplink $F_{CT}^{(u)}$ (dotted line) concurrent transmission against the locations of (a) the primary user MS_3 and (b) the ad hoc user MS_2 in the cases of $\sigma_\xi = 1$ and 6 dB, respectively.

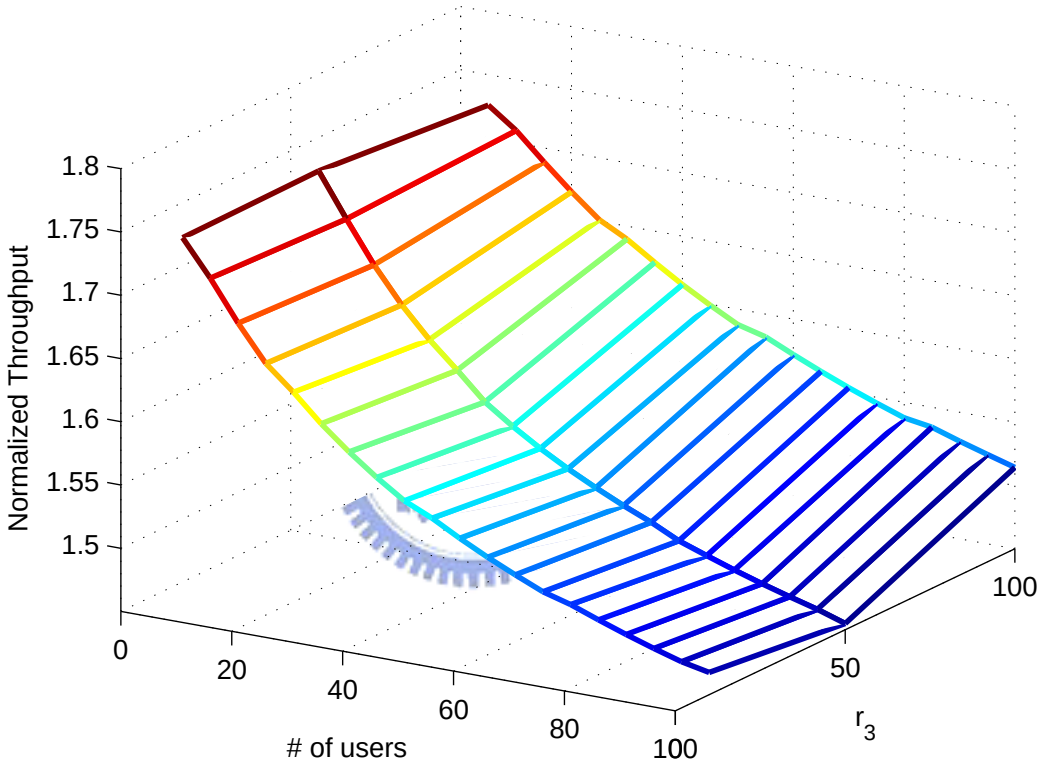

Fig. 3.8: Total throughput performance of the uplink concurrent transmission.

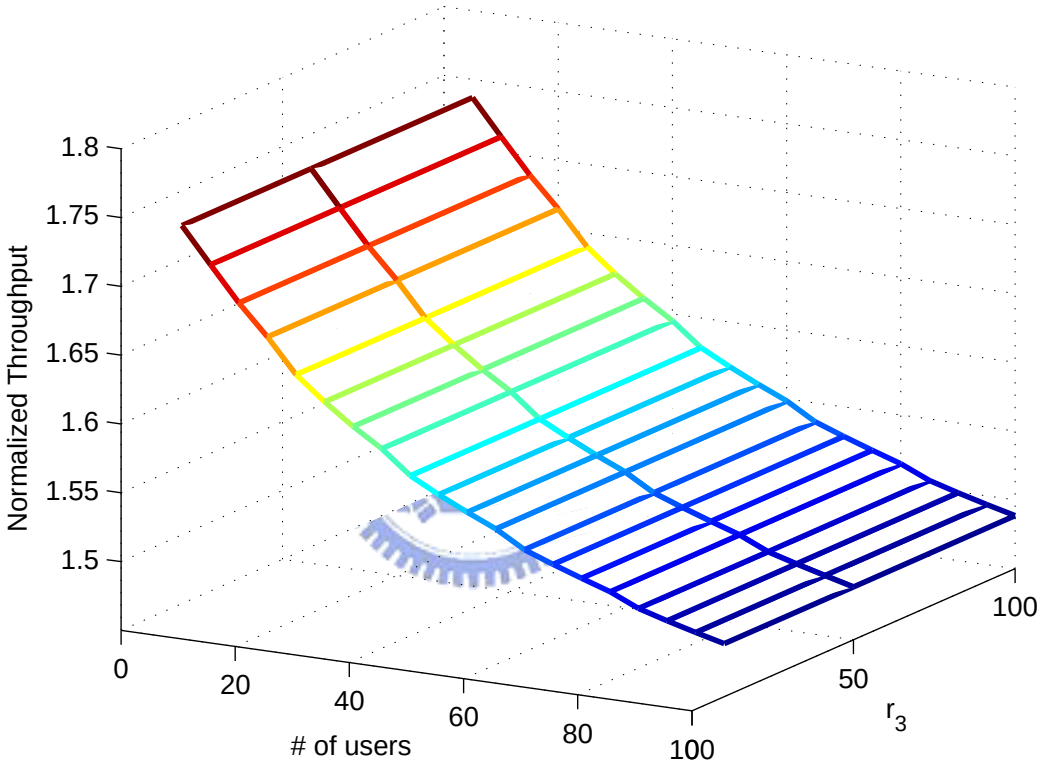

Fig. 3.9: Total throughput performance of the downlink concurrent transmission.

3.6 Conclusions

In this part, we identified a critical region R_{CT} in which the overlaying cognitive ad hoc users and the primary user can concurrently transmit data without causing interference to each other. If the location information of other nodes is available, such a concurrent transmission region can be easily identified. There are two major advantages of identifying the concurrent transmission opportunity. First, the overall throughput of the concurrently transmitted data obtained by combining both the overlaying cognitive ad hoc networks and the legacy infrastructure-based system is much higher than that of the pure infrastructure-based system. Our numerical results show that, in the uplink case, the concurrent transmission region subject to 1 dB and 6 dB shadowing standard deviation can be up to 45% out of the entire cell area with about 90% and 60% reliability, respectively. Second, if such a concurrent transmission opportunity can be identified first, it is clear that the need of the time- and energy-consuming wide-band spectrum scanning process required by most existing cognitive radio systems can be reduced dramatically.

Chapter 4

Neighbor-aware Cognitive Spectrum Access with QoS Provisioning

In this chapter, we focus on the cognitive MAC protocol design, which is different to the conventional scheme with two objectives: the avoidance of primary user's transmissions and short access delay. In additional to the objectives of high spectrum utilization and QoS provisioning in traditional networks, the cognitive MAC protocol for CR devices has to determine whether its transmission will interfere the primary user at the current and future time period. Moreover, the CR device also demands to access the channel only in a short period of time because primary users have the highest priority to access the channel. Due to the short available transmission time, the fairness from the aspect of access delay among users is more important than the amount of delivered bit for the cognitive MAC protocol, which is also different from the requirement in the legacy MAC design.

4.1 Motivation

According to [7, 8, 13], the main functionality of a cognitive MAC protocol, as shown in Fig. 1.1, can be summarized as follows:

- ***observe*** stage - to sense the surrounding environment and record the spectrum usage of the existing legacy systems;
- ***plan*** stage - to evaluate if a temporary ad hoc link can be established without interfering current users;
- ***decide*** stage - to determine the transmit power, frequency, the time and the duration of the frame transmission;

- ***act*** stage - to perform transmission with specified resources at the scheduled time.

To achieve the aforementioned objectives, we design an enhanced CSMA/CA MAC protocol for the spectrum access of secondary users. The CSMA/CA MAC protocol has the preliminary function of spectrum avoidance to the primary users. To start with, we examine the CSMA/CA MAC protocol by referring the four stages of the cognition cycle in Fig. 1.1. First, from the viewpoint of the ***observe*** stage, the cognitive MAC protocol is required to record the spectrum usage of primary users and to collect the traffic characteristics, such as the delay-sensitive or non-real-time data traffic. For the CSMA/CA MAC protocol, most recent research results, instead of identifying the interference, focus on either sensing the carrier transmission in the surrounding environment or avoiding collisions [105–107]. Thus, the functions of recording the spectrum usage and traffic characteristics are not fully considered in the current CSMA/CA MAC protocols.

Second, in the ***plan*** stage of the cognition cycle, the cognitive MAC protocol shall determine whether the requested frame transmission from the secondary user will interfere the primary user's connection. Because the cognitive MAC protocol only permits the secondary user to utilize the spectrum of the legacy system during the spare time of the primary user's transmissions, the access delay in the cognitive MAC protocol for secondary users shall be small. The standard deviation of the access delay in a cognitive MAC should be reduced to make all the secondary users have the equal opportunities of accessing the channel. However, the fairness problem in terms of equal access delay is not emphasized in many modified CSMA/CA MAC protocols [108–111]. Furthermore, a cognitive MAC protocol shall differentiate the priority for various traffic types with QoS provisioning. Although the authors in [107, 112–115] suggested adjusting the transmission probability with different contention window (CW) sizes and different lengths of black bursts to differentiate the traffic types, the issue of avoiding interference to the legacy system was not fully considered yet.

Third, in the ***decide*** stage, the cognitive MAC protocol schedules frame transmissions for secondary users to satisfy the QoS requirement, especially for delay-sensitive traffic. In previous works, some researchers suggested to reserve time slots prior to delay-sensitive frame transmissions [116–121]. However, such reservation methods require a polling process or additional handshaking procedure to coordinate frame transmissions. These methods consume battery energy and waste the valuable bandwidth in sending management frames. Thus, how to design a *distributed* mechanism to reserve the transmissions for high priority frames becomes an issue.

At last, in the ***act*** stage of the cognition cycle, the cognitive MAC protocol synchronizes stations and execute the transmission at the specified time. To synchronize the clock of each station, the methods designating a centralized controller to broadcast "*beacon*" signals or utilizing the global clock provided by Global Positioning System (GPS) were suggested in [12, 120, 121]. However, both methods require additional devices.

Here, we propose such a generic cognitive MAC protocol in overlaying ad hoc networks with emphases on achieving the aforementioned objectives: high spectrum utilization, QoS satisfactory and short access delay. Specifically, in the ***observe*** stage, we propose a mechanism of establishing the neighbor list to help stations to recognize the spectrum opportunities. In the ***plan*** stage, an improved contention resolution mechanism, consisting of the gating mechanism, linear backoff algorithm and stall avoidance scheme, is suggested to enhance the performance of throughput, access delay and fairness from the aspect of short access delay for CR devices. In the ***decide*** stage, a novel invited reservation procedure is developed to ensure a secondary user with QoS provisioning. At last, in the ***act*** stage, a distributed frame synchronization mechanism is proposed to coordinate frame transmissions among secondary users without a centralized controller.

4.2 Neighbor List Establishment in *Observe* Stage

To have the knowledge of the spectrum usage by the existing legacy system, we suggest a neighbor list establishment mechanism to record frame transmissions from primary and secondary users in the ***observe*** stage of the cognition cycle. Here, we assume the cognitive MAC protocol can cooperate with other spectrum sensing, identification, and allocation mechanisms to obtain the spectrum usage of primary users. Then, we partition the observed frames into three categories and respectively store the necessitated information into: Primary user information table (PIT), Reservation Information Table (RIT) and Contention Information Table (CIT). The functions of each table are described as follows.

- Primary user Information Table (PIT) stores the spectrum usage of primary users, including:
  - the address of the PU;
  - the repetition period of the PU's transmission;
  - the frame length of the PU's transmission.

  The PIT records the transmission time of the PU to avoid interfering the existing legacy system. Recall that the PU is assumed to periodically transmit packets using the TDMA MAC protocol. The secondary user can avoid interfering the primary user transmission by acquiring the period and frame length. On the other hand, the neighbor list establishment can incorporate with advance traffic models to estimate the information of PU's transmissions [23, 36]. With the knowledge of PU's transmissions, the secondary user can determine whether its transmission will cause the interference.

- Reservation Information Table (RIT) saves the reservation information of delay-sensitive traffic flows for secondary users including:

  - the source address of the delay-sensitive traffic flow;
  - the sequence number of the delay-sensitive traffic flow.
  - the next packet length in the delay-sensitive traffic flow;

  The RIT collects the reservation information in the MAC header of the delay-sensitive data and its corresponding ACK frames for secondary users. The header in the proposed MAC protocol is similar to that in IEEE 802.11 WLAN [12], except for the duration field in the MAC header for delay-sensitive data and its ACK frames. In our proposed cognitive MAC protocol, the duration field represents the length of the next delay-sensitive frame in the flow instead of the length of the current frame as in the IEEE 802.11 WLAN. This duration field will be set to zero if the delay-sensitive traffic flow has no remaining packets. By overhearing the MAC header of frame transmissions in all the reserved flows, CR devices can update its RIT and remove the canceled flow from the list. In addition, the RIT can also use the received order of the observed information for the sequence of reserved flow transmissions. The transmission sequence and frame length incorporating with the newly proposed distributed frame synchronization mechanism help secondary users to recognize the time whether it can transmit packet without interfering to the transmission of PUs and reserved frames, which will be detailed in Section 4.5.

- Contention Information Table (CIT) records the properties of non-real-time traffic including:

  - the source address of the non-real-time data traffic flow.
  - the transmission time of the observed frame;
  - the number of non-real-time data traffic flows;

  The CIT provides the information with the number of non-real-time traffic flows,

which will be used to reduce the collisions and improve the channel throughput in the ***act*** stage of the cognition cycle.

To correctly establish PIT, RIT and CIT, a CR user is designed to observe the status of frame transmissions around its neighborhood for an observe period T_{obv} before any frame transmission. The duration of T_{obv} must be longer than the period of the legacy system to ensure the secondary user has the knowledge of the periodic frame transmissions for primary users. Furthermore, T_{obv} shall also be longer than the maximum repetition period between two successive delay-sensitive frames to prevent unnecessary real-time traffic flow establishment. The optimal value for T_{obv} can be obtained through heuristic search but beyond the scope of this paper.

Another interesting point is that the continuous table update is inefficient in terms of energy consumption. For this issue, the proposed MAC protocol can incorporate with some well-known power management, e.g. power saving mode in IEEE 802.11 [12]. The node without packet transmissions can enter the sleeping mode, in which the station turns off all the unnecessary functions. The node will sleep over a fixed period of time and wake up to check whether other nodes have packets to itself. An extra transmission window, like ATIM window in IEEE 802.11, is preserved after all reserved frame transmissions to indicate the packet transmission in the later future. The station having packets to the sleeping node sends the indicative message in this window; otherwise, the sleeping node returns to the sleep mode until the next ATIM window or the time it has packet to send.

4.3 Contention Resolution in *Plan* Stage

In the ***plan*** stage of the cognition cycle, the cognitive MAC protocol has two major functions. One is to prevent CR users from interfering the legacy system, and the other is to make them efficiently and effectively access the unused spectrum in a short available transmission time. To this end, we suggest three improved approaches as

follows:

1. gating mechanism - to forbid the transmissions that may interfere to primary users or collide with other CR users;

2. linear backoff algorithm - to expedite the link establishment of delay-sensitive traffic flows;

3. stall avoidance scheme - to speed up the transmission of stalled non-real-time data packets.

The three above mechanisms help to achieve the objectives of high throughput, low access delay, and fairness for secondary users.

4.3.1 Gating Mechanism

The gating mechanism is used to avoid interfering the primary user of the legacy system and to reduce the collision among CR users. The basic idea is cooperating the spectrum usage information obtained from the spectrum sensing, identification and allocation techniques to prevent from interfering the primary users. Recall that the PIT stores the information of primary user transmissions. The gating mechanism postpones the secondary user transmitting packets when the primary user appears on the channel. In addition, we also suggest the modified p-persistent CSMA algorithm to improve the efficiency of spectrum usage for CR users, where the optimal value of p can be computed according to the number of *nrt-nodes* in CIT [69].

The detailed procedure of the proposed gating mechanism is described as follows:

1. When a frame of a CR user is requested for transmission, the gating mechanism first checks whether a legacy user occupies the channel from the information in PIT.

    - If so, the transmission of this CR user is deferred.

- Otherwise, the optimal transmission probability p is calculated based on the neighborhood information in CIT.

2. Apply the p-persistent algorithm to determine whether the frame can be transmitted:

   - If the frame is granted for transmission, the CR user immediately sends the frame.
   - Otherwise, the frame will be deferred and again contend for the channel access.

According to the proposed procedure, one may argue that it still cause the interference with the legacy system using the CSMA/CA MAC protocol by suppressing the bandwidth. However, most existing systems using the CSMA/CA MAC are operated on unlicensed frequency bands. Both legacy and CR devices have the equal right to access these frequency bands, and thus we believe that the bandwidth suppression is not an issue for secondary users.

4.3.2 Linear Backoff Algorithm

To expedite the channel access in supporting delay-sensitive application, we suggest that the link establishment of delay-sensitive traffic flows shall follow the linear backoff algorithm instead of increasing the CW size exponentially as in the legacy CSMA/CA MAC protocol. That is, if the request for sending the first frame of a delay-sensitive traffic flow is collided, the CW size (CW_{rt}) for that particular frame increases according to the following principle:

$$CW_{rt} = \min(CW_{max}, CW_{min} \times (N_{req} - 1)), \tag{4.1}$$

where N_{req} is the number of attempts for sending the frame; CW_{max} and CW_{min} are the maximum and minimum CW sizes in the contention resolution mechanism, respectively.

Figure 4.1 shows the CW sizes for the linear and binary exponential backoff algorithms. As shown in the figure, the CW size in the linear backoff algorithm increases less slowly than that in the binary exponential backoff algorithm. Therefore, the channel access of the first frame in a delay-sensitive traffic flow can be faster than that of the non-real-time data flows. As long as the delay-sensitive traffic flow is successfully established, the remaining frames are sent in the reserved time slot according to the proposed invited reservation procedure (which will be discussed in Section 4.4). Based on our design, because only the first frame contends for accessing the channel, the number of attempts of establishing a delay-sensitive traffic flow is much fewer than that of non-real-time traffic flows. Thus, the proposed MAC protocol can avoid the collisions issue of the linear backoff algorithm, while reducing the access delay in the link establishment of delay-sensitive traffic flows.

4.3.3 Stall Avoidance Scheme

In order to improve the fairness for the CR users, we develop a stall avoidance scheme aiming to reduce the transmission delay of the *nrt-nodes* with excessive buffered frames. The specific goal of the suggested approach is to minimize the variance of the access delay among all the *nrt-nodes*. Due to the short available transmission time of the spectrum in an overlaying cognitive ad hoc network, the small variance of the access delay makes CR users have equal opportunities to access the channel. Here, the access delay includes the waiting time in the queue and the channel access time. Therefore, obviously, reducing the variance of access delay implies to speed up the back-logged frame transmission.

The suggested stall avoidance scheme with respect to *nrt-nodes* is described as follows. Select a pre-determined threshold Q_{th} for the maximum allowable buffered data frames and the guaranteed CW size for the stalled *nrt-nodes* CW_{stall}, where

$$CW_{stall} < CW_{min}. \tag{4.2}$$

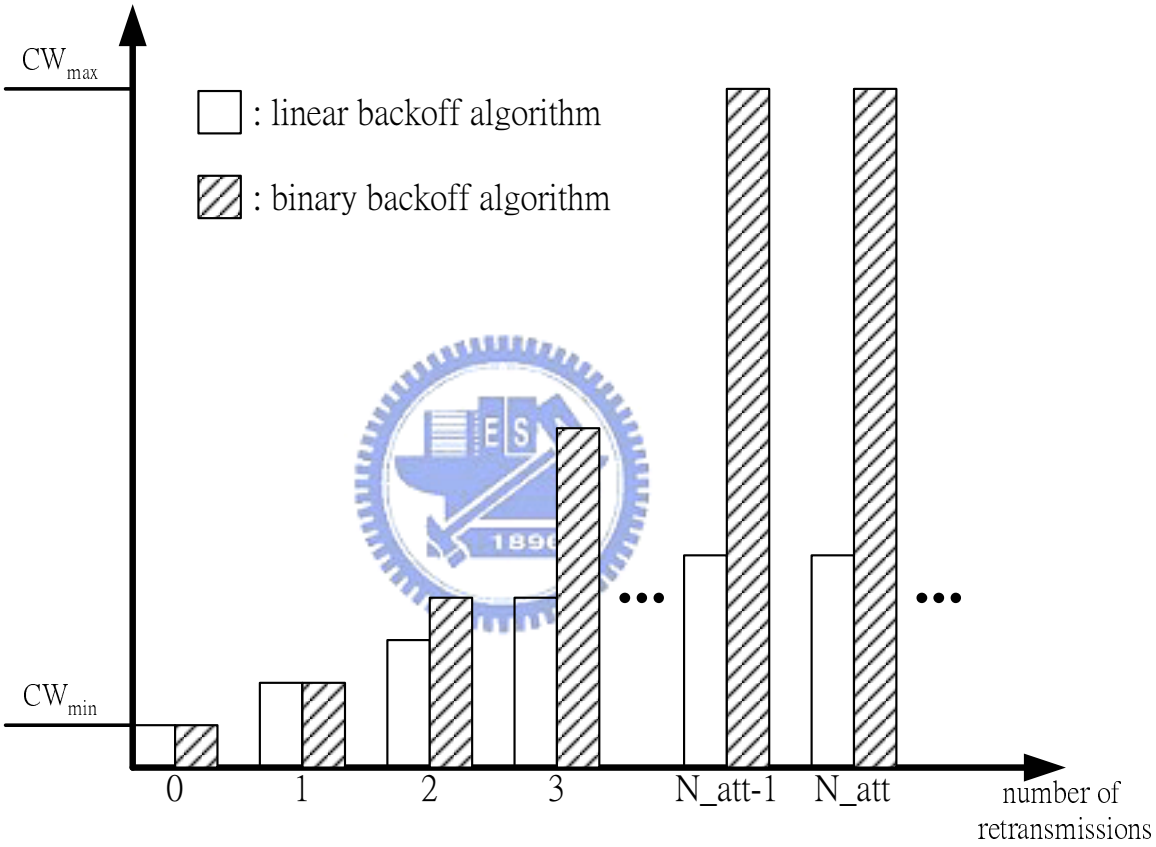

Fig. 4.1: Comparison of CW size between linear and binary exponential backoff algorithms.

If the number of buffered frames in an *nrt-node* is more than Q_{th}, the CW size of the subsequent frames in the queue is reduced to CW_{stall}. Because a smaller CW size leads to a higher transmission probability, the lagging frames in a stalled *nrt-node* with CW_{stall} can be transmitted earlier than others, thereby improving the fairness performance among *nrt-nodes*. Both Q_{th} and CW_{stall} are system parameters, which optimal values can be obtained through heuristic search but beyond the scope of this paper.

One may argue that reducing the CW size worsens the network congestion in a crowded system and thus causes the instability for a network. However, this situation may seldom happen because secondary users in a cognitive network have plenty of channels, and the number of secondary users choose and access on the same channel is small compared to the legacy system. Furthermore, our simulation results shown in the later section illustrate that the system up to 140 stations can still remain stable. Therefore, we believe the system instability is not a severe problem for the proposed MAC protocol.

4.4 Invited Reservation Procedure in *Decide* Stage

Next, another key challenge in designing the cognitive MAC protocol lies in the way of periodically transmitting delay-sensitive traffic flows because any connection in a cognitive ad hoc network cannot interfere the legacy system. To solve this problem, we propose an invited reservation procedure in the ***decide*** stage of the cognition cycle.

4.4.1 Invited Reservation Procedure

The invited reservation procedure is designed for supporting the delay-sensitive application. Based on this procedure, the receiver sends the real-time clear-to-send (rt-CTS) control frame to reserve time slots for the transmitter sending subsequent

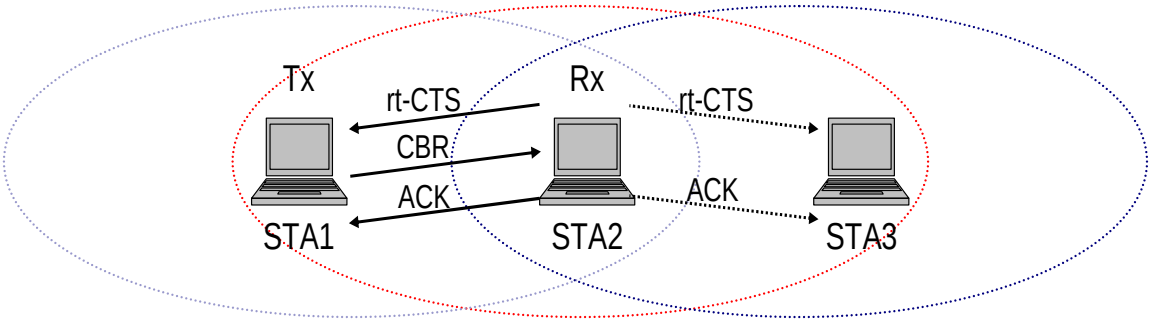

Fig. 4.2: An illustration of the invited reservation procedure.

frames of a reserved delay-sensitive traffic flow. Like the clear-to-send (CTS) control frame, the duration field of the MAC header in the rt-CTS frame defines the length of current frame transmission and thus can be used to forbid the transmissions from the stations in receiver's neighborhood. Because the delay-sensitive frame transmissions are controlled by the receiver of reserved flows, the collisions due to the hidden node problem can be somehow alleviated. For example, Fig. 4.2 illustrates a scenario where the transmitter STA 1 establishes a delay-sensitive traffic flow to the receiver STA 2 in the presence of a hidden node STA 3. In the figure, the receiver STA 2 sends rt-CTS inviting STA 1 to transmit reserved frames. Upon receiving the rt-CTS control frame for STA 1, the hidden node STA 3 recognizes the incoming reserved transmission and halts sending packets. Therefore, the invited reservation procedure can reduce the dropping rate of delay-sensitive traffic flows, especially in an environment with hidden nodes. Furthermore, recall that the MAC duration field of delay-sensitive data and its ACK frames represent the frame length of the next packet in the reserved flow. This value will be set to zero if the reserved flow is cancelled, and thus the receiver knows whether the sender has packets once the flow is established. On the other hand, since the receiver can learn the spectrum usage time of primary users in ***observe*** stage of the cognition cycle, the receiver always has the knowledge to adjust the invitation without interfering primary users.

In our design, the transmission based on the reception of rt-CTS may induce an

issue that the transmission from the hidden node of the receiver may cause collisions at the sender. In fact, assuming that the hidden node also follows the proposed MAC protocol, it can transmit packets only after it receives all the data or ACK frames from all the reserved flows in RIT. In other words, the hidden node has to wait for the end of all delay-sensitive frame transmissions and then transmits packets accordingly. Therefore, we believe the considered situation may not happen in our proposed MAC protocol.

4.4.2 Link Establishment with Invited Reservation Procedure

Next, the problem is how to establish a delay-sensitive traffic flow using the invited reservation procedure. In our design, the first packet of a delay-sensitive traffic flow is used for the link establishment through the random access on the channel by request-to-send/clear-to-send (RTS/CTS) handshaking. The first packet transmission also reserves the length and sequence for the next packet transmission. Once the link is successfully established, the receiver periodically sends the rt-CTS control frame to reserve time for the reserved delay-sensitive flow. Figure 4.3 illustrates an example for the link establishment. In Flow 2 (STA 4 → STA 3), STA 4 follows the RTS/CTS handshaking procedure to send the first packet of a delay-sensitive traffic flow during the n^{th} contention period (CP). As long as the flow is established, STA 3 periodically sends rt-CTS with reserved information to its sender STA 4. Accordingly, without contention, STA 4 transmits the rest packets of the reserved flow in succeeding contention free periods (CFPs).

However, the random access for the link establishment of a delay-sensitive traffic flow induces the collision with other non-real-time data frames and leads packet drop due to the increased access delay. To alleviate the impacts of contentions, we design the linear backoff algorithm for the first packet transmission to shorten the access delay. The linear backoff algorithm decreases the CW size of the collided frame to

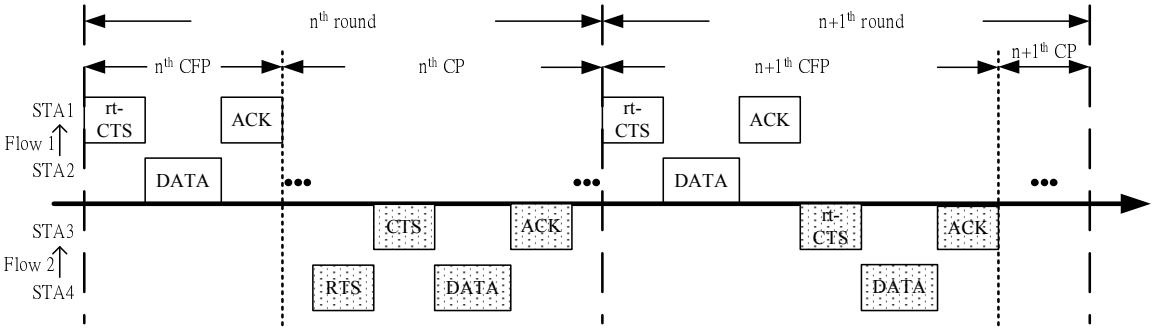

Fig. 4.3: The timing diagram for the invited reservation procedure.

expedite the link establishment of a delay-sensitive traffic flow. The simulation results in the later section demonstrate that the dropping rate of delay-sensitive frames in the proposed MAC protocol is almost negligible compared to that in the IEEE 802.11 DCF mode. Therefore, we believe the impact of contentions to the link establishment for delay-sensitive traffic is insignificant because most of packets are reserved and sent during an acceptable period.

On the other hand, for a reservation based MAC protocol, one important issue is the starvation problem for non-real-time data traffic. As shown in Fig. 4.3, the fixed total transmission time in each round is partitioned into two periods: the CFP and CP. To prevent the starvation problem, the time duration of the two periods shall be appropriately allocated so that the delay constraints for the delay-sensitive traffic flow can be satisfied, while its impact on the non-real-time data transmission can be limited to an acceptable level. However, precisely controlling the duration of CFP and CP in a distributed way is sophisticated for CR device. Instead, in this paper, the stall avoidance scheme is designed to avoid the bandwidth suppression by expediting the stalled frame transmission. Recall that the stall avoidance scheme will decrease the CW size to CW_{stall} if an *nrt-node* has excessive buffered frames, and $CW_{stall} < CW_{min}$. The stalled non-real-time data frame with the small CW size CW_{stall} can have a higher probability to win the channel contention and prohibits from *rt-nodes* establishing a new delay-sensitive traffic flow. Therefore, in this way, the

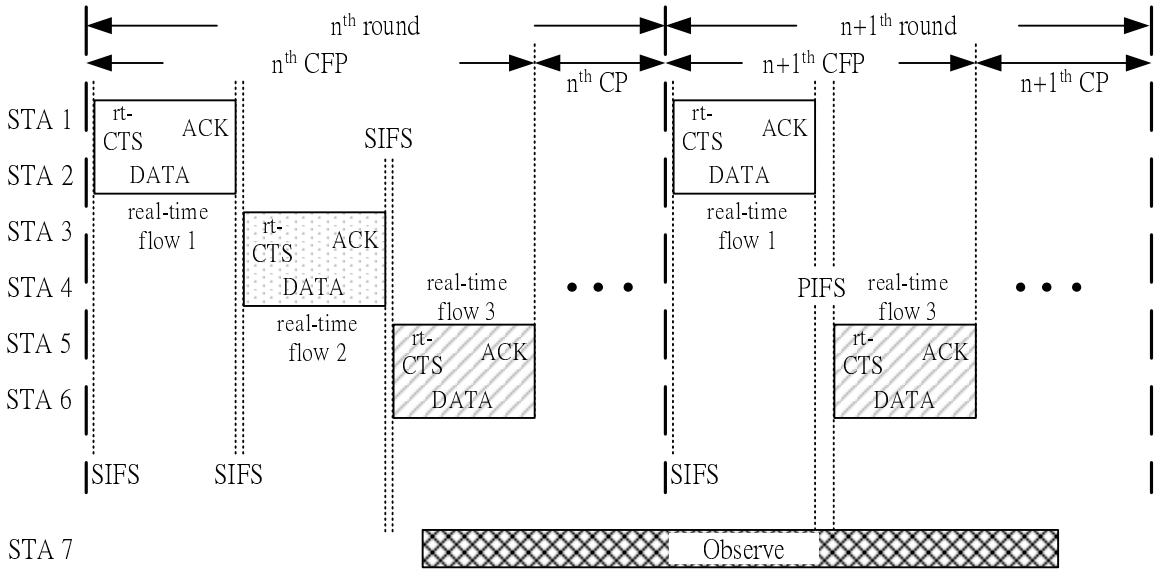

Fig. 4.4: The timing diagram for the new proposed distributed frame synchronization mechanism.

access delay of non-real-time data frames can be still controlled within a reasonable range without sacrificing the delay constraint for delay-sensitive traffic.

4.5 Distributed Frame Synchronization Mechanism in *Act* Stage

Another important issue in the ***act*** stage of the cognition cycle is to develop a distributed approach to ensure the frame synchronization among CR users. The objective of frame synchronization is to inform stations the starting time of the CFP and CP in each round. In the legacy IEEE 802.11 WLAN, the access point or the designated central controller broadcasts the "*beacon*" signal as the start of each round. However, broadcasting "*beacon*" signals not only increases energy consumption, but wastes the valuable transmission time for secondary users. To this end, we propose a new distributed frame synchronization mechanism as follows.

The basic idea of the proposed distributed synchronization algorithm is to let the secondary user transmission follow the sequence of reserved flows in RIT. Since a CR user establishes its neighbor list in the ***observe*** stage, the information in RIT can be applied to identify the first and last stations transmitting the delay-sensitive frames. Thus, when the channel is available, the receiver of the first reserved flow in RIT broadcasts rt-CTS frame to start a new CFP. During the CFP, the *rt-nodes* transmit frames based on the sequence in RIT, whereas the *nrt-nodes* wait until receiving the ACK frame from the receiver of the last flow in RIT. If the primary user become active during CFP, the receiver of the delay-sensitive traffic flow will halt sending the rt-CTS and resume it when the spectrum turns idle. Therefore, through the information stored in PIT and RIT, all the CR users can access the channel in the designated period without influencing the primary users and the transmissions in the reserved time.

Figure 4.4 illustrates an example for the proposed distributed synchronization mechanism. Assume that STAs 1∼6 establish delay-sensitive traffic flows. At the start of the n^{th} CFP, when STA 1 senses the channel is available, it immediately sends rt-CTS to start a new CFP and waits for receiving the frame from STA 2. After sending the ACK frame to STA 2, STA 1 waits for a fixed duration and repeats the above procedure until flow 1 is terminated. In the meanwhile, STAs 3 and 5 overhear the channel and recognize a new CFP. When the previous reserved transmissions are finished, STA 3 send rt-CTS to STA 4 to start flow 2. At last, when the transmissions of the last flow in RIT are ended, i.e., flow 3 from STA 6 to STA5, the CP in the n^{th} round starts. All the *nrt-nodes* are allowed to contend for the channel during this duration until the next CFP starts. Note that the proposed distributed frame synchronization is only needed when delay-sensitive traffic flows exit. The legacy CSMA/CA MAC protocol with the suggested gating mechanism is enough when only non-real-time traffic exists.

Three interesting scenarios are discussed as follows. First, when a CR user just

joins the CR network or turns on the power, it may not recognize the time when the CFP and CP start. This particular user may access the channel in CFP and collide the on-going transmission. To avoid this kind of collisions, the previously suggested neighbor list establishment mechanism has been carefully designed to resolve this problem. Recall that every CR user overhears the spectrum for at least a T_{obv} period to correctly establish PIT, RIT and CIT before transmission. Since the duration of T_{obv} is longer than the maximum repetition period between two successive frames of a reserved flow, a new user can be aware of the first and last transmissions in CFP based on the information in its RIT. Thus, it can easily recognize the starting time of the two periods in each round. Take STA 7 in Fig. 4.4 as an example. Since it observes the channel for a T_{obv} period and establishes PIT and RIT, STA 7 can recognize that CFP and CP respectively start after STAs 1 and 5 send the rt-CTS and ACK frames. Therefore, STA 7 will access the channel during CP without colliding with the transmission of primary users or reserved flows.

Another interesting issue is when some CR users can not maintain frame synchronization due to the failure reception of rt-CTS, data and ACK frames in the lossy wireless channel. Under this situation, the *nrt-node* may send the data frame in CFP and cause collisions to other reserved flows. To deal with this problem, the invited reservation procedure is designed with following principle. If not hearing the rt-CTS frame longer than a duration of PCF inter-frame spacing (PIFS), the receiver of the next reserved flow in RIT immediately sends the rt-CTS frame to reserve time slots. Note that in the IEEE 802.11 WLAN, PIFS is longer than SIFS, but shorter than data inter-frame spacing (DIFS). In this way, the rt-CTS frame always has the highest transmission priority, and thus it can protect the transmissions in CFP from the interference of unsynchronized stations. As shown in Fig. 4.4, when STA 5 identifies a new CFP, it waits for rt-CTS or data frame from STA 3 or 4. Once the channel is idle longer than PIFS as shown in the $n+1^{th}$ CFP, STA 5 directly sends rt-CTS to prevent the non-real-time frame transmissions from unsynchronized stations. There-

fore, the frame synchronization can be maintained even though some frames are lost due to signal outage.

At last, one may be curious that whether the new distributed frame synchronization mechanism is backward compatible and interoperable with the legacy DCF and PCF modes in IEEE 802.11 WLAN. On the one hand, the transmission in DCF mode has no influence to that in our invited reservation procedure. Because the maximum spacing between any two delay-sensitive frames in our MAC protocol (PIFS) is shorter than the minimum duration of two data frames in DCF mode (DIFS), i.e., PIFS $<$ DIFS. The frame transmission in DCF mode cannot disturb the reserved frame transmission in CFP. On the other hand, the neighbor list establishment helps secondary users to recognize the transmission in the PCF mode and treat them like primary user transmission. Therefore, with the gating mechanism and information in PIT, all the secondary user transmissions in our MAC protocol are postponed until the end of PCF mode to avoid interfering the transmission in PCF mode.

4.6 Throughput Analysis

In this section, we analyze the throughput of our proposed cognitive MAC protocol with mixed delay-sensitive and non-real-time data traffic flows. To ease the analysis, we make the following assumptions: (1) the spectrum usage information is correctly obtained by the spectrum sensing, identification, and allocation mechanisms; (2) the channel is ideal without transmission errors; (3) a fixed number of *nrt-nodes* always have packets to send; (4) the delay-sensitive traffic of a fixed number of *rt-nodes* is characterized by the "on/off" model with the exponentially distributed inter-arrival and departure time [122]. Recall that CR users can send packet only in the spare time of primary user transmissions. Thus, we only consider the throughput performance during the time available for CR users.

4.6.1 Mixed non-real-time and delay-sensitive traffic flows

Next, we consider a mixed traffic model with delay-sensitive and non-real-time data traffic flows. Denote M and K the number of *rt-nodes* and *nrt-nodes*, respectively, and let $n_{rt}(t)$ be the number of *rt-nodes* requesting for frame transmissions at the time instant t. For simplicity, it is assumed that only one delay-sensitive traffic flow requests to establish in each round.

The delay-sensitive traffic is assumed to be modeled by an interrupted Poisson process (IPP), as shown in Fig. 4.5(a). In the figure, the "On" state represents a talk spurt, whereas the "Off" state is for a silent spurt [122]. The durations for both states are exponentially distributed with a mean value of $1/q$ and $1/p$, respectively. In addition, an M-stage Markov-modulated Poisson process (MMPP) shown in Fig. 4.5(b) is applied to model multiple delay-sensitive traffic flows. Each state in the figure stands for the number of *rt-nodes* requesting for frame transmissions, and thus the state probability (P_i) can be expressed as

$$P_i = P\{n_{rt}(t) = i\} = \binom{M}{i} \rho^i P_0 \ , \tag{4.3}$$

where $\rho = q/p$.

Denote $T(M, K)$ the throughput of M *rt-nodes* and K *nrt-nodes* in an overlaying cognitive ad hoc network, which can be given by

$$\begin{aligned} T(M,K) &= E[\text{throughput of } M \text{ } \textit{rt-nodes} \text{ and } K \text{ } \textit{nrt-nodes}] \\ &= \sum_{i=0}^{M-1} P_i \cdot \left(\frac{iL_{rt}}{L} T_{rt} + \frac{L - iL_{rt}}{L} T_{nrt}(K) \right) \\ &= T_{nrt}(K) + (T_{rt} - T_{nrt}(K)) \sum_{i=0}^{M-1} P_i \frac{iL_{rt}}{L} \\ &= T_{nrt}(K) + (T_{rt} - T_{nrt}(K)) \frac{L_{rt}}{L} \frac{M\rho}{1+\rho} \ , \end{aligned} \tag{4.4}$$

where L is the entire duration of two secondary transmission periods, i.e., CFP and CP; L_{rt} is the total duration for sending delay-sensitive data frames as well as the

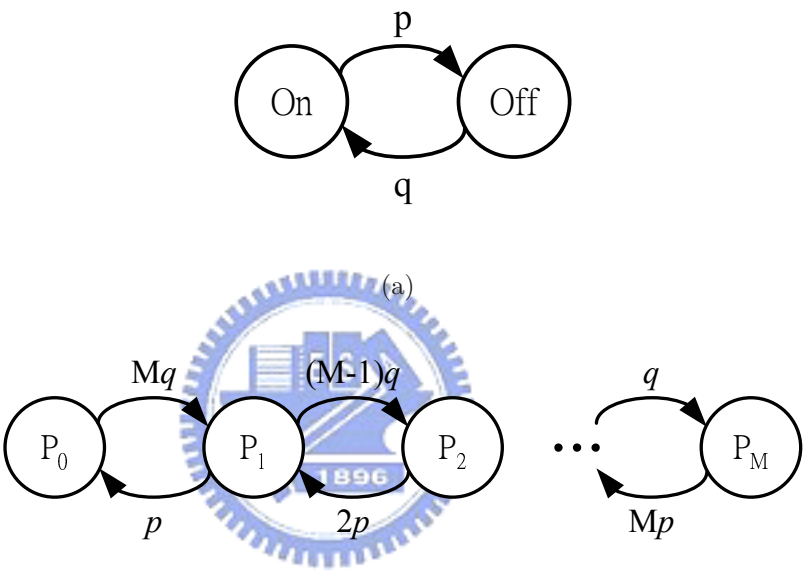

Fig. 4.5: (a) Interrupted Poisson process model for delay-sensitive traffic. (b) Markov modulated Poisson process (MMPP) model for one type delay-sensitive traffic with M users.

rt-CTS and ACK control frames; $T_{nrt}(K)$ represents the received frames from K *nrt-nodes* in the CP; T_{rt} contains the delay-sensitive data frames. Note that L is assumed to be fixed because it excludes the duration of primary user transmissions.

The above analysis can be extended to the mixed traffic model containing multiple types of delay-sensitive traffic by using a multi-dimension Markov chain. Take two delay-sensitive traffic types as an example and let N and M be the numbers of CR users sending these traffic types, respectively. Then, the state probability $P_{i,j}$ of the two-dimensional Markov chain model in Fig. 4.6 can be expressed as

$$P_{i,j} = \begin{pmatrix} N \\ i \end{pmatrix} \begin{pmatrix} M \\ j \end{pmatrix} \rho_1 \rho_2 P_{0,0} \ , \tag{4.5}$$

where $\rho_1 = q_1/p_1$ and $\rho_2 = q_2/p_2$ are similar to the definitions in (4.3). Thus, the total throughput $T(M, N, K)$ can be written as

$$T(M,N,K) = T_{nrt}(K) + (T_{rt1} - T_{nrt}(K)) \frac{L_1}{L} \frac{M\rho_1}{1+\rho_1} + (T_{rt2} - T_{nrt}(K)) \frac{L_2}{L} \frac{N\rho_2}{1+\rho_2} \tag{4.6}$$

where all the parameters are defined in (4.4).

4.7 Simulation

In this section, we demonstrate the performance of the proposed cognitive MAC protocol through the NS-2 simulator [123]. We also use the IEEE 802.11 DCF mode with the RTS/CTS handshaking for the performance comparison. The RTS/CTS DCF mode is naturally a good candidate for secondary user in a cognitive network because the carrier sensing avoids interfering primary user transmissions at the moment of any packet transmission. Furthermore, most of current cognitive MAC protocol still use the CSMA/CA MAC protocol to resolve the collisions among secondary user [36,49,59]. Thus, the performance of the CSMA/CA MAC protocol with RTS/CTS handshaking can be a baseline in a cognitive network.

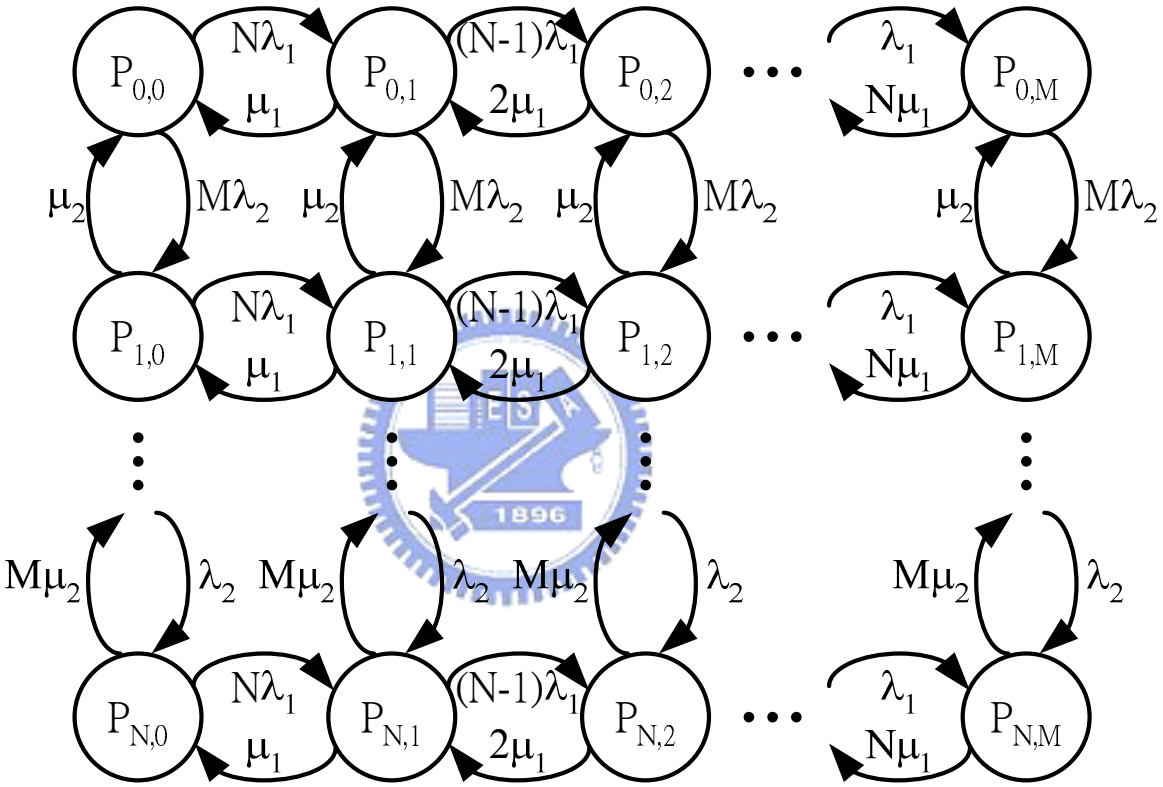

Fig. 4.6: Two-dimensional Markov chain for the analysis of two delay-sensitive traffic types.

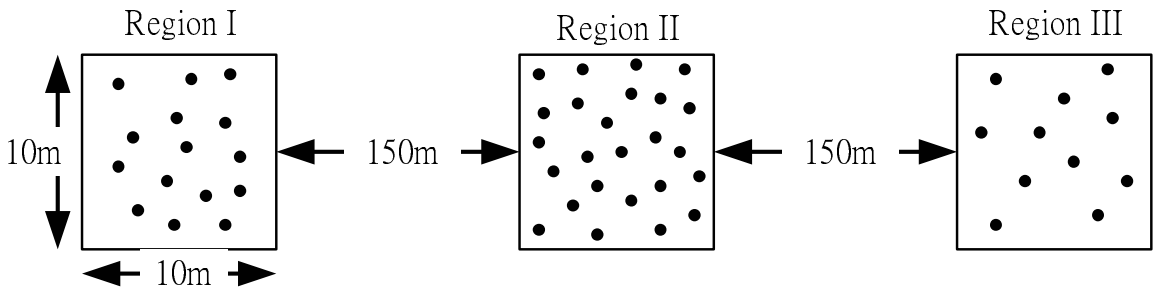

Fig. 4.7: The considered network topology for the simulation, in which nodes are distributed to three clusters in a string-type topology.

4.7.1 Simulation Environment

To begin with, we explain the considered simulation environment. In this paper, we consider two network topologies, in which nodes are 1) allocated in one cluster and 2) distributed to three clusters in string-type topology. In the first network topology, all the primary and secondary users are located in the same cluster with the area of 10 m $\times$ 10 m. On the other hand, in the second network topology, primary users are only located in Region II, but secondary users are distributed at all the three regions, as shown in Fig. 4.7. Furthermore, the nodes in region I are hidden from that in region III, and vice versa. The secondary users in regions I and III can send packets only to those in region II. In our simulation, the primary user is assumed to adopt the TDMA MAC protocol, whereas secondary users use the proposed MAC protocol or the CSMA/CA MAC with RTS/CTS handshaking for packet transmissions. In addition, it is assumed that the transmission is considered success if only one user accesses on the channel, while the collision takes place when more than one user transmit packets at the same time. The other simulation parameters are listed in Table 4.1.

Furthermore, the following traffic models are considered in the simulation.

- **Voice traffic** is characterized by an interrupted Poisson process. In the "On" state, an 164-byte packet is generated every 20.48 msec, which is equal to 64

Tab. 4.1: System Parameter for the Simulation of Cognitive MAC Protocol

Area of one cluster	10 m×10 m
Distance of each cluster	160 m
Data Rate	2 Mbps
Slot time	20 μsec
SIFS	10 μsec
PIFS	30 μsec
DIFS	50 μsec
Minimum CW size	31
Maximum CW size	1023
CW for stall avoidance (CW_{stall})	15
Maximum frame transmission times	7
Number of primary users	10
Number of rt nodes	10
Number of nrt nodes	80
Period of delay-sensitive flow	20 msec
Period of primary user transmission	20 msec
Packet size of primary user and delay-sensitive flows	164 bytes

Kbps. By contrast, the simulator stops generating any packet in the "Off" state. The duration of the "On" and "Off" states follows the exponential distribution with the average durations of 1 and 1.3 seconds, respectively.

- **Telnet data traffic** is modeled by a Poisson process with the packet length of 950 and 60 bytes. The packet inter-arrival rates are determined by the offered load.

- **FTP data traffic** is assumed that the simulator continuously generates packets with three frame sizes: 950, 500 and 60 bytes if a node successfully send the previous one.

In our simulation, only half of users have packets to send, and the others are the corresponding receivers. Without any notice in the following, the network always consists of 40 Telnet data flows in the presence of 10 voice traffic flows, which are respectively generated and received by 80 *nrt-nodes*, 10 *rt-nodes* and 10 primary users.

4.7.2 Performance Measurements

The performance of the proposed cognitive MAC protocol is evaluated in terms of the normalized throughput, mean access delay, fairness, and dropping rate. For clearance, we define these performance metrics as follows.

- **Normalized throughput** is defined as the ratio of the number of successfully received bits to the amount of total transmitted bits. Note that the successfully received bits account for both the successfully received non-real-time data frames and the delay-sensitive frames as well as the primary user frame transmissions. The received frames from delay-sensitive traffic and primary users will not be counted if the 20-msec delay constraint is not satisfied.

- **Mean access delay** accounts for the average duration a non-real-time data frame requires when it is generated by the transmitter until it is successfully

received by the receiver. By this definition, the access delay includes the waiting time in the queue and the latency of the channel access. The frame, which number of transmission times is larger than the maximum retry limit, will not be taken into account for the access delay calculation.

- **Fairness** is evaluated by the maximum standard deviation of the frame access delay among all the non-real-time traffic flows. Note that the available transmission time for the secondary user in a cognitive network is short. The reduced delay variance among traffic flows represents that all secondary users have equal opportunities to send packets on the channel during the short transmission time. Thus, the maximum standard deviation of access delay among user is more appropriate for measuring the fairness performance in a cognitive network.

- **Dropping rate** is defined as the ratio of the number of dropped frames to the total number of transmitted frames. The frame is considered to be dropped if the access delay of the delay-sensitive frame or the primary user transmission is beyond 20 msec.

4.7.3 Numerical Results

First, we examine the dropping rate of primary user transmissions in the network topology that all user are located in one cluster, as shown in Fig. 4.8. Because of the gating mechanism and the information stored in PIT, the proposed cognitive MAC protocol dynamically stops secondary users sending frames at the time when primary users access the channel. Surprisingly, the dropping rate of primary users in the legacy CSMA/CA MAC protocol is less than 3%. This phenomenon results from the carrier sensing that the node performs before sending packets. This carrier sensing satisfies the basic requirement of spectrum sensing in a cognitive network. However, the carrier sensing only detects the channel at the time instance when it executes

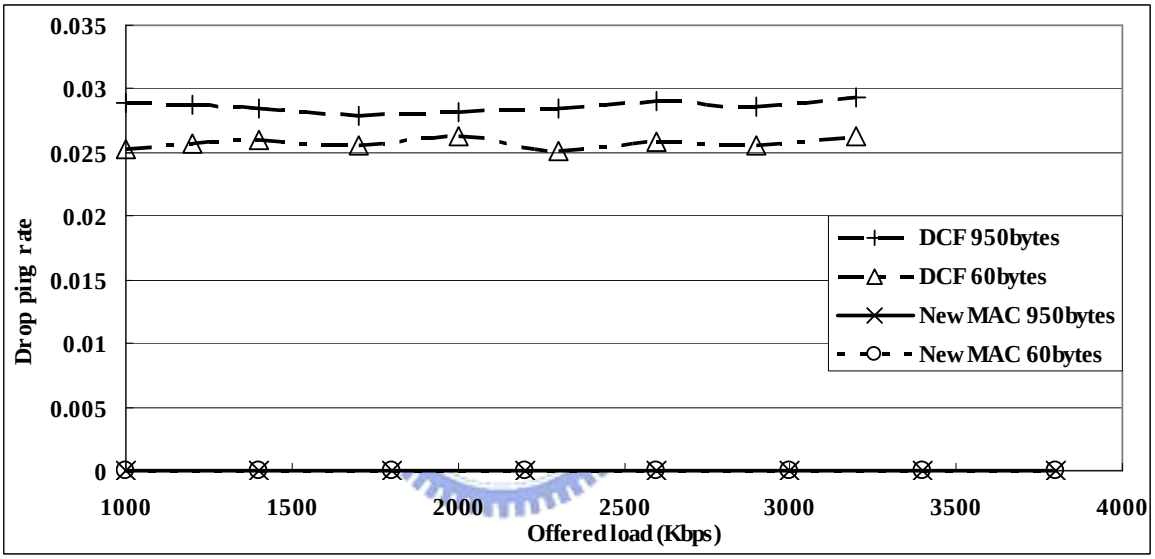

Fig. 4.8: Dropping rate of the primary user's transmissions in the network topologies that all secondary users are located in one cluster.

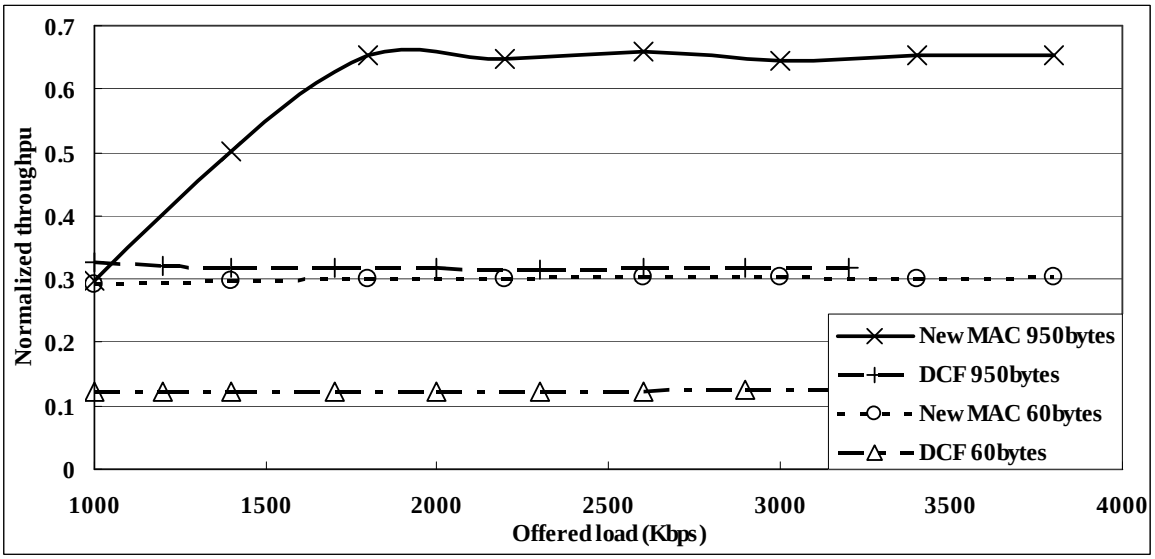

Fig. 4.9: Throughput comparison of the proposed cognitive MAC protocol with the traditional CSMA/CA MAC protocol.

instead of the whole duration for the frame transmission. The collision still happens when the primary user appears at the time during the secondary user transmission. In our proposed cognitive MAC protocol, the gating mechanism with the information in PIT ensures the entire duration of the secondary user transmission has no influence to primary users. Although the current simulation only considers the periodic traffic, the proposed method still can cooperate with other advance traffic models to estimate the time and length of primary user transmissions. Therefore, we believe the proposed scheme still provides valuable contribution for the cognitive MAC protocol design.

Figure 4.9 compares the normalized throughput of the proposed cognitive MAC protocol and the legacy CSMA/CA MAC protocol in the one-cluster network topology. For both the frame sizes of 60 and 950 bytes, the throughput in the proposed MAC protocol are 100% better than those in the CSMA/CA MAC protocol. The improvements mainly result from the invited reservation procedure, which can control the delay for the delay-sensitive frames. Thus, most of the delay-sensitive frames can be counted for throughput computation. On the contrary, all the delay-sensitive

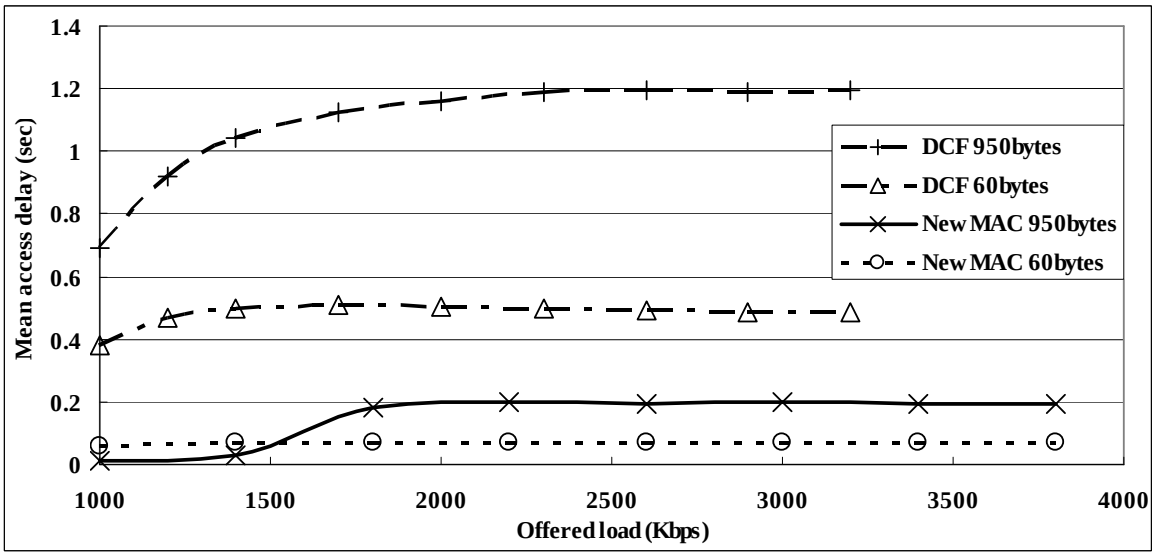

Fig. 4.10: Comparison of mean access delay between the proposed cognitive MAC protocol and the CSMA/CA MAC protocol.

frames in the legacy CSMA/CA MAC protocol still contend for the channel with other non-real-time frames. The contention leads the access delay of delay-sensitive frames is beyond the delay constraint due to retransmissions, and causes the neglect of those frame in throughput calculation. Furthermore, the gating mechanism in the proposed cognitive MAC protocol reduces the collisions in the CP. Hence, the throughput of the proposed MAC is better than that of the CSMA/CA MAC protocol in supporting mixed-type traffic flows.

Figures 4.10 and 4.11 compare the mean access delay and the fairness performances between the two MAC protocols. For the proposed cognitive MAC protocol, the mean access delay and its maximum standard deviation in sending the Telnet data frames is less than 0.2 sec and 1 sec, respectively. However, for the legacy CSMA/CA MAC protocol, the considered performance matrices are increased to 1.2 sec and 3.6 sec, respectively. The long access delay and its maximum standard deviation in the CSMA/CA MAC protocol is due to the long waiting time in the queue. However, when the non-real-time data frames are back-logged, the proposed stall avoidance

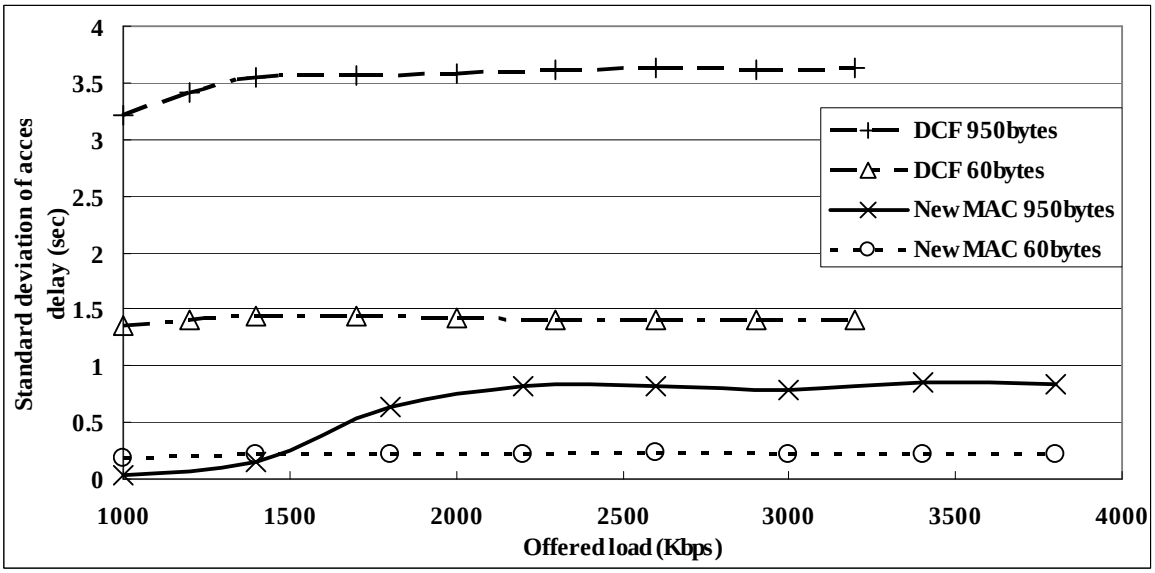

Fig. 4.11: Comparison of fairness among the proposed cognitive MAC protocol and the CSMA/CA MAC protocol.

scheme can effectively reduce the CW size of the stalled frames to expedite the transmissions. Therefore, the proposed cognitive MAC protocol can reduce the waiting time and improve the access delay and its standard deviation.

An interesting phenomenon shown in Figs.4.10 and 4.11 is that both the delay and its standard deviation become stable at high traffic load. Recall that the computation of access delay only counts the frame which the number of transmissions is less than the retry limit, i.e., seven in our simulation. Therefore, the limited number of frame transmission attempts for the calculation of access delay confines the values of its average and standard deviation even at high traffic load.

Figure 4.12 compares the dropping rate of delay-sensitive traffic for secondary users in two considered MAC protocols. As shown in the figure, the dropping rate in the proposed MAC protocol is lower than 0.1%, while in the legacy CSMA/CA MAC protocol the dropping rate can be higher than 50%. Because delay-sensitive frames in the legacy CSMA/CA MAC protocol contend for the channel with data frames using the similar priority, the retransmission due to the collisions causes the access delay

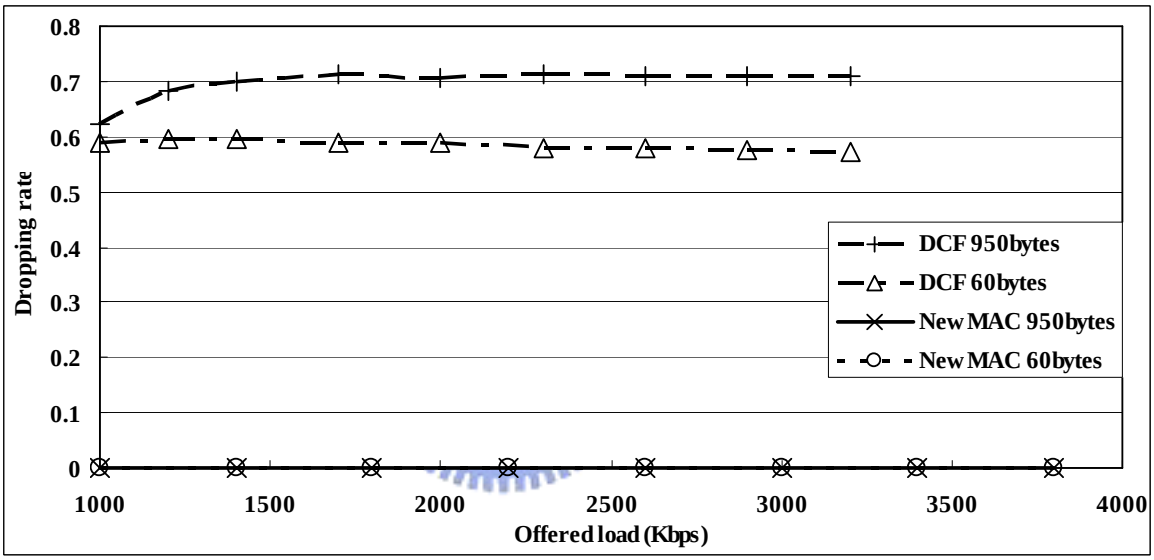

Fig. 4.12: Dropping rate of delay-sensitive traffic for secondary users.

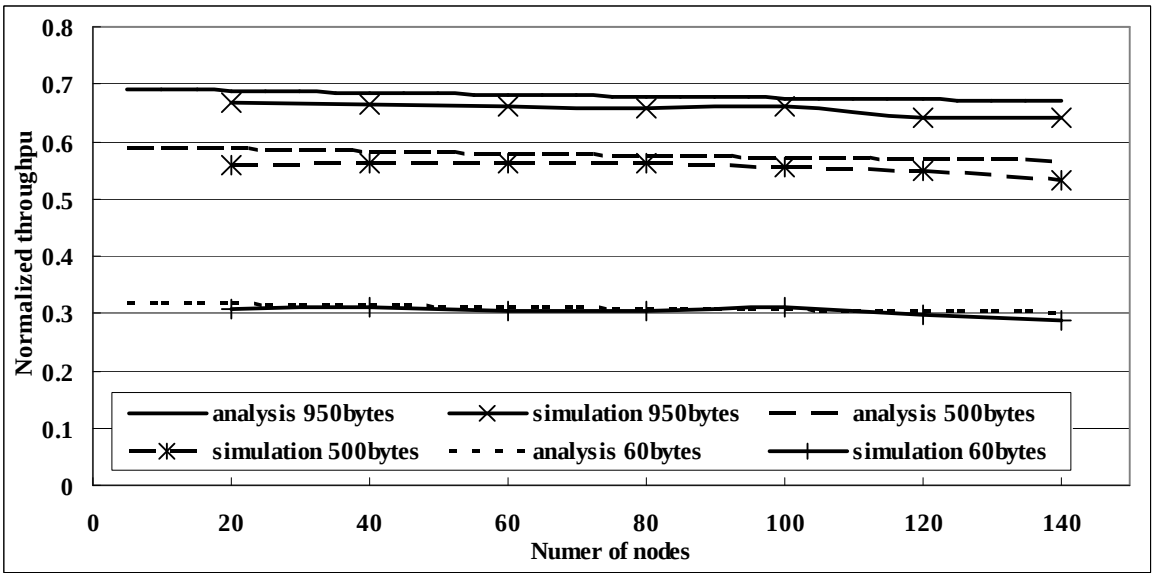

Fig. 4.13: Throughput of the proposed cognitive MAC protocol in the mixed voice and FTP data traffic.

beyond the delay constraint. By contrast, with the help of the invited reservation procedure, the proposed MAC protocol can guarantee the delay-sensitive frames to be received within the predefined constraint of 20 msec. Although, in the proposed MAC protocol, the first frame of delay-sensitive traffic flow still contends with other non-real-time data frames, the linear backoff algorithm helps to quickly establish the traffic flow and reserve the succeeding frame transmissions. Therefore, the dropping rate of the proposed MAC protocol is almost negligible compared to the CSMA/CA MAC protocol.

To validate our results, Fig. 4.13 shows the normalized throughput with the mixed delay-sensitive and non-real-time data traffic in the proposed cognitive MAC protocol by simulations and analysis. The considered scenario includes 10 *rt-nodes* and various number of *nrt-nodes* establishing voice and FTP data traffic flows, respectively. As shown in the figure, the result from the analytical model by (4.4) are close that from simulations, especially for the case with a small packet size. Even for the large packet size, the discrepancy between analysis and simulation is still less than

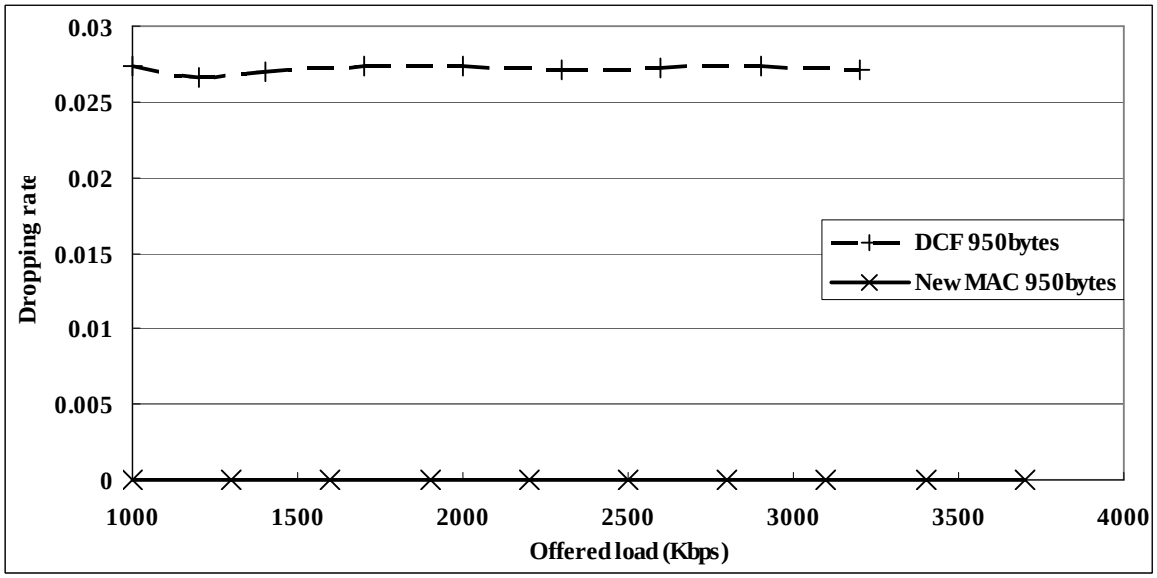

Fig. 4.14: Dropping rate of primary user transmissions in the network topology that secondary users are distributed in three separated clusters.

3%. As shown in the figure, the throughput still remains stable even in the system with more than 100 *nrt-nodes*. This observation illustrates that the use of small CW size in the linear backoff algorithm and stall avoidance scheme do not deteriorate the network stability in a crowded environment.

At last, the network topology that all secondary users are distributed in three string-type clusters, as shown in Fig. 4.7, is considered. Figure 4.14 shows the dropping rate of primary user transmission. Similar to the observation shown in Fig. 4.8, the dropping rate in the proposed cognitive MAC protocol is negligible compared to the legacy CSMA/CA MAC protocol. In addition, as shown in Figs. 4.15 and 4.16, the proposed cognitive MAC protocol for secondary user transmissions still outperforms the legacy CSMA/CA MAC protocol in terms of throughput and dropping rate. Like the RTS/CTS handshaking in the legacy CSMA/CA MAC protocol, broadcasting rt-CTS from the receiver of reserved flows in RIT reduces the collision in the reserved slot. Thus, the hidden node issue only cause a minor impact to the

throughput and dropping rate in the proposed cognitive MAC protocol.

4.8 Conclusion

In this part, we have proposed a cognitive MAC protocol to establish an overlaying cognitive ad hoc network with QoS provisioning in the presence of the legacy wireless systems. The proposed mechanisms can supplement the insufficiency of the legacy CSMA/CA MAC protocol to fulfill the goals of the cognitive wireless networks. With respect to the four stages in the cognition cycle, we suggest the following techniques:

- **Neighbor list establishment** in the ***observe*** stage: to help CR users having the knowledge of the spectrum usage by the primary and other CR users;
- **Improved contention resolution algorithm** in the ***plan*** stage: to prevent CR users from interfering the existing legacy system and to allow CR users to efficiently and fairly access the channel in the short spare time of the spectrum usage by primary users.
- **Invited reservation procedure** in the ***decide*** stage: to schedule the transmissions of delay-sensitive traffic with satisfactory QoS requirements for secondary user without interfering the legacy system and to dynamically allocate the bandwidth for various traffic types to avoid the starvation issue for low priority traffic.
- **Distributed frame synchronization** in the ***act*** stage: to distributively coordinate the frame transmissions among CR users.

Through the simulations by NS-2, we demonstrate that even in the environment with hidden nodes, the throughput performance of the proposed MAC protocol is at least 50% better than that of the legacy CSMA/CA MAC protocol. The mean access delay and its maximum standard deviation of the proposed MAC protocol are 5 times

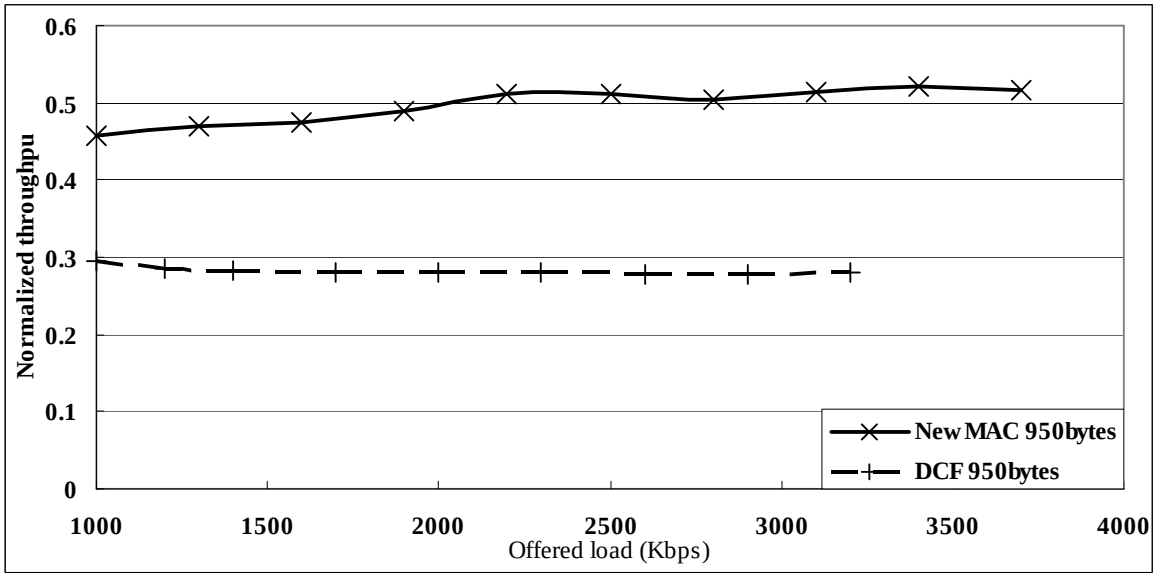

Fig. 4.15: Comparison of throughput performance between the proposed cognitive MAC protocol and the CSMA/CA MAC protocol in the network topology that secondary users are distributed in three separated clusters.

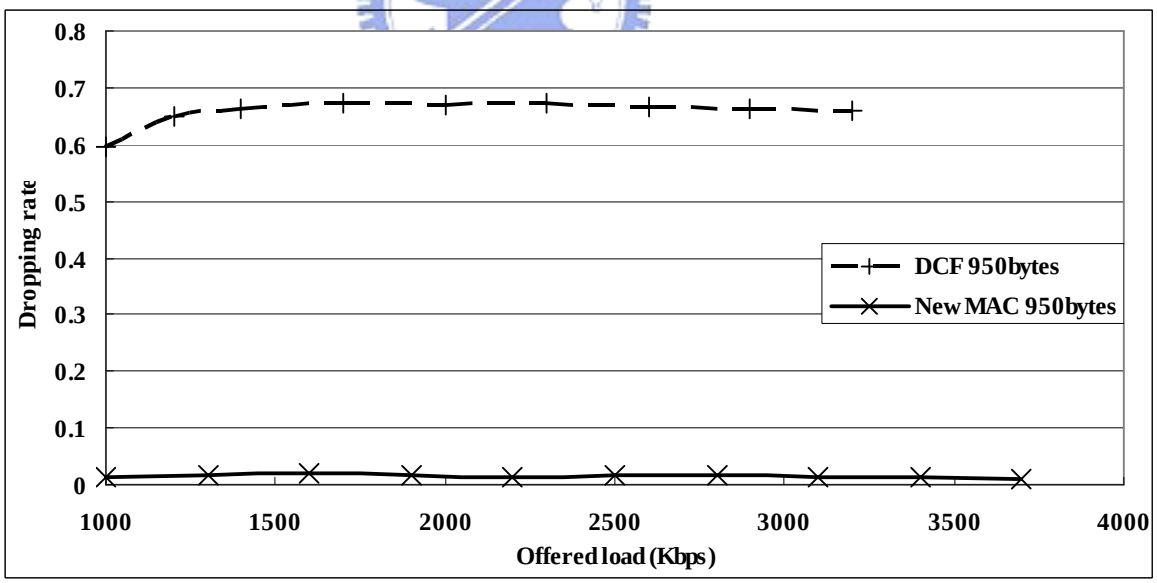

Fig. 4.16: Comparison of dropping rate for secondary users between the proposed cognitive MAC protocol and the CSMA/CA MAC protocol in the network topology that secondary users are distributed in three separated clusters.

less than the CSMA/CA MAC protocol. At last, instead of more than 50 % for the legacy CSMA/CA MAC protocol, the dropping rate of delay-sensitive traffic for the proposed MAC protocol is almost negligible.

Chapter 5

Traffic-aware Cognitive Spectrum Handoff with Preemptive Interruption

In this chapter, we discuss the link maintenance issue for CR device when the primary user accesses on the occupied channel during the period of a secondary user's transmission.

5.1 System Model

Here, we assume that both primary and secondary users uses the slotted system, in which the user's transmissions on the channel are partitioned into slots. The primary user is assumed to adopt the connection oriented medium access control (MAC) protocol for their data transmissions to meet the quality-of-service (QoS) requirement, such as GSM and WiMax. The secondary user is capable of advocating the channel in the prior slot of the primary user's transmission by overhearing the reservation information in the legacy system.

Then, we will consider three scenarios for secondary users to continue their transmissions when the primary user appears on the occupied channel. In the first scenario, the secondary user stays in the original channel and postpones its transmission when the primary user appears on the channel, as shown in Fig. 5.1. The CR user will resume the transmission after the primary user completes its transmission. This non-spectrum-handoff process will be repeated until the secondary user sends all its data. Apparently, the stalled transmission prolongs the transmission time and thus decreases the effective data rate.

The next considered scenario is that the secondary user switches to another channel to proceed its transmission when the primary user appears in the channel.

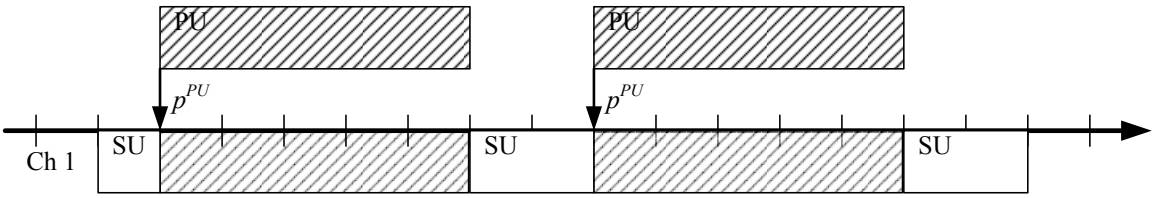

Fig. 5.1: An illustration of the transmission scenario that the secondary user stays in the original channel when the primary user accesses on the channel.

This is the so called "spectrum handoff". To the secondary user, the key issue for the spectrum handoff is the selection of the target channels to continue the on-going transmission. In this case, we categorize two possible scenarios for the target channel selection. Figure 5.2 illustrates the first channel selection scheme. As shown in the figure, the secondary user prepares the list of the target channels for the spectrum handoff before it establishes the link. The channel list can be sent to the receiver during the period of the link setup. When the primary user accesses in the occupied channel, the secondary user can change its transmission on the first channel in the list without waiting for the primary user's transmissions. Obviously, the effective data rate for secondary users can be significantly improved due to the decreasing transmission time.

However, the pre-determined channel list spectrum handoff scheme in the last paragraph relies on the accurate traffic model to estimate the usage of the primary user on the target channel. The error decision makes the secondary user continuously change its transmission on different channels. The secondary user wastes time on the handshaking for the spectrum handoff, and thus the effective data rate is also decreased due to the erroneous channel prediction. To reduce the error probability of the channel selection, another intuitive way is proposed to determine the target channel after a sensing mechanism, as shown in Fig. 5.3. In the figure, the CR device will perform a wideband radio sensing once the primary user accesses in the

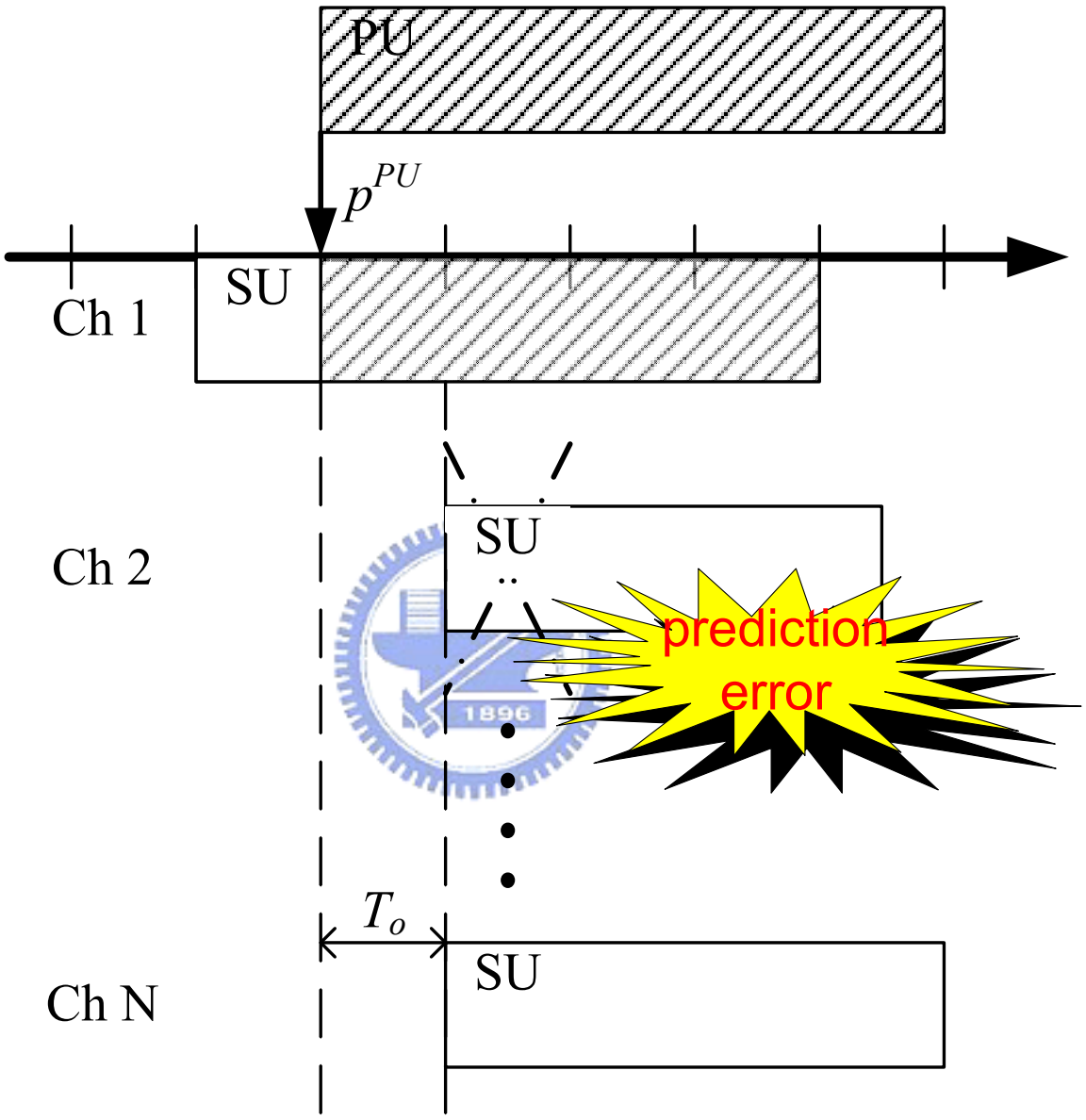

Fig. 5.2: An illustration of the spectrum handoff scenario that the secondary user determines the list of target channels before the link is established.

same channel. The secondary user then chooses and changes to the target channel according to the result obtained from the radio sensing. Clearly, the spectrum handoff with radio sensing scheme can avoid the possibility of the erroneous target channel prediction in the aforementioned method. However, this method still spends time on performing the radio sensing, which also prolongs the transmission time and decreases the effective data rate.

Another issue for the two aforementioned spectrum handoff schemes is the number of spectrum handoff trials that a secondary user has to perform during its entire transmission duration. Intuitively, the more the number of handoffs the higher the probability that a secondary user can maintain the established link, whereas the longer the transmission time that a secondary user requires to finish its transmission. Thus, it requires a way to come to a compromise between the performances of the link maintenance probability and effective data rate in the three secondary user's transmission scenarios.

5.2 Analytical Model

In the following, we will develop an analytical model to investigate the performances of the three considered transmission scenarios for secondary users. This analytical model provides an insight for the system parameter design at the given requirement of the link reliability and effective data rate for secondary users.

5.2.1 Link maintenance probability

The link maintenance probability p_m is defined as the probability that a secondary user can finish its transmission within N handoff trials. Given the secondary user transmission lasts over M slots, the link maintenance probability p_m can be written

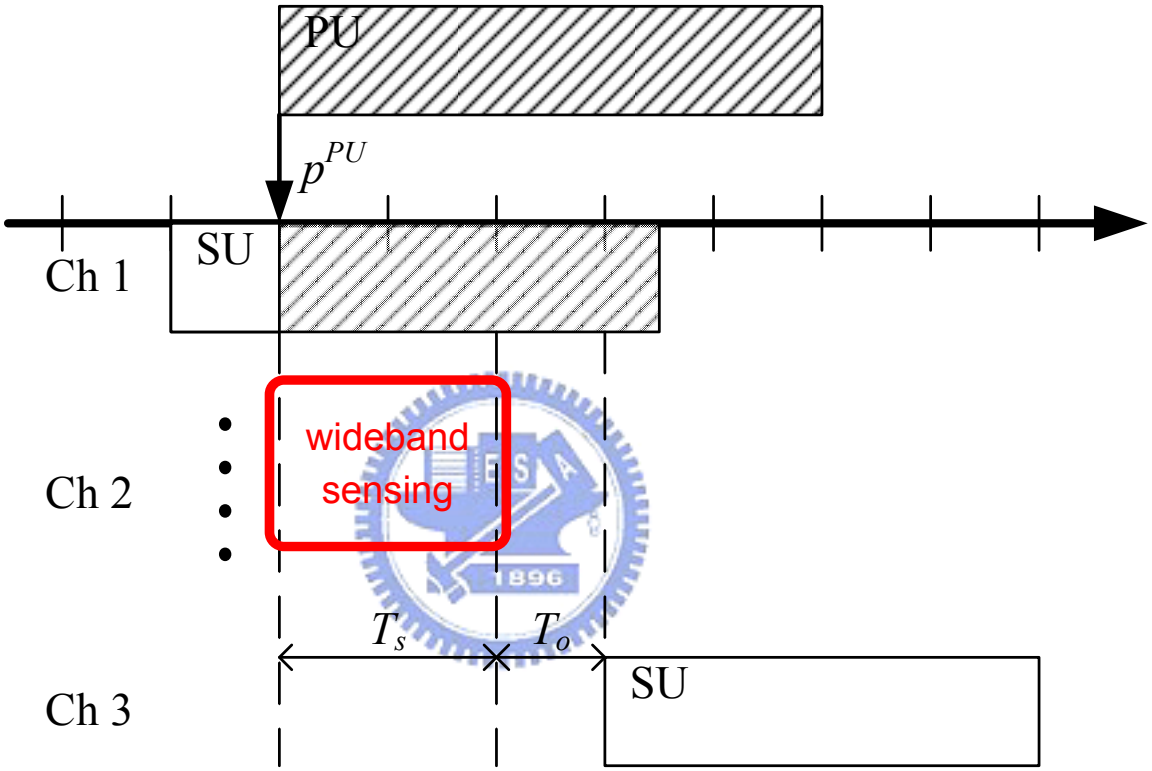

Fig. 5.3: An illustration of the spectrum handoff scenario that the secondary user performs the wideband radio sensing and then determines the target channel after the primary user appears.

by

$$p_m \triangleq Pr\{\text{the number of handoff trials required for the whole secondary user's transmission is less than N| an M-slot transmission}\} . \quad (5.1)$$

Let p be the probability that the given slot is not available for a secondary user. Assume that the primary user's transmissions on different channels are identical. Then, for the non-spectrum-handoff scenario and the pre-determined channel list spectrum handoff scheme, the link maintenance probability is determined by

$$\begin{aligned} p_m &= (1-p)^{M-1} + \binom{M-1}{1} p(1-p)^{M-1} + \cdots + \binom{M-2+N}{N} p^N (1-p)^{M-1} \\ &= \sum_{i=0}^{N} \binom{M-2+i}{i} p^i (1-p)^{M-1} , \end{aligned} \quad (5.2)$$

where $p_m = 1$ as $N \to \infty$. In these two transmission scenarios, the slot after one handoff trial may not be available for secondary users due to the continuous primary user's transmission or the erroneous target channel prediction. Thus, for a limited number of handoff trails, the link maintenance probability is always less than unity.

In addition, the non-spectrum-handoff scenario only differs with the pre-determined channel list spectrum handoff on the probability p. Suppose that the access probability p_{PU} of the primary users in a given slot is independent. Given p_e the frame outage probability of the secondary user's transmission in a slot, the probability p in the non-spectrum-handoff scenario can be expressed as

$$p = p_{PU} + (1 - p_{PU})p_e . \quad (5.3)$$

However, for the pre-determined channel list spectrum handoff, the channel prediction error probability p_s should be further taken into account. Thus, the probability p' that a secondary user is unable to transmit in the given slot for the pre-determined type spectrum handoff becomes

$$p' = p + (1 - p)p_s . \quad (5.4)$$

As for the spectrum handoff with radio sensing scheme, the link maintenance probability p_m is slightly different from the aforementioned two cases. Because the secondary user executes the radio sensing and selects the target channel while the primary user accessing the channel, at least one slot in the target channel is always available after a handoff trial. Therefore, the link maintenance probability p'_m in this case can be written by

$$\begin{aligned} p'_m &= (1-p)^{M-1} + \binom{M-1}{1} p(1-p)^{M-2} + \cdots + \binom{M-1-N}{N} p^N (1-p)^{M-1-N} \\ &= \sum_{i=0}^{N} \binom{M-1}{i} p^i (1-p)^{M-1-i} , \end{aligned} \tag{5.5}$$

where $p'_m = 1$ when $N = M$. Because the target channel decision is made right after the radio sensing, the channel prediction error probability can be negligible in the calculation of the slot availability p.

5.2.2 Effective data rate

Next, given l_{SU} the payload length of a secondary user's transmission, the effective data rate R_{SU} for secondary users can be defined as

$$R_{SU} = \frac{l_{SU}}{E[t_{SU}]} , \tag{5.6}$$

where $E[t_{SU}]$ is the average time of a secondary user's transmission, which differs from the transmission scenarios as discussed in Section 5.1.

Given T_{PU} the primary user transmission time, in the non-spectrum-handoff case, a secondary user's transmission will be delayed by T_{PU} each time when a primary user accesses in the channel, as shown in Fig. 5.1. Thus, referring to the derivations of the link maintenance probability in (5.2), the average secondary user's transmission

time $E[t_{SU}^{NSHO}]$ can be written by

$$\begin{aligned} E[t_{SU}^{NSHO}] &= (1-p)^{M-1}T_{SU} + \binom{M-1}{1}p(1-p)^{M-1}(T_{PU}+T_{SU}) + \cdots \\ &\quad \binom{M-2+N}{N}p^N(1-p)^{M-1}(NT_{PU}+T_{SU}) \\ &= \sum_{i=0}^{N}\binom{M-2+i}{i}p^i(1-p)^{M-1}(iT_{PU}+T_{SU}) \ , \end{aligned} \tag{5.7}$$

where $T_{SU} = l_{SU}/r_{SU}$, and r_{SU} is the data rate during the secondary user's transmission. As $N \to \infty$, the average transmission time converges to

$$E[t_{SU}^{NSHO}] = T_{SU} + T_{PU}\frac{(M-1)p}{1-p} \ . \tag{5.8}$$

For the pre-determined channel list spectrum handoff scheme, the secondary user's transmission is postponed by the execution time T_o of a handoff trial. Then, similar to (5.7), the average transmission time $E[t_{SU}^{SHOwoS}]$ turns into

$$E[t_{SU}^{SHOwoS}] = \sum_{i=0}^{N}\binom{M-2+i}{i}(p')^i(1-p')^{M-1}(iT_o+T^{SU}) \ , \tag{5.9}$$

where $E[t_{SU}^{SHOwoS}] = T_{SU} + T_o(M-1)p'/(1-p')$ as $N \to \infty$.

At last, the spectrum handoff with radio sensing scheme needs to performs the radio sensing and spectrum handoff for each handoff trail. Let T_s be the time a secondary user requires to accomplish a radio sensing, and then $E[t_{SU}^{SHOS}]$ becomes

$$\begin{aligned} E[t_{SU}^{SHOS}] &= (1-p)^{M-1}T^{SU} + \binom{M-1}{1}p(1-p)^{M-2}\left[(T_s+T_o)+T^{SU}\right] + \cdots \\ &\quad \binom{M-1}{N}p^N(1-p)^{M-1-N}\left[N(T_s+T_o)+T^{SU}\right] \\ &= \sum_{i=0}^{N}\binom{M-1}{i}p^i(1-p)^{M-1-i}\left[i(T_s+T_o)+T^{SU}\right] \ . \end{aligned} \tag{5.10}$$

When $N = M$, the transmission time in (5.10) can be written by

$$E[t_{SU}^{SHOS}] = T_{SU} + (M-1)p(T_o+T_s) \ . \tag{5.11}$$

Tab. 5.1: System Parameters of the Spectrum Handoff for Link Maintenance

slot time	10 μsec
PU transmission time	2.5 msec
payload length of a secondary user's transmission (l_{SU})	1500 bytes
secondary user transmission's speed (r_{SU})	12 Mbps
execution time for a spectrum handoff trial (T_o)	100μsec$\sim$10msec
the secondary user's radio sensing time (T_s)	100μsec$\sim$10msec
frame error rate for a secondary user's transmission (p_e)	10^{-2} & 10^{-1}
channel prediction error probability (p_s)	$10^{-3} \sim 10^{-1}$
primary user appearance probability in a slot (p_{PU})	$10^{-3} \sim 10^{-1}$

5.3 Numerical Results

In this section, we investigate the performances of the link maintenance probability and the effective data rate for the secondary user's transmission. Both primary and secondary users's transmissions are partitioned into slots. The primary user adopts the connection-oriented MAC protocol, in which the user first requests to establish connection and transmits data according to the information broadcasted by the base station. The secondary user overhears the broadcast messages to synchronize the timing with the legacy system and to avoid interfering the primary user's transmissions by acquiring the schedule. Here, we assume that the slot time and a primary user's transmission time are 10 μsec and 2.5 msec, respectively. Without any special notice, the values of the system parameters considered in this paper are shown in Table 7.1.

5.3.1 Performance of effective data rate for a reliable secondary user's link

First, we consider the situation when the secondary user's link can be always successfully maintained, that is $p_m = 1$. Figures 5.4(a) and (b) illustrate the impact of the primary user's traffic load on the effective data rate. As we can expect, the effective secondary user's data rate in both spectrum handoff schemes are higher that the non-spectrum-handoff transmission scenario if $p_s \leq 0.15$ or $T_s \leq 1.5$ msec. Intuitively, for the non-spectrum-handoff transmission scenario, the secondary user requires to wait a long period of time for primary user's transmissions. Thus, the effective secondary user's data rate is decreased due to the prolonged transmission time.

Also shown in Figs. 5.4(a) and (b), one can observe that the effective data rate performance is sensitive to the changes of the channel prediction error probability p_s and the radio sensing time T_o. For the pre-determined channel list spectrum handoff scheme in Fig. 5.4(a), when the prediction error p_s increases from 0.1 to 0.5, the effective data rate decreases from 35 Kbps to 10 Kbps. Similarly, for the spectrum handoff with radio sensing scheme, R_{SU} becomes from 35 Kbps to 7 Kbps as the radio sensing time T_s changes from 1 msec. to 10 msec. Obviously, increasing the radio sensing time delays the secondary user's transmission time, and thus decreases the effective data rate. On the other hand, the large prediction error raises the required number of spectrum handoff trails, and also decreases the effective data rate due to the prolonged transmission time. Therefore, from this observation, it is worthwhile to carefully design the system parameters of the spectrum handoff for both the considered schemes.

Compare the performances in Figs. 5.4(a) and (b). As $p_{PU} = 0.5 \sim 0.9$, the effective data rate for the spectrum handoff with radio sensing scheme is higher than the pre-determined channel list spectrum handoff. For example, for $p_{PU} = 0.9$, the effective data rates in the spectrum handoff schemes with and without radio sensing

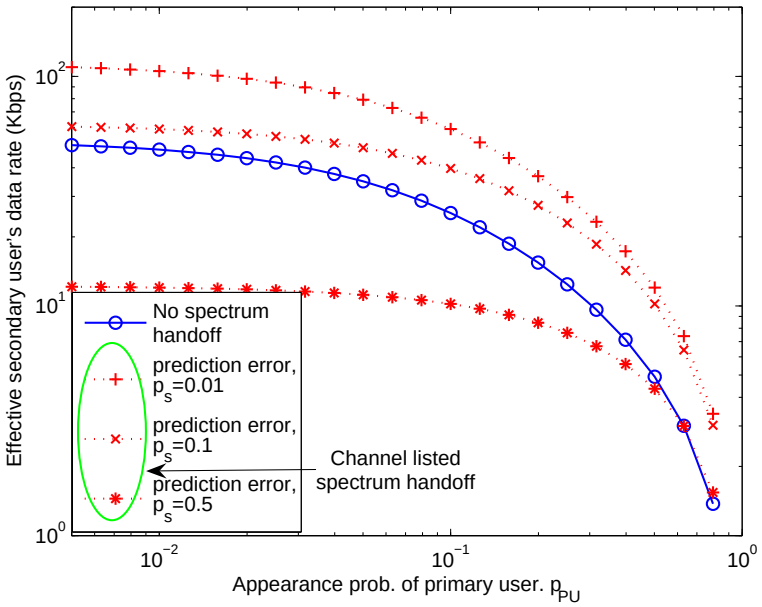

(a) Non-spectrum-handoff versus pre-determined channel list spectrum handoff schemes

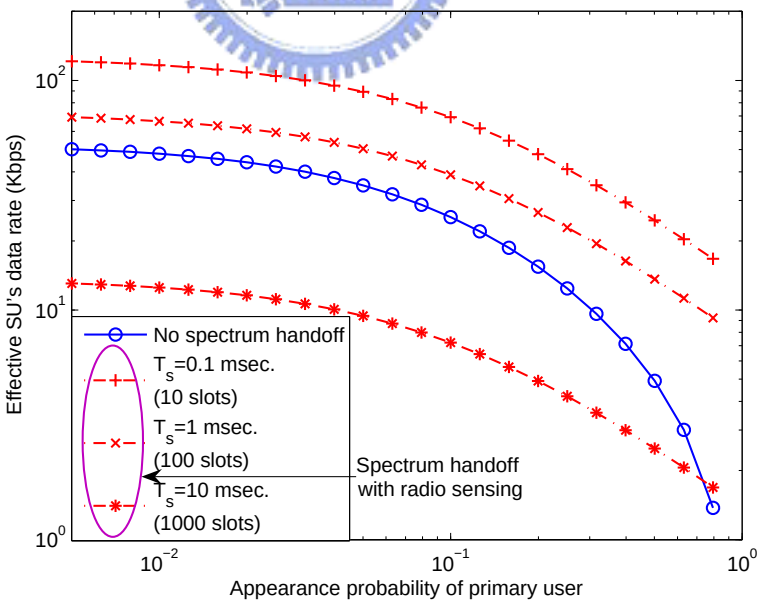

(b) Non-spectrum-handoff versus spectrum handoff with radio sensing schemes

Fig. 5.4: Impact of primary user's traffic load on the effective data rate if the secondary user's transmission is reliable.

are 9 Kbps and 3 Kbps, respectively. In this situation, the radio sensing ensures that the secondary user can select the correct target channel, and thus effectively lowers the required handoff trials. However, the erroneous channel prediction makes the secondary user require more handoff trials to maintain the link. Therefore, the effective data rate for the scheme of spectrum handoff with radio sensing is higher than the pre-determined channel list spectrum handoff in the case of the high primary user's traffic load.

Figure 5.5 shows the impacts of the spectrum handoff execution time and the frame error rate for a secondary user's transmission on the effective secondary user's data rate. Obviously, the longer the execution time the lower the effective data rate. Interestingly, in the case of the short handoff execution time, the pre-determined channel list spectrum handoff outperforms the other two schemes. This is because the secondary user can quickly switch to the target channel even to the incorrect channel, whereas the other schemes have to wait for an extra period of time for a primary user's transmission or radio sensing. Thus, the channel-listed spectrum handoff is better than the other two schemes as $T_o \leq 1.5$ msec.

On the other hand, the impact of secondary user's frame error rate (FER) is insignificant compared to the other parameters. The erroneous secondary user transmission only postpones the transmission in the later one slot, while the erroneous channel prediction makes secondary user wait an extra primary user's transmission time or radio sensing time. The duration of a slot time is much shorter than the duration of the other two time periods. Thus, the FER of the secondary user's transmission will not be an important parameter for the spectrum handoff.

5.3.2 Impacts of spectrum handoff trials

Figure 5.6 shows the link maintenance probability versus the number of spectrum handoff trials. Apparently, the more the handoff trials the higher the link maintenance probability. Furthermore, it is interesting that the required number of handoff trials

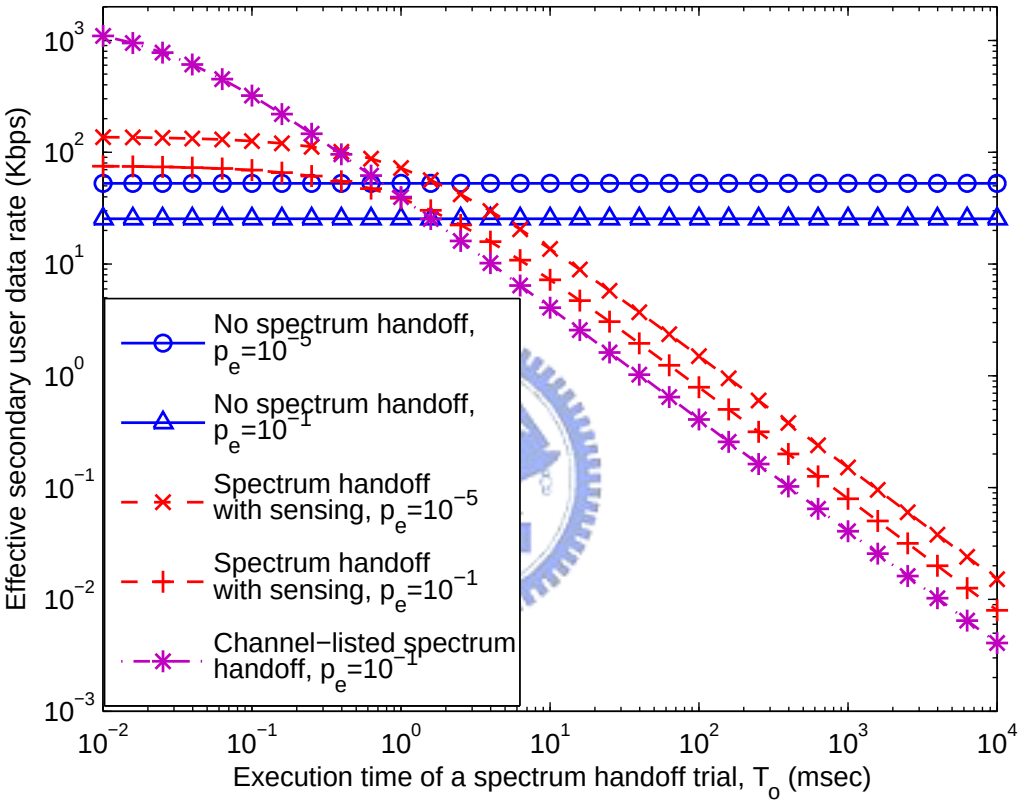

Fig. 5.5: Impact of the handoff execution time on the effective data rate if the secondary user's transmission is reliable.

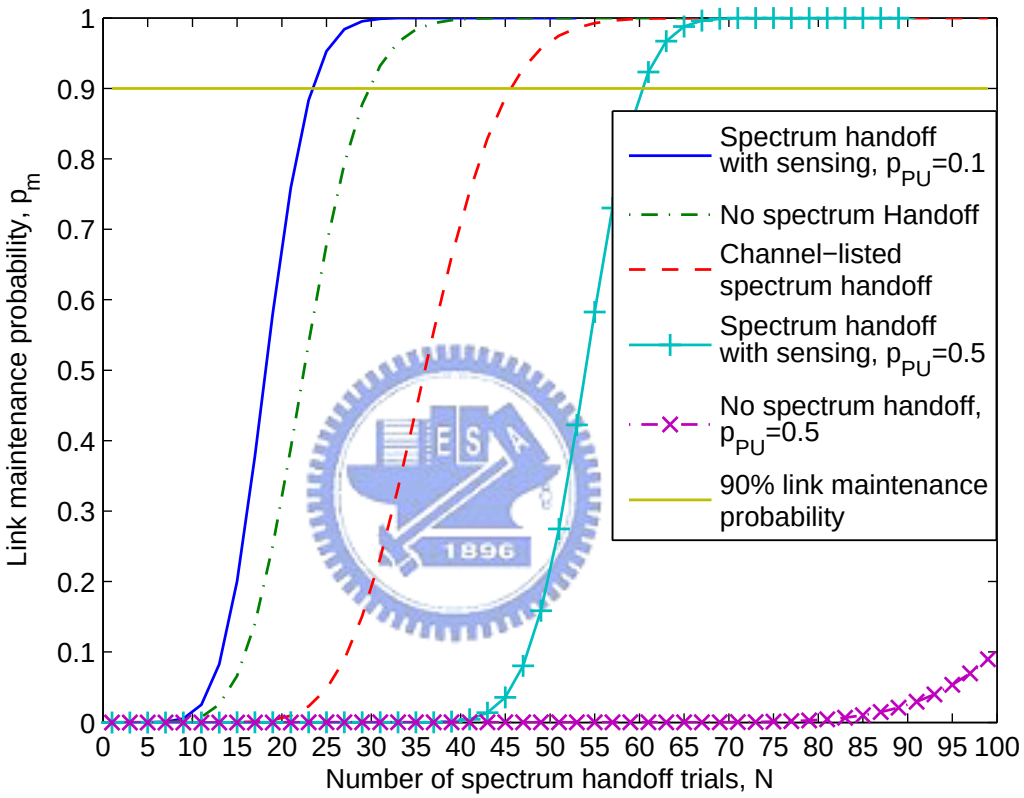

Fig. 5.6: Impact of spectrum handoff trials on the link maintenance probability of a secondary user's transmission.

for the pre-determined channel list scheme is larger than the other two schemes due to the error possibility of channel prediction. On the other hand, in the case of high primary user's traffic load, the spectrum handoff with radio sensing scheme only requires much less handoff trials than the other two schemes. This is because the former scheme can always select the correct channel lasting at least one slot for the remaining secondary user's transmissions. However, the later two schemes may encounter the situation of the continuous primary user's transmissions or the channel prediction error, both of which increase the required number of handoff trials. Thus, the scheme with radio sensing can confine the number of handoff trials within a small value.

5.3.3 Design of system parameters for spectrum handoff schemes

At last, we discuss the system parameter design for the two considered spectrum handoff schemes. Figure 5.7 (a) illustrates the required number of handoff trials N and the maximum channel prediction error probability p_s for the given effective data rates and when $T_o = 100\mu$sec. and $p_{PU} = 0.1$. Similarly, Fig. 5.7 (b) shows the required number of handoff trials N and the maximum radio sensing time T_s. Here, the presented data for the two spectrum handoff schemes have to satisfy two criteria: (1) the link maintenance probability $p_m > 0.9$ and (2) the lower average transmission time compared to the non-spectrum-handoff method. As shown in the both figures, given an effective data rate, the required number of handoff trials increases as the channel prediction error p_s or the radio sensing time increases. However, when the handoff trials is more than a certain threshold, the maximum allowable channel selection error or sensing time is decreased. This phenomenon can be explained into two folds. On the one hand, adding the number of handoff trials raises the link maintenance probability and increases the allowable error probability of channel selection or sensing time. On the other hand, when the handoff trials is too many, the average secondary

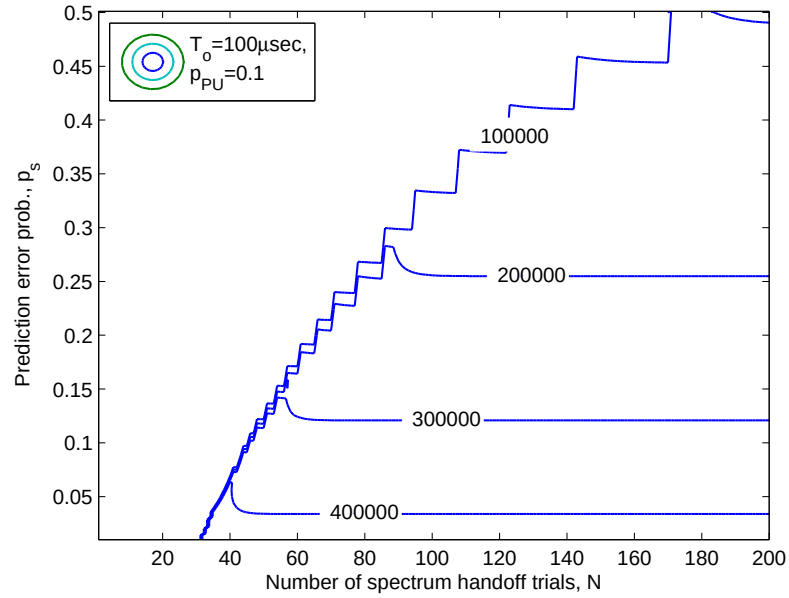

(a)

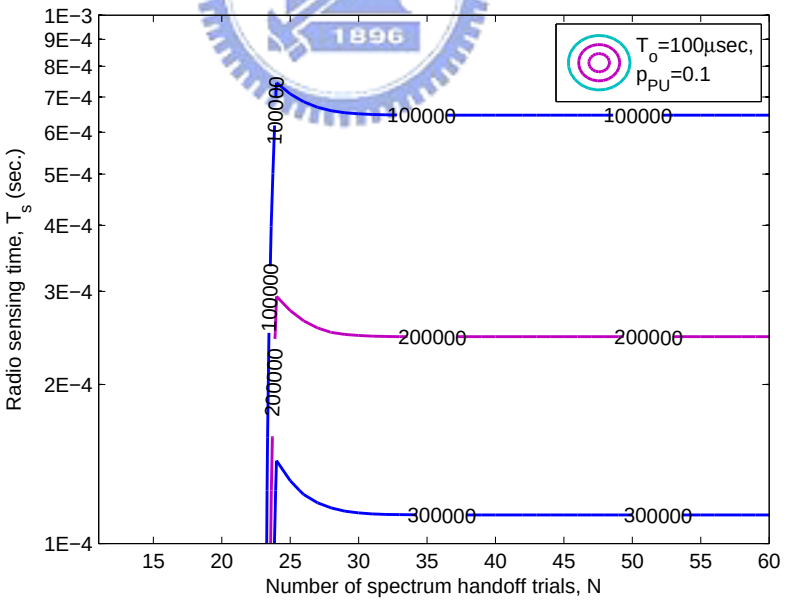

(b)

Fig. 5.7: Contour of the effective data rate for the system parameters (a) p_s and N in the pre-determined channel list spectrum handoff scheme and (b) T_s and N in the spectrum handoff with spectrum sensing scheme when $p_{PU} = 0.1$ and $T_o = 100$ μsec, respectively.

user's transmission time in the two handoff schemes becomes longer than that in the non-spectrum-handoff case. Thus, the maximum error probability and sensing time is decreased to satisfy the delay requirement.

5.4 Summary

In this part, we examined the performances of the three possible transmission scenarios for CR devices when the primary users appear in the occupied channel. The considered scenarios include: (1) non-spectrum-handoff scheme; (2) the pre-determined channel list spectrum handoff and (3) the spectrum handoff with radio sensing scheme. Based on the developed model, we investigated the impacts of the channel prediction error probability, the radio sensing time, the number of handoff trials, the primary user appearance probability, the frame error rate of the secondary user's transmissions and the handoff time. The numerical results show that the spectrum handoff with the radio sensing scheme outperforms the pre-determined channel list spectrum handoff in the case of the high primary user appearance probability due to the more successful channel selection for the handoff. The results also reveal that the performances of secondary users for the two spectrum handoff schemes is sensitive to the prediction error probability, the radio sensing time and the number of handoff trials. At last, given an effective data rate and the link maintenance probability, we provide the design guide of the system parameters so that the effective data rate of the two handoff schemes is higher than the non-spectrum-handoff case.

Chapter 6

Cross-layer Analysis for A Cognitive MAC: Single Channel CSMA/CA Case Study

The objective of this part is to develop such a cross-layer analytical model to accurately evaluate the throughput of the CSMA/CA MAC protocol. To our knowledge, in the context of the IEEE 802.11 WLAN, an analytical throughput model taking into account of the effects of a practical directional antenna pattern, capture, log-normal shadowing, multipath Rayleigh fading and the number of radio transceivers is still lacking in the literature. Here, we provide the complete derivation of the PHY/MAC analytical model and the more detailed simulation results. Furthermore, we discuss the impacts of SINR requirement, shadowing parameters, directional antenna gain patterns and the number of radio transceivers for both the uplink and downlink transmissions.

6.1 Motivation

As the demand for the WLAN services has grown dramatically recently, it becomes a crucial issue to further improve the performance for the CSMA/CA based WLAN. In the literature, there have been mainly three research directions for this issue. The first direction is from the MAC protocol perspective [111, 114, 124–127]. The authors in [114, 124] proposed a dynamic tuning algorithm to adjust the backoff window size according to the traffic load. In addition, a fast backoff procedure was proposed in [111]. Packet pipeline scheduling [125] and the out-of-band signaling [126] were proposed to reduce the possibility of frame collision. In [127], a frame concatenation mechanism was introduced to reduce the protocol overhead. The second research

direction to improve the throughput of the CSMA/CA based WLAN is to incorporate the capture effect [80, 81, 128]. With capture effect, a user can transmit data even with other simultaneously transmitting users. The third research direction is to adopt directional or smart antennas in WLAN [129–141]. The main objective of these works was to modify the MAC protocol to exploit the advantages of directional or smart antennas. These MAC protocols can be categorized into three types: 1) multiple antennas equipped with one radio transceiver and one network allocation vector (NAV) [129–132]; 2) multiple antennas equipped with one radio transceiver, but each antenna is associated with distinct directional network allocation vector (DNAV), and the new MAC protocol is designed to dynamically switch antenna to the desired users [133–136]; 3) multiple antennas and radio transceivers, each of which is also associated with independent NAV [137–141]. However, most of these MAC protocols considered only an ideal directional antenna pattern and ignore the effects of capture and frame outage.

6.2 MAC Layer Throughput Performance: Previous Analysis

In Section 6.4, we will propose a PHY/MAC cross-layer analytical model for the CSMA/CA MAC protocol that extends from [69] to further incorporate the effects of frame capture, outage and a practical gain pattern of directional antennas on the backoff process in the presence of shadowing and Rayleigh fading. To this end, we first summarize the work of [69], and then describe the method of incorporating capture effect in the CSMA/CA protocol.

6.2.1 CSMA/CA Backoff Process without Capture Effect

The backoff process aims to resolve the contention issue when multiple users access a common radio channel. According to the CSMA/CA MAC protocol, all users wait

for a random duration before transmission. The waiting time is randomly chosen between zero and the backoff window size. Previous outcomes of channel contention will affect the backoff window size. According to the IEEE 802.11 WLAN, the backoff window size is doubled in the next attempt if a frame is collided in the current attempt. When a frame is successfully transmitted or a new frame requests to send, the backoff window size will be reset to the minimum value.

In [69], the author proposed an analytical model to evaluate the saturation throughput for the CSMA/CA MAC protocol. According to the analytical model in [69], the stationary transmission probability τ can be written as follows:

$$\tau = \frac{2}{1 + W_0 + p_c W_0 \sum_{i=0}^{b-1} (2p_c)^i} \ . \tag{6.1}$$

From (7.5), it is implied that a smaller value of p_c leads to a higher transmission probability (τ). However, a higher transmission probability also results in more collisions. For N contending users, the frame collision probability (p_c) is

$$p_c = 1 - (1 - \tau)^{N-1}. \tag{6.2}$$

Jointly solving (7.5) and (6.2), we can obtain the stationary transmission probability τ for a given N and the range of the backoff window size $(W_0, 2^b W_0)$.

Define the normalized system throughput (S) as the fraction of time that the channel is used to transmit payload successfully. Also, note that the successful transmission probability (p_s) can be computed as the probability that only one user transmits frame under the condition that at least one user is active, i.e.,

$$p_s = \frac{N\tau(1-\tau)^{N-1}}{p_{tr}}, \tag{6.3}$$

where $p_{tr} = 1 - (1 - \tau)^N$ is the probability that at least one user is active.

Hence the normalized system throughput (S) can be expressed as

$$\begin{aligned} S &= \frac{E[\text{payload transmitted during one slot}]}{E[\text{slot duration}]} \\ &= \frac{p_s p_{tr} \mathrm{E}[P]}{(1 - p_{tr})\sigma + p_{tr} p_s T_s + p_{tr}(1 - p_s) T_c} \ , \end{aligned} \tag{6.4}$$

where $E[\mathrm{P}]$, T_s, T_c, and σ represent the average payload size, average successful transmission duration, average collision duration, and an empty slot time, respectively.

6.2.2 CSMA/CA with Capture Effect

In [80], the author extended the model of [69] to incorporate the capture effect. The capture probability (p_{cap}) is defined as the probability that the received SIR of a transmitted frame (γ) is higher than a required threshold z_0. That is,

$$p_{cap} = \sum_{i=1}^{N-1} R_i \cdot \Pr(\gamma > z_0 | i) \ , \tag{6.5}$$

where R_i represents the probability of the total $(i+1)$ frames contending for transmissions in the same time slot, i.e.,

$$R_i = \binom{N}{i+1} \tau^{i+1} (1-\tau)^{N-i-1} \ . \tag{6.6}$$

In [80], the successful transmission probability with capture effect is then defined as

$$p_s = \frac{N\tau(1-\tau)^{N-1} + p_{cap}}{1-(1-\tau)^N} \ . \tag{6.7}$$

Following the remaining steps in [69], the throughput performance of the CSMA/CA with capture effect can be obtained based on the modified successful transmission probability in (6.7). However, the transmission probability τ in [80] is calculated in a lossless channel based on the Bianchi's method [69], where the effects of frame outage and capture in the physical layer are not considered in the binary backoff process.

In fact, the frame outage decreases the stationary transmission probability (τ); whereas the capture effect increases it. Therefore, in our paper, we consider both the frame outage and capture effects when evaluating the stationary transmission probability in the binary backoff process. We will show how the frame outage and capture effects influence the transmission probability during the backoff process.

6.3 Physical Layer Effects

In the time varying wireless channel, a user may fail to receive the packet in the following two scenarios. First, when the received signal strength of a frame is lower than the required threshold due to large propagation attenuation even without any other contenders, the frame outage occurs and which the probability is denoted by p_o. Second, when the received signal power of the desired frame ($P_{desired}$) does not exceed the interference power of other $(N-1)$ frames with enough margin, the frame is not captured and which the probability is denoted by p_{nc}. In this section, we first derive the frame outage probability in a log-normally shadowed Rayleigh fading channel with a practical directional antenna.

6.3.1 Radio Channel Characteristics

In this paper, we consider the common channel effects: path loss, shadowing, and Rayleigh fading [142]. Path loss describes the power attenuation due to the propagation distance (r) between a user and the access point. Usually, path loss is modelled as $r^{-\eta}$, where η is the path loss exponent. Hereafter, we choose $\eta = 4$ in this paper. Shadowing is caused by terrain features and can be characterized by a log-normal random variable $10^{\xi/10}$, where ξ is a Gaussian random variable with zero mean and a standard deviation of σ dB. At last, Rayleigh fading characterizes the impact of multipath propagation.

Let P_t be the transmission power of a user and consider the antenna gain $G(\theta)$ with the incident angle θ. Then the received signal power P_r at an access point can be written as

$$P_r = P_t r^{-4} G(\theta) 10^{\xi/10} x^2 \ , \tag{6.8}$$

where x is a Rayleigh distributed random variable with unit power and has the prob-

ability density function (pdf) as follows:

$$f_X(x) = 2xe^{-x^2} \ . \tag{6.9}$$

Let $Y = X^2$. Then the cumulative density function of Y is

$$F_Y(y) = 1 - e^{-y} \ . \tag{6.10}$$

6.3.2 Outage Probability

The frame outage probability is evaluated when only one user accesses the wireless channel without other competing users. In this case, the total interference power is zero (i.e. $P_I = 0$), and the frame outage probability can be expressed as

$$\begin{aligned} p_o &= \Pr\{\text{SNR} < z_0\} \\ &= \Pr\left\{\frac{P_t r^{-4} G(\theta) 10^{\xi/10} y}{N_0} < z_0\right\} \\ &= \Pr\left\{y < z_0 \frac{N_0}{P_t} r^4 G(\theta)^{-1} 10^{-\xi/10}\right\}, \end{aligned} \tag{6.11}$$

where z_0 is the required received SNR threshold, and N_0 is the noise power. In the IEEE 802.11 standards, a WLAN device can adopt different modulation and coding schemes according to channel conditions. To evaluate the effect of different transmission rates on the outage probability, we can apply the required received SNR threshold z_0 in accordance with the selected modulation and coding scheme in (6.11).

6.3.3 Effect of Directional Antenna on Outage Probability

Now, we discuss the impact of directional antennas on the frame outage probability. Let L be the cell radius and denote θ_{3dB} the 3 dB beamwidth of the directional antenna. Assume that the users are spatially and uniformly distributed within a cell, and thus the pdf of the distance (r) and angle (θ) between the user and access point can be given by $f_r(r) = 2r/L^2$, $f_\theta(\theta) = 1/2\theta_{3dB}$, respectively [143]. From (6.10) and

(6.11), we can have

$$
\begin{aligned}
p_o &= \Pr\left\{ y < z_0 \frac{N_0}{P_t} r^4 G(\theta)^{-1} 10^{-\xi/10} \right\} \\
&= \int_{-\theta_{3dB}}^{\theta_{3dB}} \int_{-\infty}^{\infty} \int_{0}^{L} F_Y \left(z_0 \frac{N_0}{P_t} r^4 G(\theta)^{-1} 10^{-\xi/10} \right) \cdot \\
&\quad f_r(r) f_\xi(\xi) f_\theta(\theta)\, dr d\xi d\theta \\
&= \int_{-\theta_{3dB}}^{\theta_{3dB}} \int_{-\infty}^{\infty} \int_{0}^{L} \left(1 - e^{z_0 \frac{N_0}{P_t} r^4 G(\theta)^{-1} 10^{-\frac{\xi}{10}}} \right) \cdot \\
&\quad \left(\frac{e^{-\xi^2/2\sigma^2}}{\sqrt{2\pi}\sigma} \right) \cdot \left(\frac{2r}{2\theta_{3dB} L^2} \right) dr d\xi d\theta \ , \qquad (6.12)
\end{aligned}
$$

where $f_\xi(\xi) = e^{-\xi^2/2\sigma^2}/\sqrt{2\pi}\sigma$ represents the distribution of the log-normal shadowing.

Figure 6.1 shows two antenna patterns with 3 dB beamwidth of 120^o and 60^o, respectively [144, 145]. The antenna gain patterns shown in the figure will be used to evaluate the impact of directional antenna on the MAC layer throughput later. Note that inside the 3 dB beamwidth, the gains at different angles are not exactly the same. Therefore, in calculating the outage probability, we need a more practical antenna gain pattern of a sector. Furthermore, it is noteworthy that for 120^o antenna, the gain at the angle of 75^o from the main lobe is only about 6 dB less than that in the main lobe. Hence, the antenna gain outside the 3 dB beamwidth cannot be totally neglected, which is especially important in evaluating the capture effect. The impacts of an imperfect antenna on both outage performance and capture effect are not fully considered in the current literature.

6.4 Cross-layer Throughput Analysis

In this section, we introduce a cross-layer analytical model to evaluate the throughput performance for the CSMA/CA MAC protocol with capture effect and a practical directional antenna. First, we derive the frame capture probability (p_{cap}) when mul-

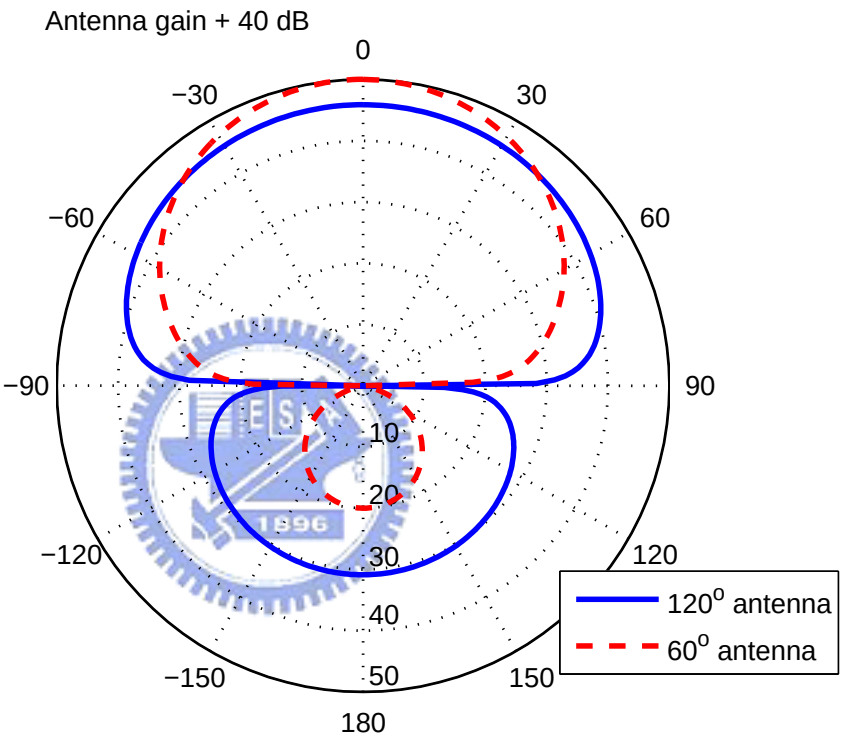

Fig. 6.1: Examples of antenna gain pattern for 120^o and 60^o directional antennas.

tiple users transmit frames at the same time. Then, we combine all the wireless channel impacts, including the frame outage, the capture effect and the gain leakage of a practical direction antenna, to evaluate the throughput of the CSMA/CA MAC protocol.

6.4.1 System Model

Figure 6.2 illustrates an access point equipped with three directional antennas. A user is usually connected to the sector antenna whose antenna gain is the largest within a cell. In the figure, users A and B communicate with antenna S1, user D communicates with antennas S2, and user C is with antenna S3.

Note that the three directional antennas can share one radio transceiver or can be associated with three independent radio transceivers. In the case with one radio transceiver, the access point can communicate only with one user within a cell by steering the antenna to receive and transmit the signal. On the contrary, in the case with three radio transceivers, the access point simultaneously transmits data frames to three users in three corresponding sectors. For example, if the access point equips with three radio transceivers, users A, C, and D in the figure can simultaneously transmit frames to the access point via antennas S1, S2, and S3, respectively.

6.4.2 Capture Effect

Capture effect is the phenomenon that a communication link is established in the presence of other interfering users, while maintaining a satisfactory SINR. Since the interference power is usually higher than the noise power, the signal-to-interference ratio (SIR) is usually used when evaluating the capture probability.

Consider N users (labelled from 1 to N) that are sending the data frames to the

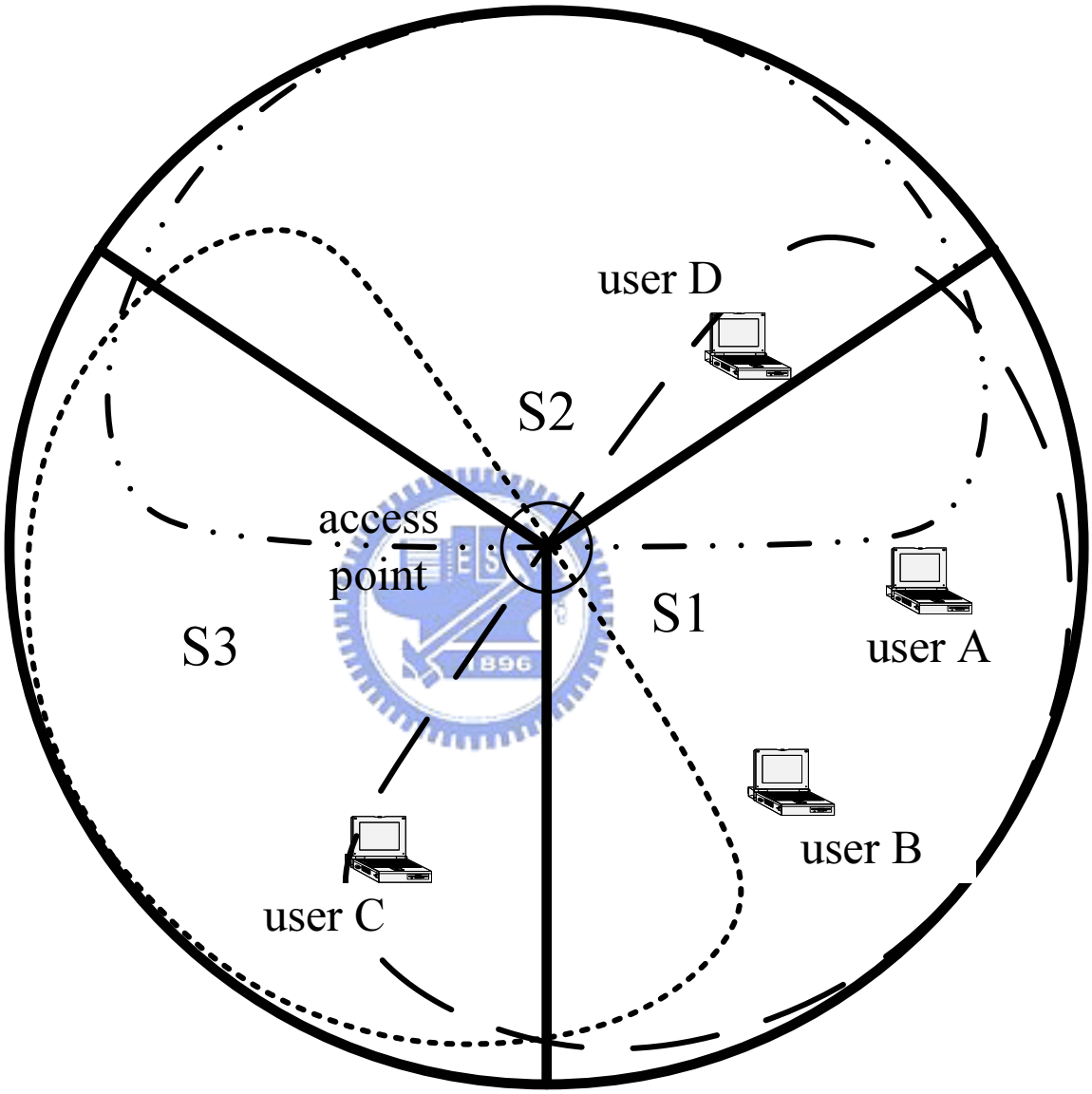

Fig. 6.2: The coverage pattern of a tri-sector cell with three 120^o directional antennas.

access point. The total frame capture probability ($p_{cap}(N)$) is defined as [146]

$$p_{cap}(N) = \Pr\left\{\left(\frac{P_1}{\sum_{i=2}^{N} P_i} > z_0\right) \cup \cdots \cup \left(\frac{P_N}{\sum_{i=1}^{N-1} P_i} > z_0\right)\right\}, \tag{6.13}$$

where z_0 is the required SIR threshold and P_i is the interference power from user i. Denote the frame capture probability of user "1" by $p_{cap,1}(N)$. From (6.8), the received power from user "1" and that from all the interfering users can be written by $P_1 = r_1^{-4} G(\theta_1) 10^{\frac{\xi_1}{10}} y_1$ and $\sum_{i=2}^{N} P_i = \sum_{i=2}^{N} r_i^{-4} G(\theta_i) 10^{\frac{\xi_i}{10}} y_i$, respectively. Thus, it is followed that

$$\begin{aligned} p_{cap,1}(N) &= \Pr\left\{P_1 > z_0 \sum_{i=2}^{N} P_i\right\} \\ &= \Pr\left\{y_1 > z_0 \sum_{i=2}^{N} \left(\frac{r_i}{r_1}\right)^{-4} \frac{G(\theta_i)}{G(\theta_1)} 10^{\frac{\xi_i - \xi_1}{10}} y_i\right\}. \end{aligned} \tag{6.14}$$

Represent $\boldsymbol{r} = (r_2, \cdots, r_N)$, $\boldsymbol{\theta} = (\theta_2, \cdots, \theta_N)$, and $\boldsymbol{\xi} = (\xi_2, \cdots, \xi_N)$ the distance, angle and the shadowing components between user i ($i = 2, \cdots, N$) and the access point, respectively. The frame capture probability of user "1" for a given $(\boldsymbol{r}, \boldsymbol{\theta}, \boldsymbol{\xi})$

can be expressed as

$$
\begin{aligned}
& p_{cap,1}(N, r_1, \theta_1, \xi_1 | \boldsymbol{r}, \boldsymbol{\theta}, \boldsymbol{\xi}) \\
&= \int_0^{\infty} \cdots \int_0^{\infty} \exp\left(-z_0 \sum_{i=2}^{N} y_i 10^{\frac{\xi_i - \xi_1}{10}} \frac{G(\theta_i)}{G(\theta_1)} \left(\frac{r_i}{r_1} \right)^{-4} \right) \cdot \\
&\quad e^{-y_2} \cdots e^{-y_N} dy_2 \cdots dy_N \\
&= \int_0^{\infty} \cdots \int_0^{\infty} \exp\left(-\sum_{i=2}^{N} y_i \left(1 + z_0 10^{\frac{\xi_i - \xi_1}{10}} \frac{G(\theta_i)}{G(\theta_1)} \left(\frac{r_i}{r_1} \right)^{-4} \right) \right) \\
&\quad \cdot dy_2 \cdots dy_N \\
&= \prod_{i=2}^{N} \frac{1}{1 + z_0 10^{(\xi_i - \xi_1)/10} \frac{G(\theta_i)}{G(\theta_1)} \left(\frac{r_i}{r_1} \right)^{-4}} \cdot
\end{aligned}
\tag{6.15}
$$

Assume all the interfering users are uniformly distributed in the cell coverage. Averaging over $\boldsymbol{r}$, $\boldsymbol{\theta}$, and $\boldsymbol{\xi}$, the capture probability of user "1" ($p_{cap,1}(N, r_1, \theta_1, \xi_1)$) is

$$
\begin{aligned}
& p_{cap,1}(N, r_1, \theta_1, \xi_1) \\
&= \int_{-\infty}^{\infty} \int_{-\pi}^{\pi} \int_0^1 \left[\prod_{i=2}^{N} \frac{1}{1 + z_0 10^{(\xi_i - \xi_1)/10} \frac{G(\theta_i)}{G(\theta_1)} \left(\frac{r_i}{r_1} \right)^{-4}} \right] \cdot \\
&\qquad f_r(\boldsymbol{r}) f_\theta(\boldsymbol{\theta}) f_\xi(\boldsymbol{\xi}) d\boldsymbol{r} d\boldsymbol{\theta} d\boldsymbol{\xi} \\
&= \left[\int_{-\infty}^{\infty} \int_{-\pi}^{\pi} \int_0^1 \frac{2 r_i \cdot e^{-\frac{\xi_i^2}{2\sigma^2}} \, dr_i d\theta_i d\xi_i}{2\pi \cdot \sqrt{2\pi}\sigma \cdot \left[1 + z_0 10^{\frac{\xi_i - \xi_1}{10}} \frac{G(\theta_i)}{G(\theta_1)} \left(\frac{r_i}{r_1} \right)^{-4} \right]} \right]^{N-1} .
\end{aligned}
\tag{6.16}
$$

To ease illustration, we denote the integral part of (6.16) by I(r_1, θ_1, ξ_1), i.e.,

$$I\left(r_1, \theta_1, \xi_1\right) = \int_{-\infty}^{\infty} \int_{-\pi}^{\pi} \int_{0}^{1} \frac{2r_i \cdot e^{-\frac{\xi_i^2}{2\sigma^2}}\, dr_i d\theta_i d\xi_i}{2\pi \cdot \sqrt{2\pi}\sigma \cdot \left[1 + z_0 10^{\frac{\xi_i - \xi_1}{10}} \frac{G(\theta_i)}{G(\theta_1)} \left(\frac{r_i}{r_1}\right)^{-4}\right]} \cdot \tag{6.17}$$

Since users 1 to N are assumed to be uniformly distributed and P_i are independent with each other, it can be shown that the average per user capture probability is the same for all users, i.e., $p_{cap,i}(N) = p_{cap,1}(N)$ for $i = 1$ to N. Averaging over r_1, θ_1 and ξ_1 in (6.16) to obtain the average per station capture probability $p_{cap,1}(N)$ and then following the definition in (6.13), we can obtain the total frame capture probability for N users $p_{cap}(N)$ as follows:

$$\begin{aligned} p_{cap}(N) &= N \cdot \int_{-\infty}^{\infty} \int_{-\theta_{3dB}}^{\theta_{3dB}} \int_{0}^{1} p_{cap,1}(N, r_1, \theta_1, \xi_1) \cdot \\ &\qquad f_r(r_1) f_\theta(\theta_1) f_\xi(\xi_1) dr_1 d\theta_1 d\xi_1 \\ &= \int_{-\infty}^{\infty} \int_{-\theta_{3dB}}^{\theta_{3dB}} \int_{0}^{1} N \cdot \left[I\left(r_1, \theta_1, \xi_1\right)\right]^{N-1} \cdot \\ &\qquad \left(\frac{2r_1}{2\theta_{3dB}}\right) \cdot \left(\frac{e^{-\frac{\xi_1^2}{2\sigma^2}}}{\sqrt{2\pi}\sigma}\right) dr_1 d\theta_1 d\xi_1 \ . \end{aligned} \tag{6.18}$$

Note that the integration over the distance in (6.17) and (6.18) takes into account of the relative distance from users to the access point, which is in the range (0,1].

According to [146], the integral in (6.17) can be simplified as

$$I\left(r_1,\theta_1,\xi_1\right)=\int_{-\pi}^{\pi}\int_{-\infty}^{\infty}\frac{e^{-\frac{\xi_i^2}{2\sigma^2}}}{2\pi\cdot\sqrt{2\pi}\sigma}\cdot \left[1-r_1^2\sqrt{z_0 10^{\frac{\xi_i-\xi_1}{10}}\frac{G(\theta_i)}{G(\theta_1)}}\cdot\arctan\left(\frac{1}{\sqrt{z_0 10^{\frac{\xi_i-\xi_1}{10}}\frac{G(\theta_i)}{G(\theta_1)}}}\right)\right] \cdot dr_i d\xi_i d\theta_i \ . \tag{6.19}$$

Then, applying the Hermite and Gaussian integration method of [142], the integrals with respect to variables ξ_1 and ξ_i in (6.18) and (6.19) can be simplified by a weighted sum of a function evaluated at some roots.

Furthermore, in (6.17) we also take into account of the interference from all the users in all the three sectors. Because the gain at the angle outside the 3 dB beamwidth cannot be neglected for a practical directional antenna, the interfering users may also be located in neighboring sectors. As shown in Fig. 6.2, users C and D in sectors S_3 and S_2 may interfere user A in sector S_1. Therefore, the first integration of $I(\cdot)$ in (6.17) needs to integrate from $-\pi$ to π, which is different from the case in evaluating the outage probability in (6.14).

So far we only focus on the uplink analysis when a user sends packets to the access point. The above analysis can be also extended to the the downlink transmission. In the downlink case, $N-1$ users are potential interferers. The capture probability in the downlink case, $p_{cap}^{'}(N)$, can be expressed by

$$p_{cap}^{'}(N)=\Pr\left\{y_1 \ > \frac{z_0}{G(\theta_1)}\sum_{i=2}^{N}\left(\frac{r_i}{r_1}\right)^{-4}10^{\frac{\xi_i-\xi_1}{10}}y_i\right\}. \tag{6.20}$$

As seen from (6.20), the role of the directional antenna on the capture effect in the downlink transmission is to increase the signal strength of the desired user. However, in the uplink transmission, not only can the directional antenna increase the the signal strength of the desired user, but suppress the interference from other users due to smaller $G(\theta_i)$ in (6.14) as $|\theta_i|$ increases. Since $p_{cap}^{'}(N)$ in (6.20) is a special case

of $p_{cap}(N)$ in (6.14), hereafter we will only consider the capture probability in the uplink transmission.

6.4.3 Probability of Packet Loss

Now, we investigate the impacts of frame outage and capture in the physical layer on the performance of the CSMA/CA MAC protocol. According to [69], the backoff process in the CSMA/CA MAC protocol are mainly characterized by the stationary transmission probability (τ) and collision probabilities (p_c). To establish the cross-layer interaction between the physical and MAC layers, the probability of packet loss (p_L) is introduced to replace p_c in the pure MAC layer analysis. Specifically, p_L is equal to the sum of the frame outage and non-capture probabilities in the presence of single and multiple users, respectively. That is, for N users, we can write

$$\begin{aligned}
p_L(N) = &\Pr\{\text{the channel is bad when only one user} \\
&\text{intends for transmission}\} + \\
&\Pr\{\text{the signal of the desired user is not captured} \\
&\text{in the presence of other interfering users}\} \\
=&\sum_{i=1}^{N-1}\binom{N-1}{i}(\tau^*)^i(1-\tau^*)^{N-i-1}(1-p_{cap}(i+1)) \\
&+(1-\tau^*)^{N-1}p_o \qquad (6.21) \\
\approx&(1-p_{cap}(N))\sum_{i=1}^{N-1}\binom{N-1}{i}(\tau^*)^i(1-\tau^*)^{N-i-1} \\
&+(1-\tau^*)^{N-1}p_o \\
=&(1-p_{cap}(N))\left[1-(1-\tau^*)^{N-1}\right] \\
&+(1-\tau^*)^{N-1}p_o\ . \qquad (6.22)
\end{aligned}$$

As shown in Fig. 6.3, the total frame capture probability is insensitive to the number of interfering users N as N increases. This phenomenon is also observed in [146–148]

through simulations. Thus in (6.22), we assume that $p_{cap}(2) = \cdots = p_{cap}(N)$ to reduce the calculation complexity. In Section 6.5, we validate the accuracy of this approximation by OPNET simulation tools.

At last, replacing p_L with p_c in (7.5), we rewrite the stationary transmission probability (τ^*) in the PHY/MAC cross-layer analysis as

$$\tau^* = \frac{2}{1 + W + p_L(N)W \sum_{i=0}^{b-1} (2p_L(N))^i} \ . \tag{6.23}$$

6.4.4 PHY/MAC Cross-layer Throughput

The PHY/MAC cross-layer throughput of the CSMA/CA MAC protocol in the composite log-normally shadowed and Rayleigh fading channel can be obtained by modifying (6.4). Incorporating the frame outage probability (p_o) and capture probability (p_{cap}) with the stationary transmission probability (τ^*) and its success probability (p_s^*) takes account of the physical layer impacts into calculating the MAC layer throughput.

Consider N users served within an access point. We define n as the effective number of users served by one radio transceiver for an access point equipped with multiple directional antennas. Note that n is dependent of the number of radio transceivers in an access point with multiple directional antennas. For a tri-sector cell, $n = N$ when the access point has only one radio transceiver; while $n = \frac{N}{3}$ if it equips with three radio transceivers. Here, for simplicity, we neglect the contentions from the stations outside the main lobe of a practical directional antenna.

Following (6.4), the throughput performance $S(n)$ delivered by one radio transceiver can be written by

$$S(n) = \frac{p_{tr}^* p_s^* \mathrm{E}[P]}{(1 - p_{tr}^*)\sigma + p_{tr}^*(1 - p_s^*)T_c + p_{tr}^* p_s^* T_s} \ , \tag{6.24}$$

where $p_{tr}^* = 1 - (1 - \tau^*)^n$. Furthermore, in (6.24), p_s^* is the successful transmission

probability in a network, which is function of p_{cap} and p_o, i.e.,

$$\begin{aligned} p_s^*(n) &= \frac{1}{p_{tr}^*} \cdot \Pr\{\text{the transmitted frame is captured and} \\ &\qquad \text{not subject to outage}\} \\ &= \frac{1}{1-(1-\tau^*)^n}[n\tau^*(1-\tau^*)^{n-1}(1-p_o)+ \\ &\quad \sum_{i=1}^{n-1}\binom{n}{i+1}(\tau^*)^{i+1}(1-\tau^*)^{n-i-1}p_{cap}(N)] \\ &\approx \frac{1}{1-(1-\tau^*)^n}[n\tau^*(1-\tau^*)^{n-1}(1-p_o)+ \\ &\quad (1-(1-\tau^*)^{n-1})p_{cap}(N)] \ . \end{aligned} \tag{6.25}$$

Note that the frame capture probability $p_{cap}(N)$ has to consider the total interference from all the sectors in an access point even when it is equipped with multiple radio transceivers due to the leakage gain of a practical directional antenna. As for the throughput performance for the particular user "i" ($S(n,i)$), (6.24) still can be reused, where the probabilities p_{tr}^* and $p_s^*(n)$ shall be changed to $p_{tr}^* = \tau^*$ and,

$$\begin{aligned} p_s^*(n,i) = \frac{1}{\tau^*}\big[&(1-\tau^*)^{n-1}(1-p_o)+ \\ &(1-(1-\tau^*)^{n-1})p_{cap,i}(N)\big] \ , \end{aligned} \tag{6.26}$$

respectively. The capture probability $p_{cap,i}(N)$ for user "i" in (6.26) can be obtained from (6.16).

To summarize, the PHY/MAC cross-layer throughput of the CSMA/CA MAC protocol can be calculated as follows:

1. Determine the required received SIR threshold (z_0) in (6.11) and (6.14) for the corresponding modulation and coding scheme. By choosing an appropriate z_0, the above analysis from (6.12) to (6.24) can be applied to the case with different transmission rates.

2. Calculate p_o and $p_{cap}(N)$ for the corresponding z_0 based on (6.12) and (6.18), respectively.

3. Find the stationary transmission probability τ^* by substituting p_L of (6.22) into (6.23), where $p_{cap}(N)$ and p_o affecting p_L are calculated in Step 2.

4. Determine the effective number of users n according to the number radio transceivers in an access point.

5. Calculate the successful transmission probability $p_s^*(n)$ by substituting τ^*, p_o, and $p_{cap}(N)$ into (6.25).

6. Obtain the throughput $S(n)$ of a radio transceiver in a multiple directional antenna system by substituting the stationary transmission probability τ^* and successful transmission probability p_s^* into (6.24).

The above throughput analysis are suitable for two cases: 1) multiple directional antennas sharing with one NAV and one radio transceiver; and 2) multiple directional antennas, each of which has an individual NAV and radio transceiver. It can be applied to the case of multiple directional antennas sharing with one radio transceiver and multiple DNAVs. However, this requires to model the dynamically changing number of effective contending users when switching directional antenna to the desired user based on the detail procedure of the DNAV-based MAC protocol. This is an interesting research topic in the future, but beyond the current scope of this paper. Nevertheless, we conjecture that the throughput of this DNAV-based MAC protocol will fall between the case of using one radio transceiver with one NAV shared by multiple antennas and that of using multiple radio transceivers with multiple NAVs.

6.5 Numerical Results

In this section, we present numerical results to compare the throughput performance of the CSMA/CA MAC protocol in WLAN with and without radio channel impacts. We consider a circular coverage area with the radius of 100 m and the shadowing

standard deviation equal to 6 dB. In our evaluation, we choose the IEEE 802.11b direct sequence spread spectrum (DSSS) mode for an access point with omni-directional and directional antennas. Figure 6.1 shows the antenna gain patterns of the directional antennas, and Table 6.1 lists other system parameters in both the analysis and simulation.

To demonstrate the channel impacts on the required capture threshold, two different packet lengths are studied with the requirement of frame error rate (FER) less than 8×10^{-2} [12]. Table 6.2 lists the required received SNR threshold (z_0) and the frame outage probability for the omni-directional, 120^o and 60^o directional antennas, respectively. A smaller packet of 60 octets requires smaller z_0 and can still achieve the same FER performance as the larger-sized 2,000 octet packet. Moreover, comparing the frame outage probability for both the omni-directional and directional antenna cases, one can find that the directional antenna can increase the received signal power and therefore reduce the frame outage probability.

6.5.1 Effect of Large Number of Contenders on Capture Probability

Figure 6.3 shows the frame capture probability versus the number of contending users with different capture thresholds, where the shadowing standard deviation is 6 dB. We can observe that the capture probability is almost the same when the number of contending users is more than 10. In fact, the phenomenon that the capture probability is insensitive for a large number of stations N can be explained from the derived analytical formulas (6.16) and (6.18). Based on (6.16), the per station capture probability for user 1 (denoted by $p_{cap,1}(N, r_1, \theta_1, \xi_1)$) decreases as the number of users N increases since there are more interfering users. However, according to (6.13), as N increases, the total capture probability for N users may also increase because all N users' signals are possibly captured. Combining both the impacts, the average total capture probability $p_{cap}(N)$ in (6.18) becomes insensitive to the number of users. This

Tab. 6.1: System Parameters of the Performance Evaluation for the Single Channel CSMA/CA MAC Protocol

MAC header	224 bits
PHY header	192 bits
ACK	304 bits
RTS	352 bits
CTS	304 bits
Bit rate	1Mbit/s
Propagation delay	1μs
Slot time	20μs
SIFS	10μs
DIFS	50μs
Minimum contention window	32
Maximum backoff stage	5
Transmission power, $P_{transmit}$	20 dBm
Noise power, N_0	-90 dBm

Tab. 6.2: Required SNR Threshold and Outage Probability for Different Packet Lengths

		Antenna type		
Packet length	z_0	Omni-directional	120^o	60^o
60 bytes	-1 dB	0.000685	0.000226	0.0000896
2000 bytes	0 dB	0.000861	0.000284	0.000113

phenomenon is also observed in [146–148] by simulations. It helps us to reduce the complexity in the proposed analytical model by using the approximation in (6.22).

6.5.2 Throughput Comparison for Different Approaches

Figure 6.4 compares the normalized throughput of the CSMA/CA MAC protocol based on different approaches. One can see that for the case without capture effect, the system throughput degrades severely when the number of users increases. This phenomenon is because frame collisions occur more frequently. For example, when the number of users increases from 50 to 100, the throughput decreases from 0.65 to 0.55. However, the throughput with capture effect only decreases from 0.75 to 0.65 when number of contenders increases from 50 to 100. Because the capture effect increases the successful transmission probability, the frame collision problem can be alleviated. Thus, the throughput performance can be improved, especially for large number of users.

Note that the improvement resulted from the capture effect is not much when the number of contenders is few. In this situation, the concurrent transmissions are so few that the performance improvement due to the capture effect is insignificant. However, based on the previous approach in [80], the improvements resulted from the capture effect seems too optimistic. Take $N = 10$ as an example. The throughput is about 0.8 in the case without capture, while the throughput based on the previous approach in [80] is 0.94. This is because the capture effect and frame outage is inherently assumed to be independent of the backoff window size in [80], thereby causing the overestimate of the throughput performance. Based on our analytical model, the throughput is 0.85 for $N = 10$, which provides a more reasonable evaluation.

Meanwhile, to validate the accuracy of our proposed analytical model, we also use OPNET simulation to verify the throughput performance in the CSMA/CA MAC protocol. In the simulation, the access point is located in the center of the cell, and all the users are spatially and uniformly located in the cell with radius 100 m. All

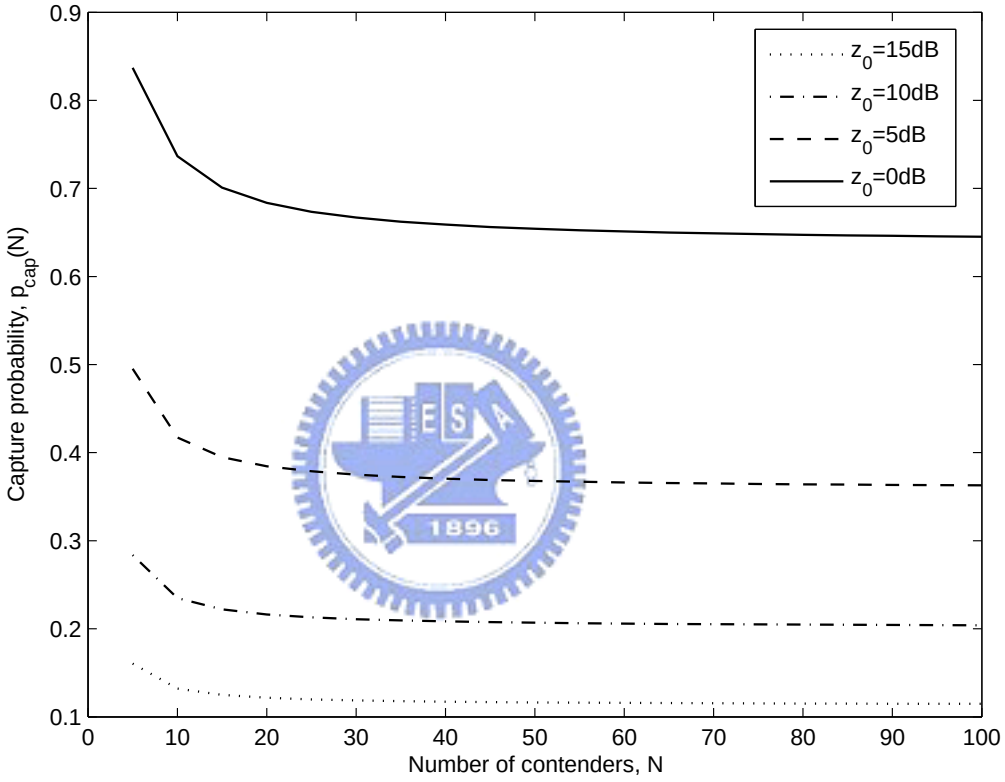

Fig. 6.3: The relation between the frame capture probability and number of contending nodes under the 6 dB shadowing standard deviation with different SIR threshold.

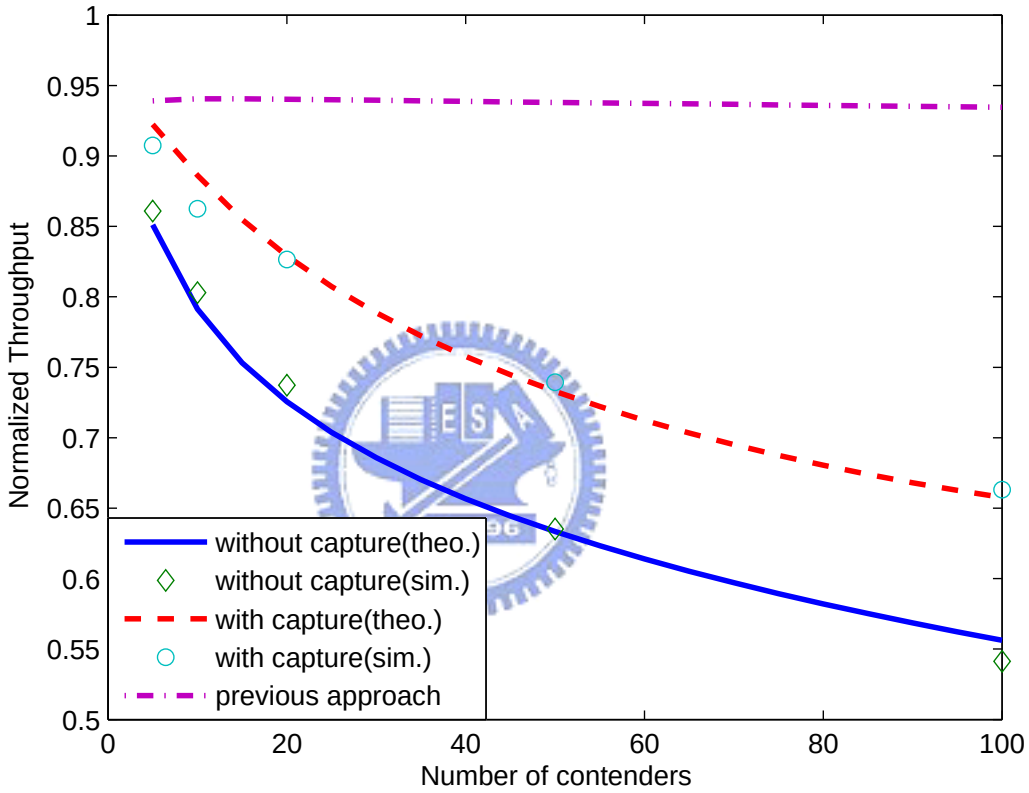

Fig. 6.4: Capture effect on the throughput of the CSMA/CA MAC protocol with an omni-directional antenna.

the users always transmit frames to the access point with frame length 2000 bytes. A frame is successfully captured by the access point if the received SIR is larger than the SIR threshold (z_0). The other parameters used in the simulation are listed in Table 6.1. As shown in the figure, both the simulation and analytical results almost match with each other, especially for a large amount of users. The discrepancy between the analysis and simulation with small number of users results from the approximation in (6.22). As shown in Fig. 6.3, the capture probability does not converge as N is small. Thus, there exists a difference between the exact and approximation values. However, the discrepancy between the analysis and simulation is small, and the developed model still has a certain level of accuracy.

6.5.3 Effect of Shadowing on the Throughput Performance

Figure 6.5 compares the throughput for various shadowing standard deviations (σ_ξ = 2 and 6 dB) and SIR thresholds (z_0 = 0 and 5 dB). As expected, the larger the SIR threshold, the lower the throughput because a more stringent SIR requirement results in more frame errors and higher frame outage probability. More interestingly, as shown in the figure, the throughput seemingly does not depend on the shadowing standard deviation. According to (6.24), the throughput S is determined by the probability of successful transmission p_s^* and stationary transmission τ^*, both of which are dominated by the capture probability. In [143,146–148], the authors were observed that the capture probability is insensitive to the shadowing parameters but only relates to the SIR threshold. Hence, the phenomenon observed in this paper regarding the shadowing effect on the throughput performance can be justified.

6.5.4 Effect of Direction Antennas on Capture Probability

Figure 6.6 compares the capture probability of the WLAN system with omni-directional and 120^o directional antennas. Obviously, higher requirement on the received SIR decreases the capture probability for both the omni-directional and directional cases.

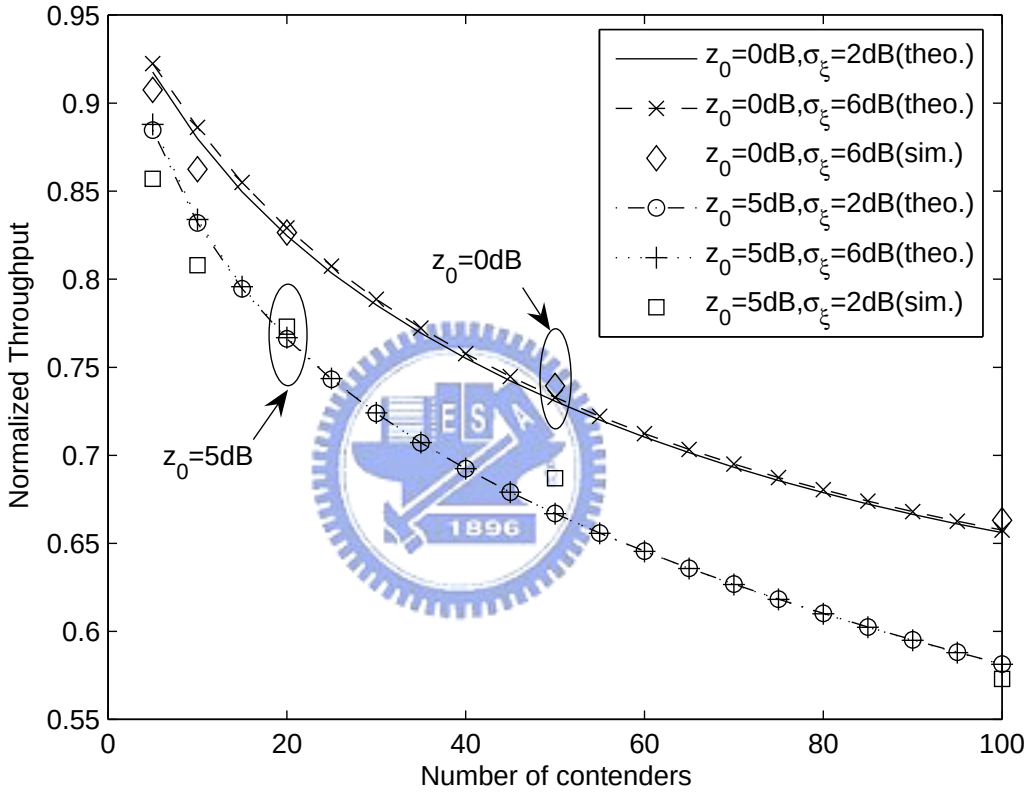

Fig. 6.5: Shadowing effect on the throughput of the CSMA/CA protocol with various SIR thresholds.

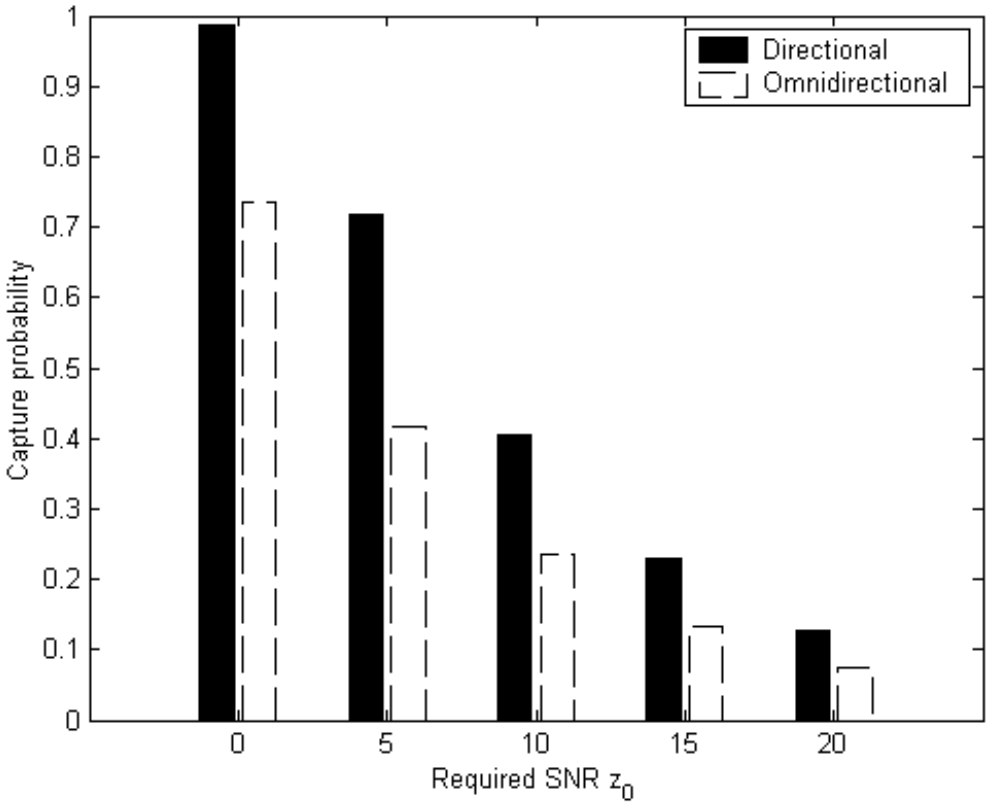

Fig. 6.6: Comparison of capture effect between omni-directional and directional antennas.

However, for the directional antenna case, the coverage area of an access point is divided into three sectors. Hence, the number of interfering users in a sector is less than that in an omni-directional antenna case. As a result, for the same capture probability, the required SIR for directional antenna case is about 5 dB less than that in omni-directional antenna case. The improvement for the capture probability between omni-directional and 120^o directional antennas approximates to the reduction ratio for the number of users in one sector (i.e. $10\log(3) = 5\ dB$).

6.5.5 Effect of Directional Antenna on Throughput Performance

Figure 6.7 shows how different kinds of directional antennas affect the throughput of the CSMA/CA MAC protocol. We consider a tri-sector access point, and each sector is equipped with a 60^o or 120^o directional antenna, respectively. In addition, two node configurations in the access point are considered: one with a single radio transceiver shared by three antennas and the other with three individual radio transceivers. From (6.24), the throughput performance $S(n)$ counts the information bits delivered by one radio transceiver. Thus, the performance in the figure for the multiple radio transceivers case represents the throughput of a single sector; whereas for the single transceiver case, it is the overall cell throughput.

For the case with one shared radio transceiver and the number of user $N = 100$, the normalized throughput is 66%, 70%, and 76% for omni-directional antenna, 120^o and 60^o directional antennas, respectively. Compared to the omni-directional antenna, the interference imposed at the angle of the side lobe of an directional antenna is lower due to a smaller antenna gain. Moreover, a directional antenna usually has higher antenna gain in the main lobe than an omni-directional antenna. Therefore, the throughput performance of an access point with directional antennas is higher than the throughput over the omni-directional access point even with one radio transceiver.

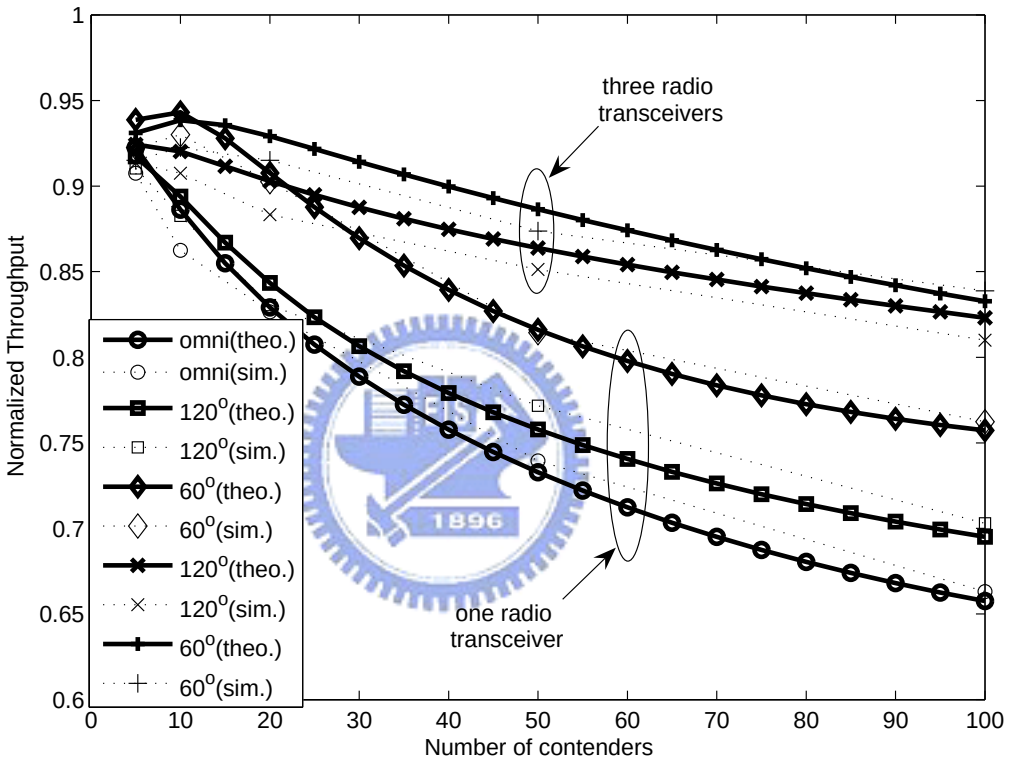

Fig. 6.7: Effects of multiple directional antenna with single/multiple radio transceivers and channel effects on the throughput of the CSMA/CA protocol.

Note that with three radio transceivers, the throughput of a single section can be further improved to 83% and 85% for 120^o and 60^o directional antennas, respectively. In the case of using multiple radio transceivers, the network is equivalent to one in which the coverage is divided into multiple independent sectors, thereby lowering the number of contenders per radio transceiver and decreasing collisions.

In Fig. 6.7, we also illustrate both the simulation and analytical results. In the simulation, the access point equips with three directional antennas with the gain patterns shown in Fig. 6.1. Due to the imperfect antenna gain pattern, in the simulation, the users in the region outside the main lobe may contend with that inside the main lobe; whereas the developed model neglects these users. Therefore, the contentions from the users in the side lobe and back lobe result in the discrepancy between the simulation and analytical results.

6.6 Conclusions

In this part, we demonstrate that the throughput of the CSMA/CA MAC protocol is insensitive to the shadowing parameters but only relates to the SIR threshold. In addition, directional antennas can improve the throughput up to 10% even with one radio transceiver. If the access point can be equipped with one radio transceiver for each directional antenna, the throughput of a single section can improve up to 20% due to the improved SIR and fewer effective contenders. This work can be the basis for some interesting research topics, such as the per station throughput evaluation or the overall throughput of the multiple directional antennas with multiple DNAVs in multi-hop networks.

Chapter 7

Resource Partition for A Hybrid MAC Based on Contention-oriented Cognitive Multi-channel CSMA/CA and Connection-oriented OFDMA/TDD

This chapter presents an analytical approach to determine the optimal number of reserved sub-channels and time slots for the random access scheme in the multi-channel contention-and connection-oriented MAC protocol, such as the OFDMA-based IEEE 802.16e system. We formulate an optimization problem to maximize the efficiency of the reserved radio resources while meeting the delay requirement for supporting real-time applications. It is noteworthy that we consider a multi-channel random access scheme based on the truncated binary backoff algorithm. Because multiple channels are reserved for contention, unlike the traditional carrier-sense multiple access (CSMA) MAC protocol in IEEE 802.11 WLAN, the multi-channel random access scheme can allow multiple users to access the sub-channels concurrently. Moreover, to resolve collisions during the contention period, the truncated binary backoff algorithm is implemented in the IEEE 802.16e WiMax system to adjust the user's transmission time according to the number of collisions in his previous attempt. Based on the proposed approach, performance enhancement can be achieved without changing the specifications of the IEEE 802.16e WiMax. To our knowledge, there have been few reports on the performance analysis of this kind of multi-channel random access scheme with the truncated binary backoff and its impact on the design of the optimal number of the reserved sub-channels and time slots in the OFDMA systems.

7.1 Motivation

Several previous studies have reported reducing access latency in the IEEE 80216e WiMax system. The authors in [149] suggested a method to simplify the conventional network entry/re-entry process. In [150], a new contention resolution algorithm was proposed for the multi-channel random access in OFDMA systems, in which data are transmitted at abundant sub-channels so that collisions and access delay are decreased. In [151, 152], a new set of orthogonal signals were designed to reduce the number of attempts for ranging, i.e., adjusting the uplink transmission power and timing. In [153], the authors suggested a sub-carrier permutation algorithm to improve the link reliability and to decrease the number of retransmissions. It seems that most of the aforementioned approach may require modifying the specifications of the current IEEE 802.16e WiMax system.

7.2 Background

7.2.1 Frame Structure and Link Establishment Procedures in the OFDMA-TDD Mode

Figure 7.1 illustrates the frame structure in the IEEE 802.16e OFDMA-TDD mode. As shown in the figure, a frame consists of two portions: the downlink and uplink sub-frames. A downlink sub-frame starts with preamble symbols followed by downlink map (DL-MAP) and uplink map (UL-MAP), which are used to inform the users of their allocated sub-channels and time slots for downlink and uplink transmissions, respectively. Next, downlink data are transmitted at allocated sub-channels and time slots. After an additional transmit/receive transition gap (TTG), the ranging and bandwidth request as well as users' data are transmitted in the uplink direction according to the UL-MAP. After a receive/transmit transition gap (RTG), the same

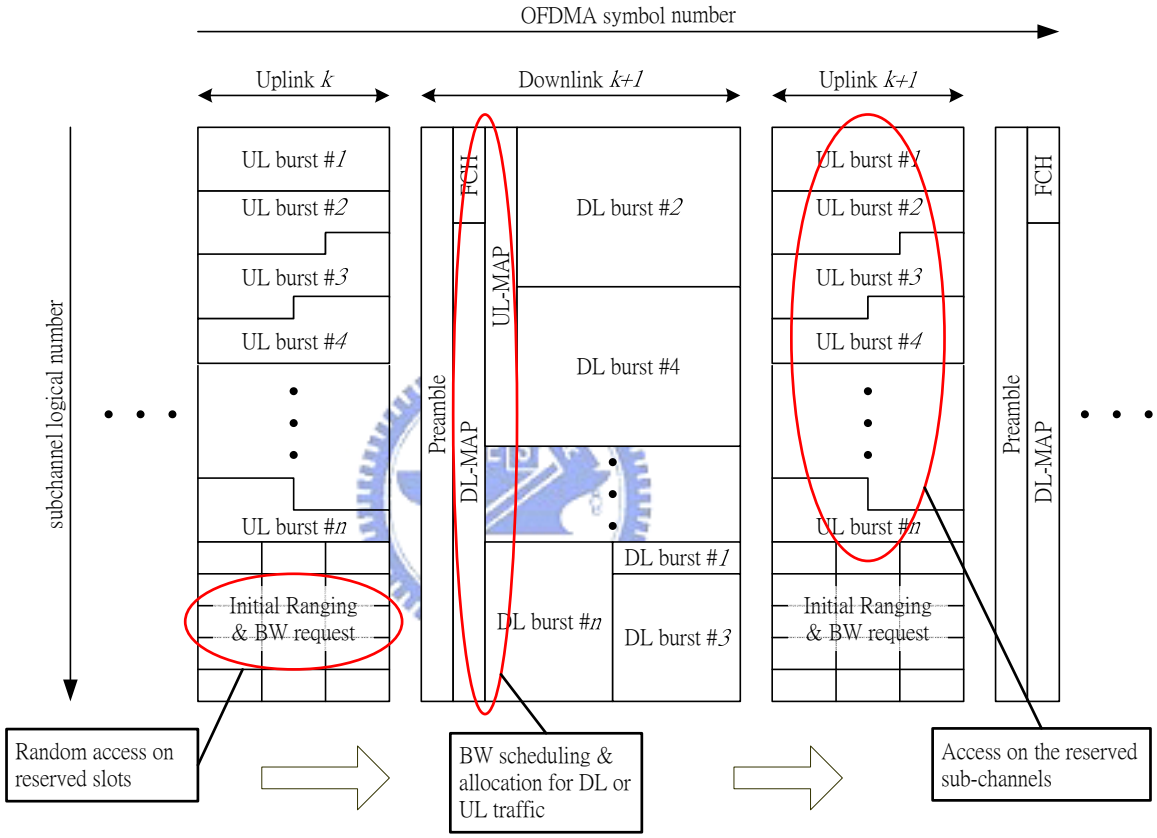

Fig. 7.1: Frame structure and Link Establishment of TDD-OFDMA mode in IEEE 802.16.

procedures are repeated for another pair of downlink and uplink sub-frames.

The IEEE 802.16e WiMax system adopts a connection-oriented MAC protocol. In this kind of MAC protocol, mobile stations must make a reservation with the base station before transmitting data. Consider the uplink transmission first. In Fig. 7.1, with packets ready to send in the *uplink sub-frame* k, mobile stations first transmit bandwidth requests to the base station at the reserved ranging/bandwidth request sub-channels. Receiving these requests, the base station allocates the sub-channels in the UL-MAP of the next *downlink sub-frame* $k+1$. In the downlink case, the base station negotiates the QoS requirements by using the dialog of dynamic service addition/change (DSA/DSC) messages on the mobile station's basic connection identifier (CID). After receiving the grant from the mobile station, the users' data are transmitted at the reserved sub-channels and time slots according to the DL-MAP.

To summarize, the base station coordinates the frame transmissions of all mobile stations in both the uplink and downlink based on the bandwidth request procedures and DSA/DSC dialog. However, a certain amount of resources must be reserved for the bandwidth request procedure and ranging in the network re-entry process, in which the mobile stations contend with each other. Thus, we must determine how large a chunk of sub-channels and time slots should be reserved for mobile stations to send the messages of bandwidth request. In the next section, we will formulate an optimization problem to design these parameters.

7.2.2 Multi-channel Random Access Protocol with Collision Avoidance

To transmit the initial ranging and bandwidth request messages, the IEEE 802.16e WiMax system adopts the multi-channel random access with the truncated binary exponential backoff algorithm [154,155]. This backoff algorithm is used to resolve the contentions between mobile stations in the process of random channel access. For a given initial backoff window size, a mobile station first selects a random number of

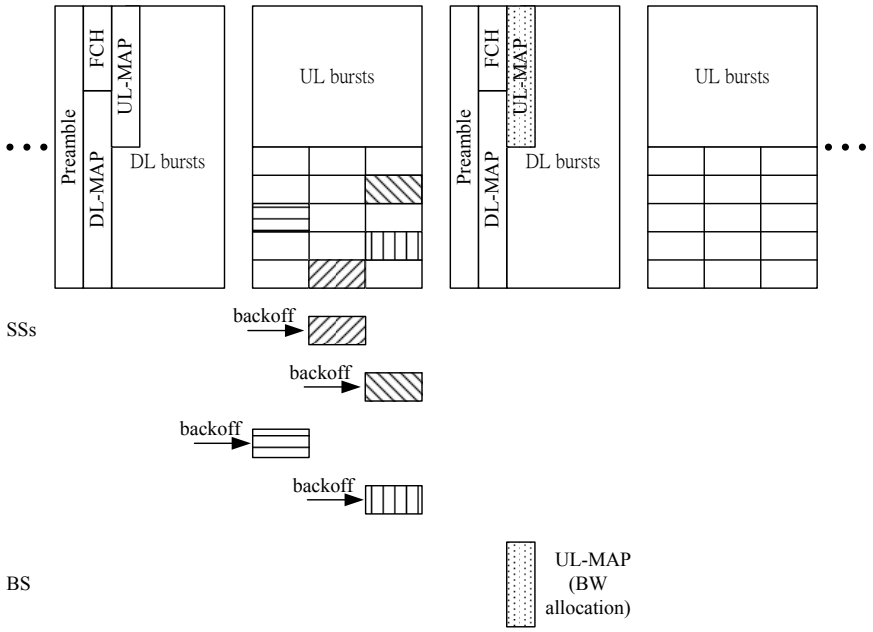

(a) The transmission succeeds at the first attempt.

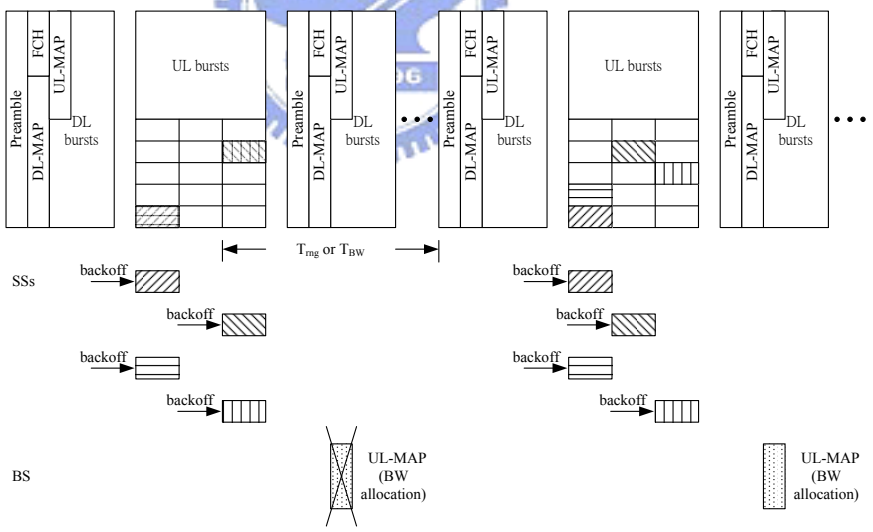

(b) Retransmission occurs when the previous attempt has a collision.

Fig. 7.2: Illustrations of the multi-channel random access for the initial ranging and bandwidth request in IEEE 802.16.

time slots smaller than the backoff window size. It is implied that a mobile station defers its transmission until the end of the selected time period. After waiting for this period, the mobile station randomly selects sub-channels and sends the bandwidth request and the ranging request (RNG_REQ) frames. Once the base station successfully receives the request, it allocates the sub-channels and time slots for the new connection in the next DL-MAP or UL-MAP, as shown in Fig. 7.2(a). However, as shown in Fig. 7.2(b), collisions may occur when the bandwidth/ranging request frames are transmitted. If the base station fails to response the bandwidth/ranging request frames after a timeout duration, T_{rng} or T_{bw_req}, the mobile station doubles its backoff window size and repeats the aforementioned procedures until reaching the maximum number of transmission attempts. Here, T_{rng} or T_{bw_req} are defined as the waiting periods for the ranging response (RNG_RSP) frame and the bandwidth grant frame, respectively.

For clarity, we explain the difference of the multiple-channel random access MAC protocol with collision avoidance used in the IEEE 802.16e WiMax system and the CSMA/CA MAC protocol used in the IEEE 802.11 WLAN system. Unlike the CSMA/CA MAC protocol, the base station in the IEEE 802.16e WiMax system is capable of receiving the requests from multiple mobile stations at the same time since the mobile stations can transmit at different sub-channels. In this case, a frame collision occurs when more than one station accesses at the same chunk of sub-channels and time slots.

7.3 Resources Partition Optimization

Now we formulate an optimization problem with the objective of maximizing the efficiency of the reserved chunk of sub-channels and time slots for random access subject to the delay constraint of supporting real-time services. Intuitively, reserving more radio resources for random access can yield shorter access latency due to fewer

collisions. However, it also leads to more idle radio resources. With the optimal numbers of reserved sub-channels and time slots for random access, we can optimize radio resource partitioning for the time-division OFDMA system.

The above optimization problem can be solved by a mixed-integer nonlinear programming (MINLP) technique. Define the efficiency η as the ratio of the reserved chunk of sub-channels and time slots on which bandwidth request and ranging requests frames are successfully transmitted over the total reserved radio resources. Denote r and m as the numbers of the reserved sub-channels and time slots for random access, respectively. It will be shown later that the considered efficiency η is a non-linear function of r and m as well as the number of mobile users (denoted by k). With the above definitions, a MINLP optimization problem is formulated to maximize the efficiency $\eta(r, m, k)$ by determining the optimal values of r and m for a given k, i.e.,

$$\underset{r,m}{\text{MAX}} \ \eta(r, m, k) \ , \tag{7.1}$$

subject to the following constraints:

$$a) \quad r \leq N_f \ ;$$

$$b) \quad m \leq N_t \ ;$$

$$c) \quad D(r, m, k) \leq D_{max} \ .$$

Later in Section 7.5, we will find that the maximization of the efficiency η is equivalent to the optimization of the reserved resources left for the data transmission.

Clearly, both integers r and m are constrained by the total number of sub-channels in the frequency domain (N_f) and the total number of time slots in the time domain (N_t). Furthermore, to support the delay-sensitive services, the access delay D of sending the bandwidth request and ranging request frames is required to be shorter than the pre-defined maximal delay (D_{max}). Note that the access delay D is a continuous value and is a nonlinear function of r, m and k. Since both $\eta(\cdot)$ and $D(\cdot)$ are nonlinear functions of r, m, and k, and conditions a), b) and c) are the constants

for both the discrete and continuous values, (7.1) becomes a MINLP optimization issue. The next important step to solve the above optimization problem is to derive $\eta(r, m, k)$ and $D(r, m, k)$, which will be discussed in the next section.

7.4 Analysis

Now we develop the analytical models for the average access latency and the spectrum efficiency for random access. It is assumed that each mobile station always has frames to send, and collisions occur when more than one station access the same sub-channel and time slot.

7.4.1 Efficiency of Reserved Radio Resources

Denote N_s as the number of successfully transmitted bandwidth and ranging requests during one uplink sub-frame, and N'_s as that during one time slot. It is assumed that each request asks for a chunk of one time slot at one sub-channel. Then, based on the previous definition, the average spectrum efficiency η of the reserved radio resources for random access can be expressed as

$$\eta(r, m, k) = \frac{\mathrm{E}[N_s]}{mr} \tag{7.2}$$

$$= \frac{m\mathrm{E}[N'_s]}{mr} , \tag{7.3}$$

where m and r are the numbers of reserved time slots and sub-channels for random access. According to the random access procedure in the standard, it is worth to note that the contention at each time slot and sub-channel is independent to the others.

Denote T as the event that at least one mobile station transmits in a time slot and the probability of event T is equal to $P_T = 1-(1-\tau)^k$, where τ is the probability that a station transmits a frame in a given time slot. Thus, it follows that

$$\mathrm{E}[N'_s] = P_T \cdot \mathrm{E}[N'_s|T] . \tag{7.4}$$

Given $\overline{W}$ the average backoff time slots that a mobile station defers before each transmission attempt, the transmit probability τ that a station transmits a request in a reserved slot can be expressed as

$$\tau = \frac{1}{\overline{W}} \ . \tag{7.5}$$

Note that based on the random access procedure in the standard, the backoff count is decreased by one for each reserved slot in a frame, while it is frozen in the other slots of a frame and continues to count down in the next frame. Therefore, the transmit probability τ is equal to the inverse of the average backoff counts because both of these factors only consider the reserved slots instead of the whole of a frame.

Then, let W_{min} and f be the initial backoff window size and the maximum number of transmission attempts, respectively. Because the users with colliding frames double their backoff window sizes in the next transmission in order to avoid collisions, the average number of backoff slots for the i-th retransmission W_i can be written as

$$W_i = \frac{2^i W_{min} + 1}{2} \ , \tag{7.6}$$

for $i = 0, \cdots, f$. Given T_o the timeout duration[4], a station has to defer an extra duration of $m\lceil T_o/T_f \rceil$ slots before the retransmission according to the random access procedure. With the random backoff time slots W_i for the i-th retransmission, the

[4] The timeout duration T_o for the initial ranging request is different from that of the bandwidth request. As specified in the standard, $T_o = 10$ and 200 msec for the bandwidth request and initial ranging, respectively.

average backoff slots $\overline{W}$ then becomes

$$\begin{aligned}
\overline{W(m)} &= (1-p_c)W_0 + p_c(1-p_c)(W_1 + m\lceil\frac{T_0}{T_f}\rceil) + \cdots \\
&\quad + p_c^f(1-p_c)(W_f + m\frac{T_0}{T_f}) + p_c^{f+1}(W_f + m\frac{T_0}{T_f}) \\
&= (\frac{1}{2} + m\lceil\frac{T_0}{T_f}\rceil)\left[(1-p_c)(1+p_c+\cdots+p_c^f) + p_c^{f+1}\right] - m\lceil\frac{T_0}{T_f}\rceil(1-p_c) + \\
&\quad \frac{W_{min}}{2}\left[(1-p_c)(1+2p_c+\cdots+(2p_c)^f) + p_c(2p_c)^f\right] \\
&= \frac{1}{2} + m\lceil\frac{T_0}{T_f}\rceil p + \frac{W_{min}}{2}\frac{1-p_c-p_c(2p_c)^f}{1-2p_c} \ , \qquad (7.7)
\end{aligned}$$

where p_c is the collision probability, which is defined as the probability that more than one station transmit frames at the same sub-channel and time slot given that a station transmits. Assuming that each station randomly selects one of r reserved sub-channels to access with the probability $1/r$, the collision probability p_c can be written by

$$\begin{aligned}
p_c &= \binom{k-1}{1}\tau(1-\tau)^{k-2}\frac{1}{r} + \binom{k-1}{2}\tau^2(1-\tau)^{k-3}(1-(1-\frac{1}{r})^2) + \cdots \\
&\quad + \binom{k-1}{k-1}\tau^{k-1}(1-(1-\frac{1}{r})^{k-1}) \\
&= \sum_{i=1}^{k-1}\binom{k-1}{i}\tau^i(1-\tau)^{k-1-i}(1-(1-\frac{1}{r})^i) \\
&= 1-(1-\frac{\tau}{r})^{k-1} \ . \qquad (7.8)
\end{aligned}$$

Note that in (7.7), $p_c^i(1-p_c)$ represents the success probability for the i-th retransmission. Thus, the transmission probability τ can be obtained by jointly solving (7.5) $\sim$ (7.8).

In addition, because each station has the probability $\frac{\tau}{r}$ to access one chunk of the reserved sub-channel and time slot, the average number of successful transmissions for the initial ranging or bandwidth request given at least one station transmits $E[N_s'|S]$ becomes

$$E[N_s'|T] = \frac{1}{P_S}\cdot r\binom{k}{1}\frac{\tau}{r}(1-\frac{\tau}{r})^{k-1} \ . \qquad (7.9)$$

By substituting (7.4) and (7.9) into (7.2), the efficiency η of the reserved radio resources is given by

$$\eta(r,m,k) = k\frac{\tau(m)}{r}(1-\frac{\tau(m)}{r})^{k-1} \ . \tag{7.10}$$

7.4.2 Average Access Latency

As defined previously in Section 7.3, the average access latency D is equal to the overall duration that a mobile station waits until successfully transmitting a bandwidth/ranging request frame. Given the average number of overall slots $E[W_D]$ before a successful request transmission and the frame duration T_f, the average access latency D can be written as

$$D = \left\lceil \frac{E[W_D]}{m} \right\rceil \cdot T_f \ . \tag{7.11}$$

Here, we only count the latency in terms of frame duration because the slot time is much shorter than a frame duration.

Suppose that each bandwidth/ranging request frame transmission only occupies one reserved slot in a frame. Then, considering the collision probability p_c, the average backoff slots at the i-th retransmission W_i and the timeout duration T_o, the average overall backoff slots $E[W_D]$ given the request is successfully transmitted is equal to

$$\begin{aligned} E[W_D] &\triangleq E[\text{the total number of the required slots for a successful transmission} \\ &\quad |\text{the request is successfully transmitted}] \\ &= \underbrace{W_0}_{\text{success at the first attempt}} + \underbrace{(W_1 + m\lceil\frac{T_o}{T_f}\rceil)p_c}_{\text{success at the second attempt}} + \cdots + \\ &\quad \underbrace{(W_{f-1} + m\lceil\frac{T_o}{T_f}\rceil)p_c^{f-1}}_{\text{success at the } f\text{-th attempt}} + \underbrace{(W_f + m\lceil\frac{T_o}{T_f}\rceil)\frac{p_c^f}{1-p_c}}_{\text{success after the } f\text{-th attempt}} \qquad (7.12) \\ &= \frac{(1-2p_c)(1+W_{min}) + W_{min}p_c(1-(2p_c)^f)}{2(1-2p_c)(1-p_c)} + m\lceil\frac{T_o}{T_f}\rceil\frac{p_c}{1-p_c} \ . \qquad (7.13) \end{aligned}$$

By substituting (7.8) and (7.13) into (7.11), the average access latency D can be obtained. Note that the collision probability p_c, as shown in (7.8), is affected by

the number of reserved sub-channels r. Thus, the average overall slots $E[W_D]$ and access latency D are also the functions of r.

7.5 Numerical Results

In this section, we investigate the effectiveness of the proposed radio resource partition technique to determine the optimal number of reserved sub-channels and time slots for random access in the time division OFDMA system. Referring to the IEEE 802.16e WiMax system, we consider the following parameters, including an uplink sub-frame with 70 sub-channels and 48 time slots, frame duration $T_f = 5$ msec, the bandwidth request and initial ranging timeout duration 10 and 200 msec, respectively. Other related system parameters are listed in Table 7.1.

7.5.1 Performances of Default Radio Resource Partition

First, we evaluate the performance of an OFDMA system with the parameters listed in Table 7.1, in which one and six sub-channels as well as three time slots are reserved for the random access. According to (7.10), the efficiency of the reserved radio resources for the random access versus various numbers of stations is plotted in Figs. 7.3(a) and (b). From the figures, the highest efficiency of the reserved random access radio resources occurs for the number of users $k = 85$ and 160 when $r = 1$ and $T_o = 10$ and 200 msecs, respectively. This phenomenon can be explained by two factors. On the one hand, when the number of stations is smaller, the reserved radio resources are more likely to become idle and thus the efficiency decreases. On the other hand, as the number of station increases, the contentions among users result in more collisions and reduce the efficiency. Thus, there exist an optimal number of stations to achieve the maximum efficiency for various timeout values. Similar results can also be observed in the multi-channel case.

Furthermore, Figs. 7.3 (a) and (b) also show the difference between the single

Tab. 7.1: System Parameters of the Performance Evaluation for the Multi-channel Random Access with Truncated Binary Exponential Backoff

Frame duration, T_f	5 msec
Timeout duration for the bandwidth request	10 msec
Timeout duration for the initial ranging	200 msec
Initial backoff window size, W_{min}	16
Maximum transmission attempts, f	7
Number of stations, k	100
Default number of reserved time slots	3
Default number of reserved sub-channels	6
Maximum number of reserved time slots	48
Maximum number of reserved sub-channels	70
VoIP delay constraint, D_{max} [156]	25 msec

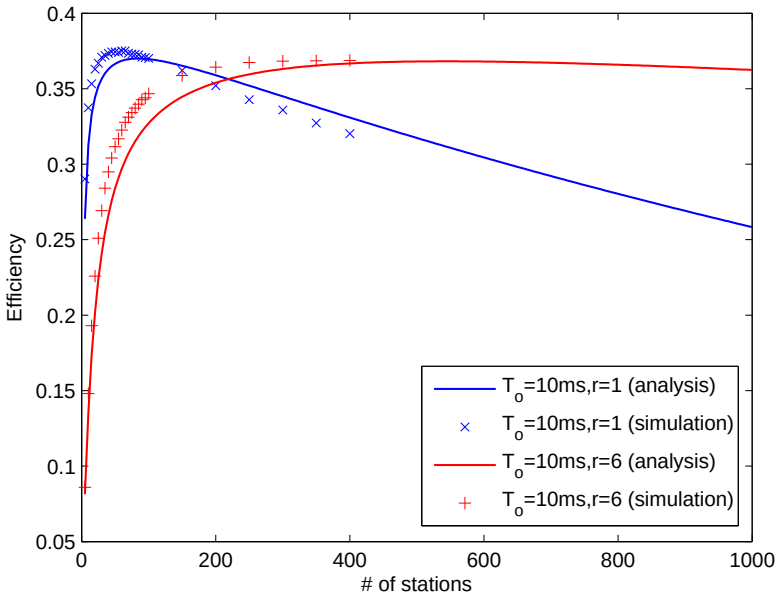

(a) $T_o = 10$ msec.

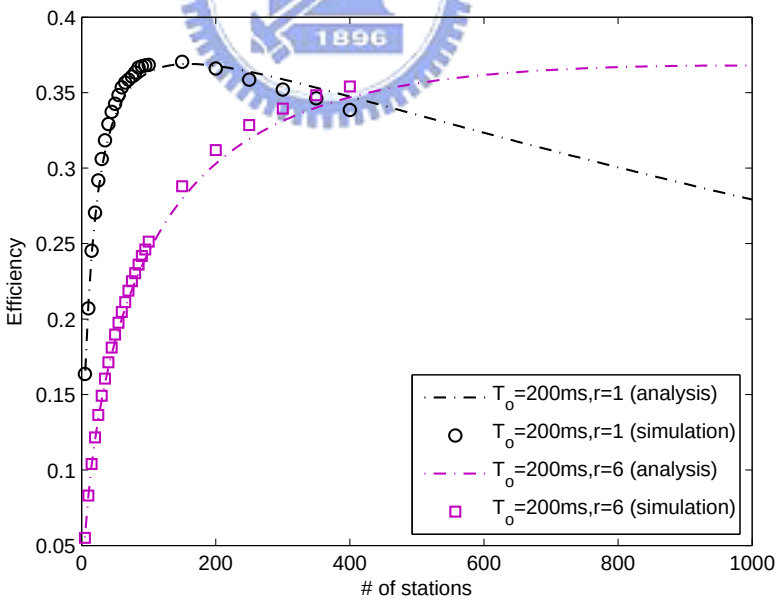

(b) $T_o = 200$ msec.

Fig. 7.3: Efficiency of the reserved radio resources based on the multi-channel random access MAC protocol with three time slots per frame and one/six sub-channels to send bandwidth/ranging requests in an OFDMA system by simulation and analysis.

and multiple channel random access. Interestingly, one can observe that the multi-channel random access has slowly increasing efficiency as the number of stations grows compared to the single channel case. This phenomenon results from the abundant reserved resources for resolving the contentions so that the system is capable of accepting more contentions among stations. Nevertheless, its payoff is the low efficiency of the reserved resources for the case of few stations due to the wasted sub-channels.

Next, based on (7.11), Fig. 7.4 shows the average latency of the multi-channel random access MAC protocol in the OFDMA system for various numbers of stations and timeout values. Consider the delay constraint $D_{max} = 25$ msec for supporting real-time services. Subject to the above delay requirement, the system can support only up to 25 stations sending the bandwidth request based on the default partition scheme, i.e. three sub-channels and six time slots are designated for random access out of the total 70 sub-channels and 48 time slots. As for the initial ranging transmission, the system with the default partition scheme cannot satisfy the delay constraint due to the long timeout duration before any retransmission. Clearly, the more radio resources reserved for the random access the shorter the access latency because of the less retransmission. However, from the figure, only one partition scheme can satisfy the delay requirement for real-time services. Therefore, it is necessary to investigate some alternative resource partition schemes through the presented analytical models for the efficiency and access delay of the multi-channel random access MAC protocol in the OFDMA system, which will be discussed next.

7.5.2 Performances of Alternative Radio Resource Partitions

In Fig. 7.5, we investigate the effects of various numbers of sub-channels r and time slots m on the efficiency of the reserved radio resources based on the multi-channel random access MAC protocol in the considered OFDMA system with 100 stations. We have the following two observations:

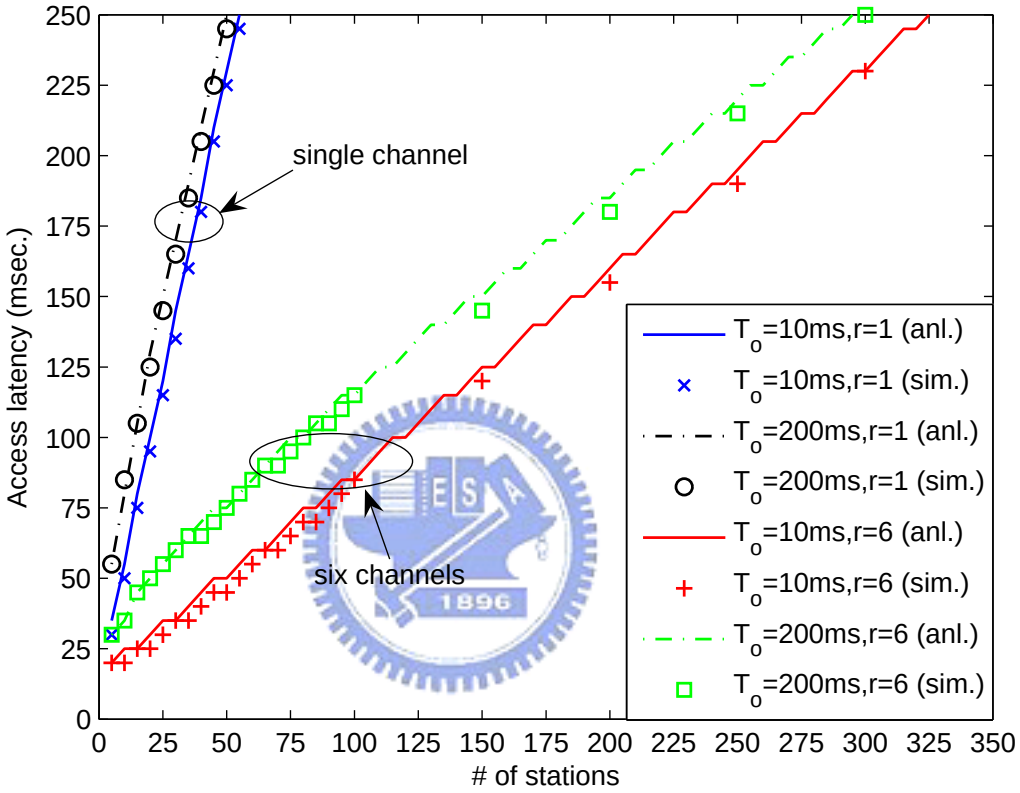

Fig. 7.4: Average latency of the reserved radio resources based on the multi-channel random access MAC protocol with three time slots per frame and one/six sub-channels to send bandwidth/ranging requests in an OFDMA system by simulation and analysis.

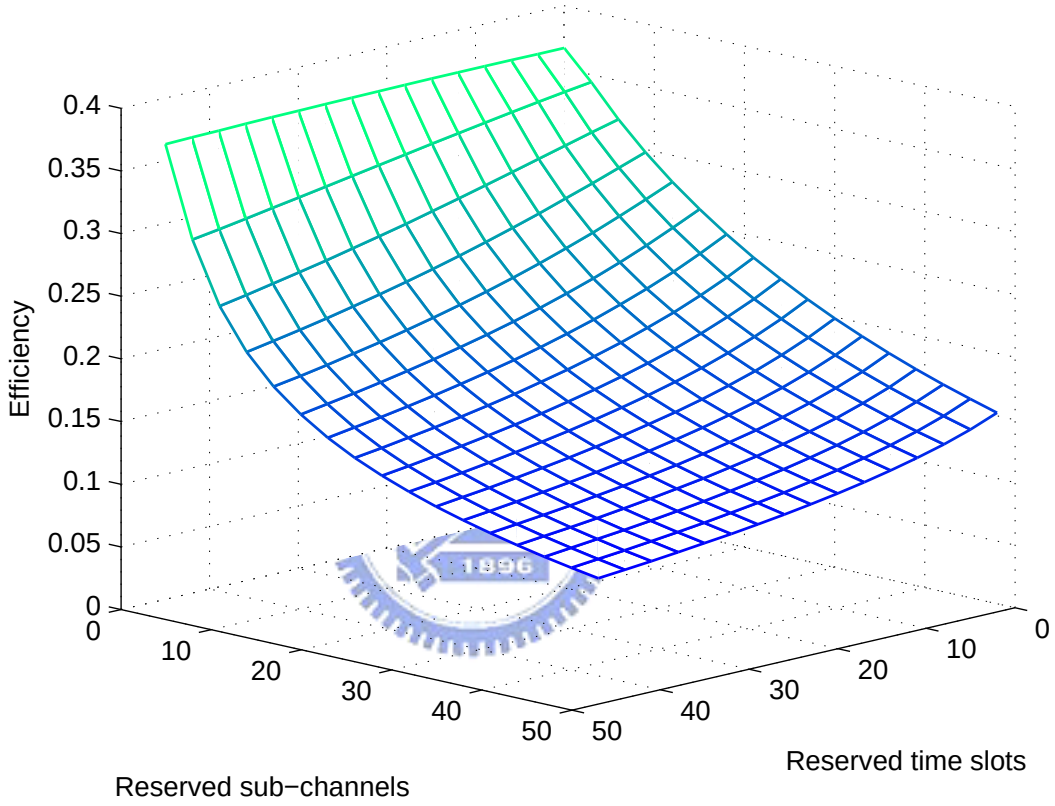

Fig. 7.5: Effects of various sub-channels and time slots on the efficiency of the reserved radio resources based on the multi-channel random access MAC protocol in an OFDMA system with 100 stations.

- As shown in the figure, the efficiency of the reserved radio resources is monotonously decreasing as the number of the reserved time slots or sub-channels in a frame grows. This is because too many reserved radio resources may cause them staying idle. For example, when the number of reserved slots $m = 3$, the efficiency η for the number of reserved sub-channels $r = 1 \sim 50$ decreases from 0.37 to 0.15. Similarly, as $r = 6$, $\eta = 0.35 \sim 0.3$ for $m = 1 \sim 48$. The phenomenon of monotonously decreasing efficiency with the increasing number of reserved sub-channels represents that the maximization of efficiency performance is also to optimize the reserved resources left for the data transmissions for the given access latency requirement. Thus, although we aim to maxize the efficiency by adjusting the numbers of reserved sub-channels and time slots, this problem is also an optimization problem for the reserved resource left for the data transmission.

- Furthermore, as shown in the figure, the efficiency of the reserved radio resources seems to be more sensitive to the changes of the number of reserved sub-channels in the frequency domain than that of the number of reserved time-slots in the time domain. We will try to explain this situation by investigating the effect of the reserved radio resources in the frequency and time domains on the collision probability of the multi-channel random access MAC protocol next.

By means of (7.8), Fig. 7.6 shows the effects of various reserved sub-channels and time slots on the collision probability of the multi-channel random access MAC protocol in the considered OFDMA system with 100 stations. Clearly, reserving more radio resources for random access can yield a lower collision probability. However, it is interesting to investigate in which domain of the OFDMA system, frequency domain or time domain, is more effective in improving the efficiency and latency performances for the system adopting the multi-channel random access MAC protocol. As shown in the figure, increasing the number of the reserved sub-channels r can reduce the collision probability more effectively than changing the number of reserved time slots

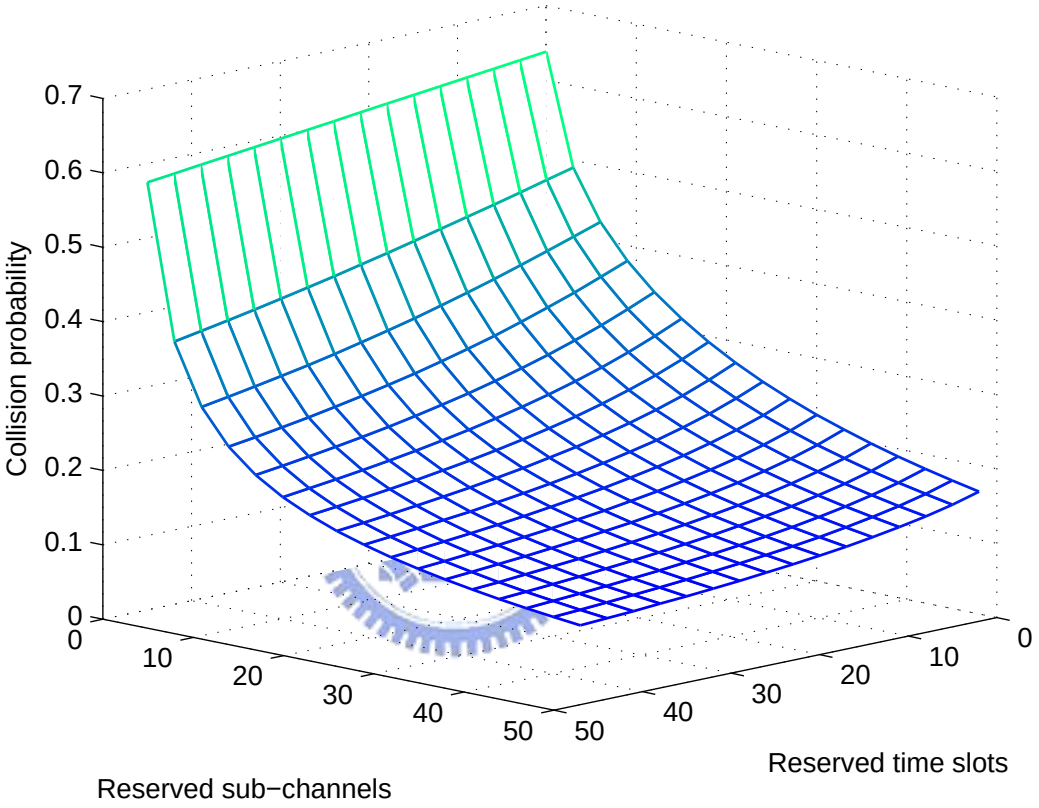

Fig. 7.6: Effects of various reserved sub-channels and time slots on the collision probability of the multi-channel random access MAC protocol in the considered OFDMA system with 100 stations.

m. For $m = 6$, changing $r = 6$ to 48 can lower the collision probability p_c from 0.64 to 0.17. By contrast, the collision probability p_c decreases from 0.49 to only 0.4 when m changes from 2 to 48 for $r = 6$. By comparing (7.8) and (7.10), one can easily see that a lower collision probability leads to a higher efficiency for the reserved random access radio resources. Hence, from Fig. 7.6, one can explain why in Fig. 7.5 changing the amount of reserved radio resource for random access in the frequency domain of the OFDMA system can more significantly affect the efficiency than in the time domain of the OFDMA system.

Figure 7.7 illustrates the effects of various reserved sub-channels and time slots on the average latency of the multi-channel random access MAC protocol in the OFDMA system with 100 stations. In contrast to the phenomenon observed in Fig. 7.5, the number of the reserved time slots dominates the latency performance compared to that of the reserved sub-channels. For example, the access latency for $r = 6$ decreases from 95 msec to 10 msec as m changes from 2 to 48. On the contrary, when r increases from 2 to 50 , the latency for $m = 6$ is reduced only from 95 msec to 20 msec. Intuitively, the more reserved time slots help stations to resolve the contentions earlier and to send the request in the prior frame. Although, from (7.11), increasing the number of reserved sub-channels can lower the collision probability, it is not as effective as increasing the time slots from the aspect of reducing the access latency because the station waits more frames to count down the backoff slots in the case of few reserved slots. Notably, it is important to combine Figs. 7.5 and 7.7 to determine a set of (r, m) with the maximum efficiency and satisfactory delay performance. For the case $k = 100$ and $T_o = 10$ msec, $(r, m) = (2, 29)$ can achieve the highest efficiency under the constraint of $D_max = 25$ msec.

7.5.3 Performance of Optimum Radio Resources Partitions

Now we apply the systematic MINLP optimization approach introduced in Section **??**.B to determine the optimal values of (r^*, m^*), which represent the sub-

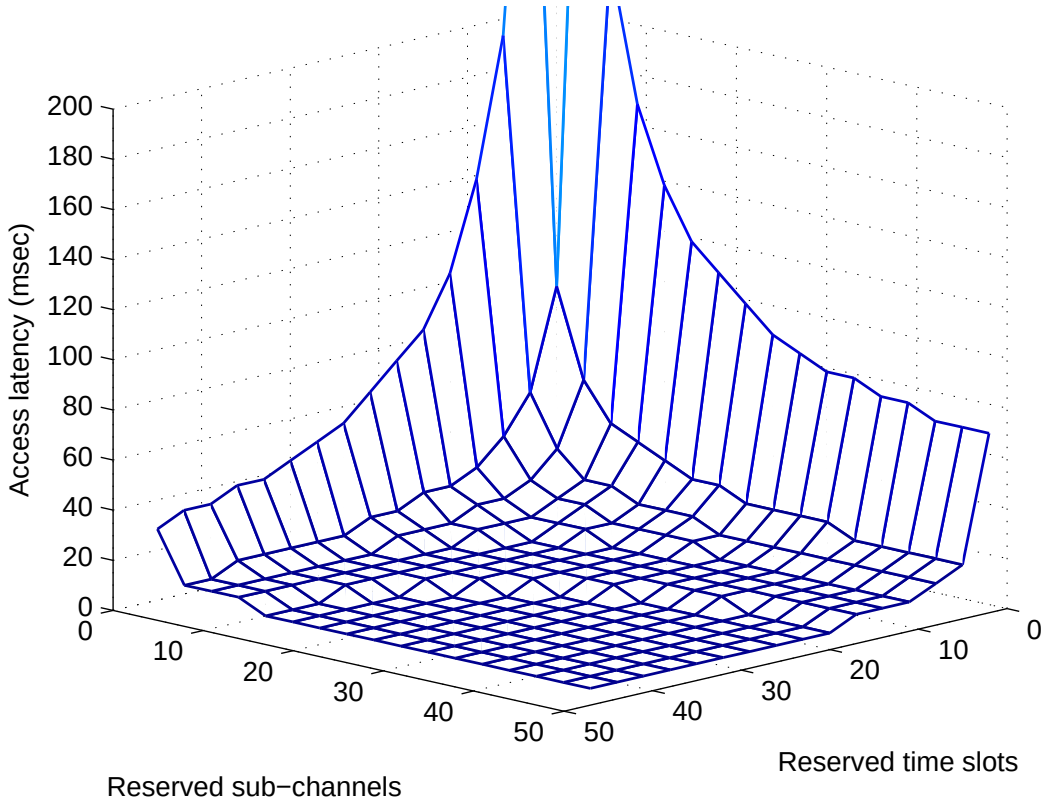

Fig. 7.7: Effects of various reserved sub-channels and time slots on the average latency of the multi-channel random access MAC protocol in the considered OFDMA system with 100 stations.

Tab. 7.2: Optimal parameters values for bandwidth request transmissions (T_o=10 msec)

Number of stations	Number of reserved time slots	Number of reserved sub-channels
10	7	1
30	18	1
50	29	1
100	29	2
150	42	2
200	38	3

Tab. 7.3: Optimal parameters values for initial ranging transmissions (T_o=200 msec)

Number of stations	Number of reserved time slots	Number of reserved sub-channels
10	20	1
30	30	2
50	34	3
100	40	5
150	43	7
200	40	10

channels and the time slots reserved for random access in the frequency domain and the time domain of the OFDMA system, respectively. In the previous subsection, an exhaustive search method is used to find the optimal (r^*, m^*) for the number of users $k = 100$. According to (7.1), Tables 7.2 and 7.3 list the optimal (r^*, m^*) for $T_o = 10$ msec and 200 msec with an objective of maximizing the efficiency of the reserved sub-channels and time slots for random access in the considered OFDMA system subject to the constraint of $D_{max} = 25$ msec, respectively. For $k = 100$ and $T_o = 10$ msec, the optimal $(r^*, m^*) = (2, 29)$ obtained by the suggested MINLP optimization approach is the same as that obtained by the exhaustive search method. Once the optimum (r^*, m^*) for various numbers of mobile stations is generated off-line and stored into a table, the base station can dynamically adjust the reserved radio resources for random access to enhance the performance of the OFDMA system.

Furthermore, from the optimal values shown in Tables 7.2 and 7.3, we can infer that the system rather reserves the more time slots than the sub-channels to meet the delay requirement for real-time applications. Although both sub-channels and time slots are used to resolve the contentions among users, the more reserved time slots let the station wait fewer frames to send the request. Thus, the access latency can

be easily satisfied the delay requirement. Despite the excess reserved sub-channels cannot be used to lower the waiting time due to the backoff before the transmission, the number of sub-channels is still the dominating factor to reduce the collisions among users and to decide the system capacity.

Figure 7.8 compares the efficiency of the reserved radio resources for random access and the access latency of the considered MAC protocol according to the above optimal radio resource partition scheme of Tables 7.2 to that according to the default partition scheme $(r, m) = (6, 3)$ in the case of $T_o = 10$ msec. Figure 7.9 also illustrates the same comparison according to Table 7.3 for $T_o = 200$ msec. As shown in Figs. 7.8 (b) and 7.9 (b), unlike the default partition that can meet the delay requirement of $D_{max} = 25$ msec only for the bandwidth request transmission and the number of users $k < 10$, the proposed optimum resource partition scheme can satisfy the delay requirement with k up to 200. For both cases of $T_o = 10$ and 200 msec, the efficiency of the reserved radio resource based on the optimal partition scheme is significantly higher than the default partition scheme especially for the case of few contending stations.

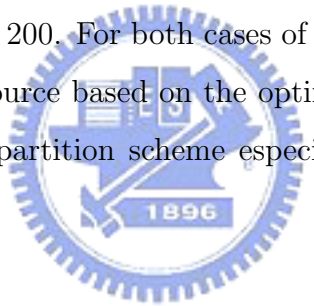

7.6 Conclusions

In this part, we have derived the analytical expressions for the efficiency of the reserved resources and the latency of the contention-based multi-channel random access MAC protocol. Based on the developed analytical models, we evaluated the impact of the number of reserved sub-channels and time slots on the efficiency and latency performances of the OFDMA systems using the contention-based MAC for link establishment. From the efficiency standpoint, we find that the number of reserved sub-channels is a more dominant factor than the number of of reserved time slots. From the latency viewpoint, however, the number of the reserved time slots becomes a dominating factor instead.

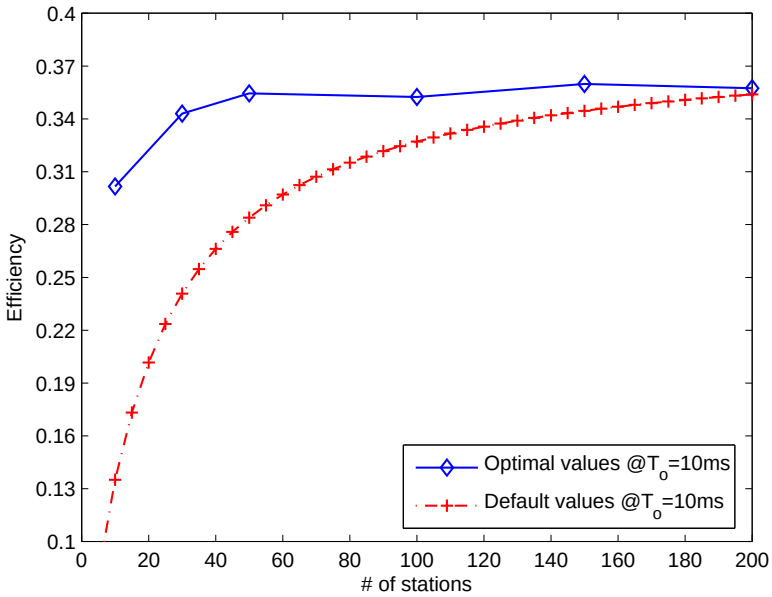

(a) Efficiency

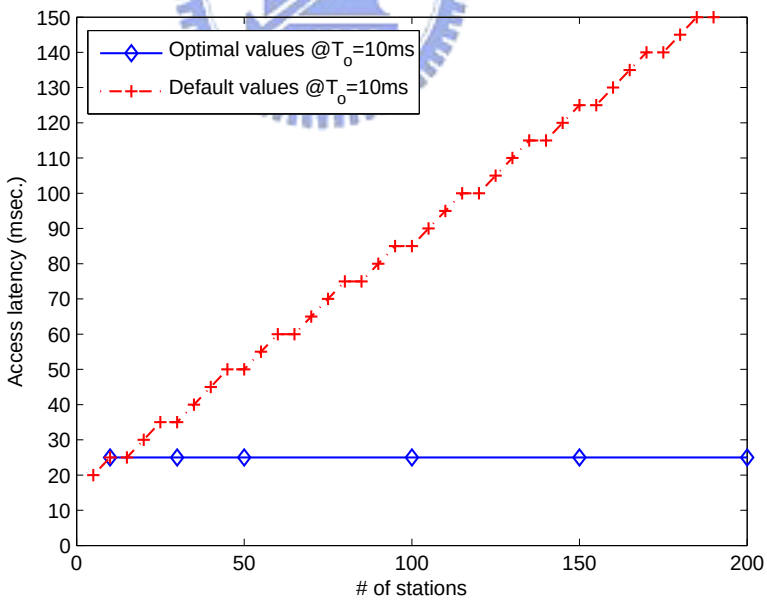

(b) Access latency

Fig. 7.8: Performance comparisons of the optimal radio resource partition scheme according to Table 7.2 and the default partition scheme $(r, m) = (6, 3)$ in terms of (a) efficiency and (b) access latency, where $T_o = 10$ msec.

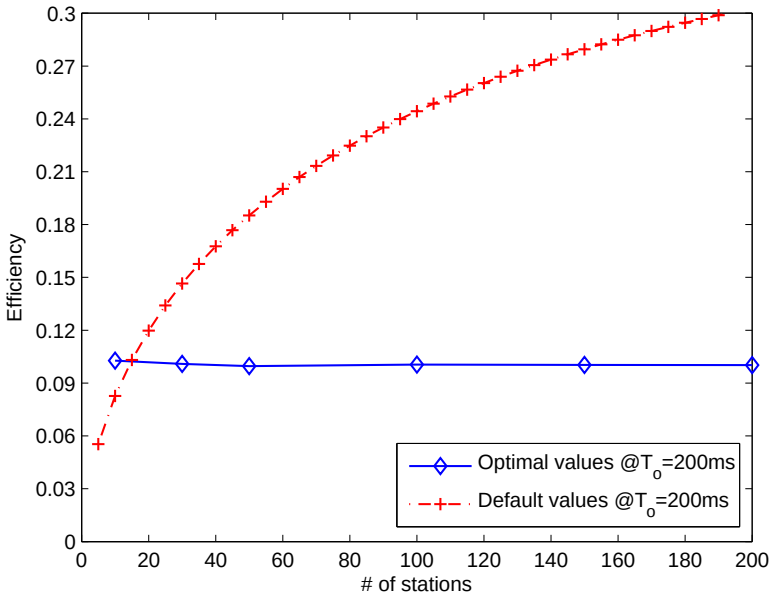

(a) Efficiency

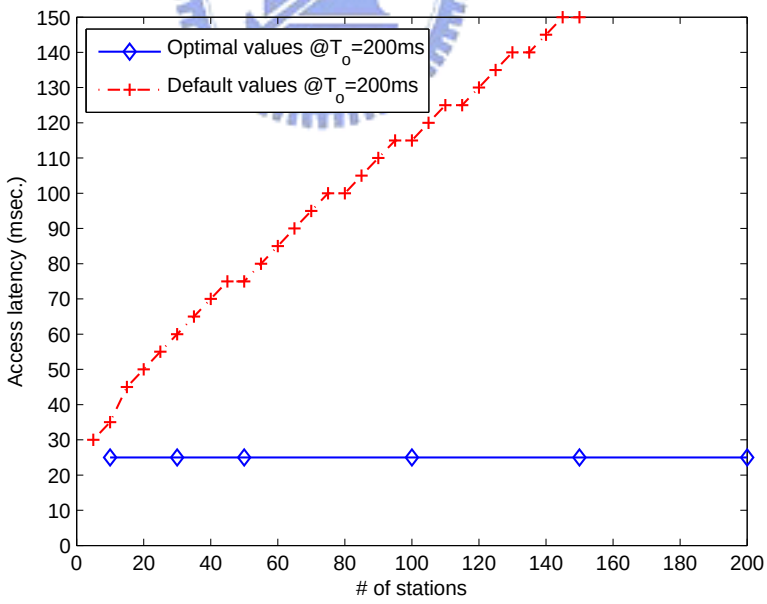

(b) Access latency

Fig. 7.9: Performance comparisons of the optimal radio resource partition scheme according to Table 7.3 and the default partition scheme $(r, m) = (6, 3)$ in terms of (a) efficiency and (b) access latency, where $T_o = 200$ msec.

By using both exhaustive and the proposed MINLP optimization approaches, we also have discussed how to find the optimal partition scheme, in which r^* sub-channels and m^* time slots are reserved for random access during link setup process. It is shown that with the optimal (r^*, m^*) the efficiency of the reserved radio resources can be maximized regardless of the number of contending users, while still satisfying the delay requirement of real-time services.

Chapter 8

Conclusion

In this dissertation, we have investigated three important issues for the cognitive radio network: wideband spectrum sensing, the cognitive MAC protocol and the spectrum handoff mechanism for the link maintenance. For the first issue, we suggested the new point of view from the location awareness to aid the spectrum sensing. Then, we designed an enhanced CSMA/CA based MAC protocol for CR devices. At last, we discussed the link maintenance probability and effective data rate of the two spectrum handoff schemes for the link maintenance. Furthermore, we also developed a cross-layer analysis to investigate the throughput, delay and resource usage efficiency for single and multiple channels CSMA/CA MAC protocol. This dissertation includes the following research topics.

- Location-aware Concurrent Transmission
- Neighbor-aware Cognitive MAC Protocol
- Spectrum Handoff for Link Maintenance
- Cross-layer Analysis for Single Channel CSMA/CA
- Cross-layer Analysis for Multiple Channels CSMA/CA

The contribution from these research works are list as follows.

1. Investigate the feasibility of location aided spectrum sensing.
2. Dimension the concurrent transmission region where the CR device can establish the concurrent transmission with the legacy system.

3. Design an enhanced CSMA/CA MAC protocol with QoS provisioning for CR device.

4. Study the link maintenance probability and effective data rate for two spectrum handoff schemes.

5. Provide the design guide of system parameters for CR devices to perform the spectrum handoff.

6. Develop the cross-layer analytical models for the single and multiple channels CSMA/CA MAC protocols.

7. Inspect the impacts of capture effect, multipath fading, shadowing, directional antennas and multiple transceivers on the throughput performance of CSMA/CA MAC protocol.

8. Optimize the reserved resources for contention-oriented multi-channel CSMA/CA MAC protocol.

In the following, we summarize the results from the above contributions.

8.1 Location-aware Concurrent Transmission

In summary, the results presented in this part provide a design paradigm for cognitive radio systems from an alternative perspective – identifying spectrum opportunity cannot just rely on wide-band spectrum sensing techniques. Location awareness also provides another important resource to help a cognitive radio system identify the opportunities of *concurrently using* the spectrum of the primary user in the spatial domain, instead of just *sharing* the spectrum in the time domain. It is hoped that our work has shed some light in this promising area of research. Nevertheless, there are still many unsolved open issues to realize the idea of exploiting the concurrent transmission opportunity by taking advantages of location awareness. Many interesting

research topics, including the concurrent transmission MAC protocol design, the efficient mechanism of location information exchange, and the theoretical upper bound on the maximum concurrent transmission links overlaying the legacy infrastructure-based systems, are worthwhile to be investigated further.

8.2 Neighbor-aware Cognitive MAC Protocol

In summary for this part, taking advantages of the obtained information in the ***observe*** stage of the cognition cycle, the proposed cognitive MAC protocol can avoid interfering the primary user. We also show how to utilize the collected information for other performance enhancements: (1) to increase the throughput for the contention-based channel access protocol; (2) to schedule the transmission of delay-sensitive frames with QoS provisioning; (3) to distributively synchronize the transmissions among ad hoc CR users. With suggested moderate modifications, the legacy CSMA/CA MAC protocol can be reshaped to an appropriate MAC protocol for overlaying CR ad hoc networks. Although the results are appealing, the proposed mechanisms just shed some lights in the direction of designing a cognitive MAC protocol, but by no means an optimal solution. For example, the current proposed cognitive MAC protocol only takes advantage of spectrum opportunity in terms of time. Thus, one interesting open issue that can be extended from this work is to develop a mechanism to identify spectrum opportunity in terms of both location and time and to develop an associated space-time-cognitive MAC protocol.

8.3 Spectrum Handoff for Link Maintenance

In this part, we have inspected the three possible transmission scenarios for CR devices when the primary users appear on the occupied channel. In the non-spectrum-handoff scenario, the secondary user stays in the original channel and resumes its transmission

after the primary user leaves the channel. The pre-determined channel list spectrum handoff scheme establishes a channel list, and the CR device changes the channels following the sequence to continue its transmissions. As for the spectrum handoff with sensing scheme, the secondary user senses and determines the target channel only when the primary user interrupts its transmissions. We also developed an analytical mode to investigate the performances of the link maintenance probability and the effective data rate of the secondary user for the three transmission scenarios. At last, based on the model, we investigate the impacts of the error sensing probability, the radio sensing time, the number of handoff trials, the frame error rate of the secondary user's transmission and the handoff time on the performances of spectrum handoff. Furthermore, through this model, we can design appropriate system parameters for the CR device to perform the spectrum handoff.

8.4 Cross-layer Analysis for Single Channel CSMA/CA

In this part, we have developed a PHY/MAC cross-layer analytical model to take account of the physical layer effects, including the capture effects and a practical directional antenna, into the throughput evaluation of the CSMA/CA MAC protocol. We have derived explicit expressions for the frame outage and capture probability of a directional antenna system in the presence of log-normal shadowing and multipath Rayleigh fading. We integrate this PHY layer model with the MAC throughput analytical model of the CSMA/CA protocol. We find that it is crucial to incorporate the channel effects into both the stationary transmission probability and the backoff window size of a station. By doing so, we can model the interaction of the physical layer effect and the MAC layer throughput more accurately. Through OPNET simulations, we verify the accuracy of the proposed PHY/MAC cross-layer analytical model.

8.5 Cross-layer Analysis for Multiple Channels CSMA/CA

In this part, based on a multi-channel random access MAC protocol with a collision avoidance binary bacoff algorithm, we formulated a MINLP optimization problem to determine the most suitable number of sub-channels and time slots that should be reserved in the frequency and time domain of the OFDMA system for sending the bandwidth/ranging requests. The objective of the proposed optimization issue is to maximize the efficiency of the reserved radio resources under the delay constraint of supporting the real-time services.

We derived the analytical expressions for the efficiency of the reserved resources and the latency of the contention-based multi-channel random access MAC protocol. Based on the developed analytical models, we evaluated the impact of the number of reserved sub-channels and time slots on the efficiency and latency performances of the OFDMA systems using the contention-based MAC for link establishment. From the efficiency standpoint, we find that the number of reserved sub-channels is a more dominant factor than the number of of reserved time slots for the considered OFDMA system. From the latency viewpoint, however, the number of the reserved time slots becomes a dominating factor instead.

There are many interesting research issues that can be extended from this work for further investigation. Specific issues include the impact of the physical layer channels on the contention-based multi-channel random access MAC protocol with collision avoidance, the impact of the co-channel interference on the performance of the contention-based multi-channel random access MAC protocol, and joint resource partition and allocation issue for OFDMA systems.

8.6 Suggestions for Future Research

In this dissertation, we have discussed some preliminary issues for cognitive radio. Other possible interesting research topics that can be extended from this dissertation are listed as follows:

- **Wideband spectrum sensing:**
  1. Extend the system with multiple secondary links coexisting with the primary user's connection.
  2. Develop the CR-enabled location exchange mechanism and ad hoc positioning system.
- **Cognitive MAC protocol:**
  1. Develop an accurate spectrum usage model to characterize other sophisticated non-TDMA-based legacy systems, e.g. IS-95 and WCDMA system.
  2. Design the multiple channels cognitive MAC protocol that enables the CR device to transmit data over various number of idle channels.
- **Spectrum handoff:**
  1. Investigate the impacts of the primary user's traffic and the contentions among secondary users on the link maintenance probability and effective data rate.
  2. Design a notification mechanism using inband signaling to let secondary users acknowledge the presence of primary users.

A famous slogan by a worldwide communication company is said, "human technology". Through the CR technique, we believe that the dream of freely connecting people anywhere anytime is no longer an impossible mission but will be come true in

the near future. After all, the development of technology is to satisfy the need that people want.

Appendix

A.1 Derivation of (3.4)

The region $R_{CT}^{(u)}$ shown in (3.4) is composed of three sections with the areas of $\pi(\frac{d_{23}}{z_a^{1/\alpha}})^2$, A_1, and A_2. Figure A.1 shows all the parameters used in deriving the area of A_1 and A_2 in (3.5) and (3.6), respectively. In (3.5), the section A_1 is composed of two fan-shaped areas with the measures of $(\frac{d_{23}}{z_a^{1/\alpha}})^2(\pi-\theta')$ and $R^2\theta$, and two identical triangles with the lengths of R, r_2, and $\frac{d_{23}}{z_a^{1/\alpha}}$, where

$$\theta = cos^{-1}\frac{R^2+r_2^2-\frac{d_{23}}{z_a^{1/\alpha}}}{2Rr_2}\ , \tag{A.1}$$

$$\theta' = cos^{-1}\frac{r_2^2+(\frac{d_{23}}{z_a^{1/\alpha}})^2-R^2}{2r_2(\frac{d_{23}}{z_a^{1/\alpha}})}\ , \tag{A.2}$$

$$\Delta = \sqrt{s(s-R)(s-r_2)(s-\frac{d_{23}}{z_a^{1/\alpha}})}\ , \tag{A.3}$$

and

$$s = \frac{R+r_2+\frac{d_{23}}{z_a^{1/\alpha}}}{2}\ . \tag{A.4}$$

Similarly, in (3.6), the section A_2 is also made up by two fan-shaped areas with the measures of $(\frac{d_{23}}{z_a^{1/\alpha}})^2\phi$ and $(r_3 z_i^{1/\alpha})^2\phi'$, and the triangle with the lengths of r_2, $r_3 z_i^{1/\alpha}$, and $\frac{d_{23}}{z_a^{1/\alpha}}$, where

$$\phi = cos^{-1}\frac{r_2^2+(\frac{d_{23}}{z_a^{1/\alpha}})^2-(r_3 z_i^{1/\alpha})^2}{2r_2(\frac{d_{23}}{z_a^{1/\alpha}})}\ , \tag{A.5}$$

$$\phi' = cos^{-1}\frac{r_2^2+(r_3 z_i^{1/\alpha})^2-(\frac{d_{23}}{z_a^{1/\alpha}})^2}{2r_2(r_3 z_i^{1/\alpha})}\ , \tag{A.6}$$

$$\Delta' = \sqrt{s'(s'-r_2)(s'-r_3 z_i^{1/\alpha})(s'-\frac{d_{23}}{z_a^{1/\alpha}})}\ , \tag{A.7}$$

and

$$s' = \frac{r_2 + r_3 z_i^{1/\alpha} + \frac{d_{23}}{z_a^{1/\alpha}}}{2} . \quad (A.8)$$

A.2 Derivation of (3.10) and (3.11)

The distances between the base station to the intersections by the two circles with the radii of $r_3 z_i'^{1/\alpha}$ and $r_2 z_a'^{1/\alpha}$ and centered at (r_3, θ_3) and (r_2, θ_2) are denoted by r^+ and r^-, respectively. Given the locations of intersections (x, y), they can be obtained by jointly solving the equations as follows:

$$\begin{cases} (x - r_2 cos\theta_2)^2 + (y - r_2 sin\theta_2)^2 = (r_2 z_a'^{1/\alpha})^2 \ ; \\ (x - r_3 cos\theta_3)^2 + (y - r_3 sin\theta_3)^2 = (r_3 z_a'^{1/\alpha})^2 \ . \end{cases} \quad (A.9)$$

The distances between the base station and the intersections r^+ and r^-, respectively, shown in (3.10) and (3.11) can be obtained by solving the locations (x, y) from (A.9).

A.3 Derivation of (3.13)

In the infrastructure downlink case, when $max(r^+, r^-) \leq R$, the region $R_{CT}^{(d)}$ is composed of three sections with the areas of $\pi(d_{23} z_a'^{1/\alpha})^2$, A_1, and A_2. Figure A.2 details the parameters used to calculate the areas of these sections in (3.14) and (3.15). In (3.14), the region A_1 is made of two fan-shaped areas with the measures of $(r_2 z_a'^{1/\alpha})^2(\pi - \theta')$ and $R^2\theta$, and two identical triangles with the lengths of R, r_2, and $r_2 z_a'^{1/\alpha}$, where

$$\theta = cos^{-1} \frac{R^2 + r_2^2 - (r_2 z_a'^{1/\alpha})}{2 R r_2} , \quad (A.10)$$

$$\theta' = cos^{-1} \frac{r_2^2 + (r_2 z_a'^{1/\alpha})^2 - R^2}{2 r_2 (r_2 z_a'^{1/\alpha})} , \quad (A.11)$$

$$\Delta = \sqrt{s(s - R)(s - r_2)(s - r_2 z_a'^{1/\alpha})} , \quad (A.12)$$

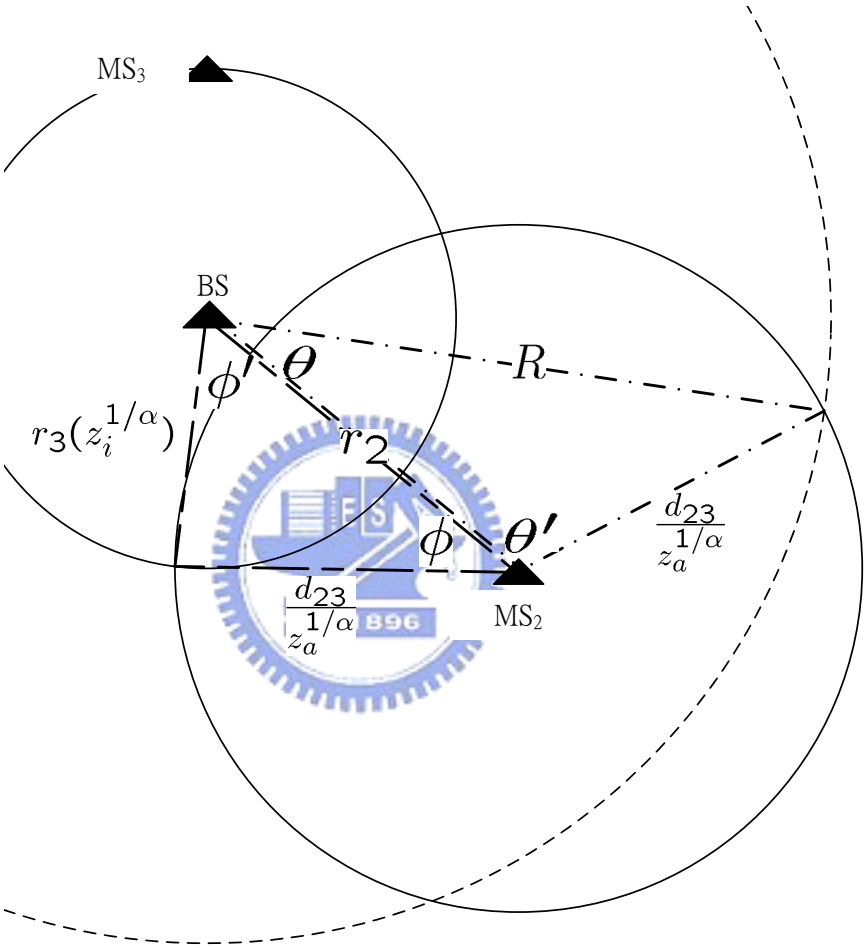

Fig. A.1: Definition of parameters in the calculation of the area of region $R_{CT}^{(u)}$ in the infrastructure uplink case.

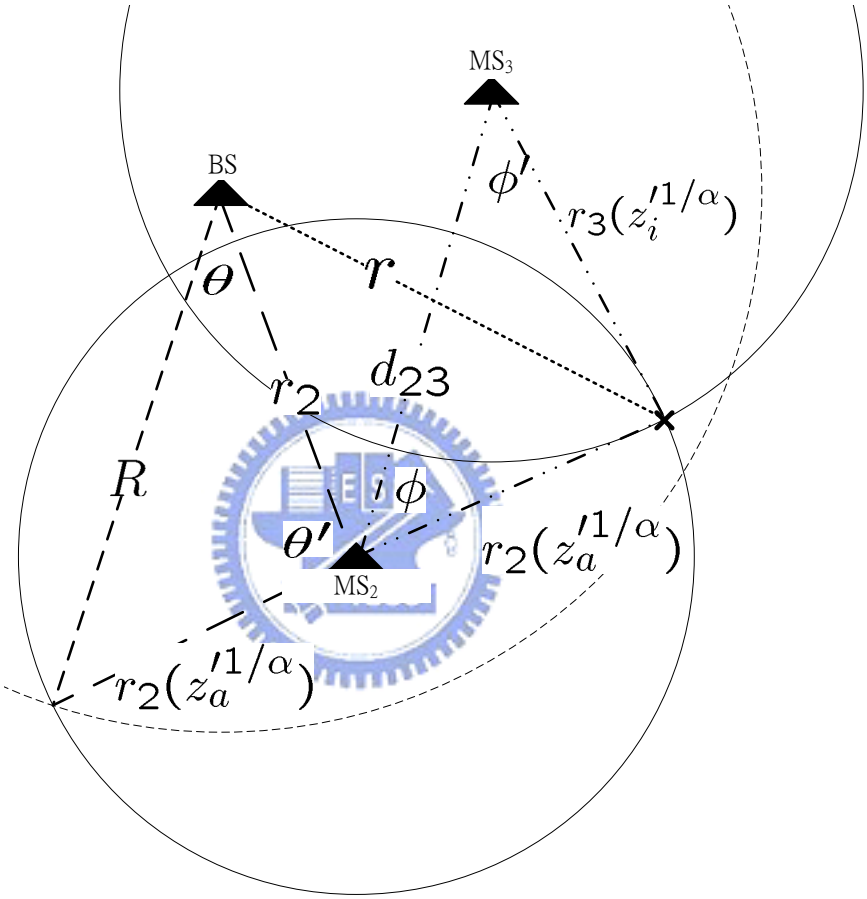

Fig. A.2: Definition of parameters in the calculation of the area of region $R_{CT}^{(d)}$ in the infrastructure downlink case when $max(r^+, r^-) \leq R$.

and

$$s = \frac{R + r_2 + r_2 z_a'^{1/\alpha}}{2} . \tag{A.13}$$

Similarly, the section A_2 in (3.15) is also composed of two fan-shaped areas with the measures of $(r_2 z_a'^{1/\alpha})^2\phi$ and $(r_3 z_i'^{1/\alpha})^2\phi'$, and the triangle with the lengths of d_{23}, $r_2 z_a'^{1/\alpha}$, and $r_3 z_i'^{1/\alpha}$, where

$$\phi = cos^{-1}\frac{d_{23}^2 + (r_2 z_a'^{1/\alpha})^2 - (r_3 z_i'^{1/\alpha})^2}{2d_{23}(r_2 z_a'^{1/\alpha})} , \tag{A.14}$$

$$\phi' = cos^{-1}\frac{d_{23}^2 + (r_3 z_i'^{1/\alpha})^2 - (r_2 z_a'^{1/\alpha})^2}{2d_{23}(r_3 z_i'^{1/\alpha})} , \tag{A.15}$$

$$\Delta' = \sqrt{s'(s' - d_{23})(s' - r_3 z_i'^{1/\alpha})(s' - r_2 z_a'^{1/\alpha})} , \tag{A.16}$$

and

$$s' = \frac{d_{23} + r_2 z_a'^{1/\alpha} + r_3 z_i'^{1/\alpha}}{2} . \tag{A.17}$$

A.4 Derivation of (3.16)

When $max(r^+, r^-) > R$, the region $R_{CT}^{(d)}$ can be separated into four sections with the areas of $\pi(d_{23} z_a'^{1/\alpha})^2$, A_1, A_2, and A_3. Figure A.3 shows all the parameters in deriving (3.17), (3.18), and (3.19). In (3.17), the section A_1 can be divided into two fan-shaped areas with the measures of $(r_2 z_a'^{1/\alpha})^2(\pi - \theta')$ and $R^2\theta$, and the triangle with the lengths of R, r_2, and $r_2 z_a'^{1/\alpha}$, where

$$\theta = cos^{-1}\frac{R^2 + r_2^2 - (r_2 z_a'^{1/\alpha})}{2Rr_2} , \tag{A.18}$$

$$\theta' = cos^{-1}\frac{r_2^2 + (r_2 z_a'^{1/\alpha})^2 - R^2}{2r_2(r_2 z_a'^{1/\alpha})} , \tag{A.19}$$

$$\Delta = \sqrt{s(s - R)(s - r_2)(s - r_2 z_a'^{\frac{1}{\alpha}})} , \tag{A.20}$$

and

$$s = \frac{R + r_2 + r_2 z_a'^{\frac{1}{\alpha}}}{2} . \tag{A.21}$$

In addition, the section A_2 is made of two fan-shaped areas with the measures of $(r_2 z_a'^{1/\alpha})^2\phi$ and $(r_3 z_i'^{1/\alpha})^2\phi'$, and the triangle with the lengths of d_{23}, $r_3 z_i'^{1/\alpha}$, and $r_2 z_a'^{1/\alpha}$, where

$$\phi = cos^{-1}\frac{d_{23}^2 + (r_2 z_a'^{1/\alpha})^2 - (r_3 z_i'^{1/\alpha})^2}{2d_{23}(r_2 z_a'^{1/\alpha})}\ , \tag{A.22}$$

$$\phi' = cos^{-1}\frac{d_{23}^2 + (r_3 z_i'^{1/\alpha})^2 - (r_2 z_a'^{1/\alpha})^2}{2d_{23}(r_3 z_i'^{1/\alpha})}\ , \tag{A.23}$$

$$\Delta' = \sqrt{s'(s'-d_{23})(s'-r_3 z_i'^{\frac{1}{\alpha}})(s'-r_2 z_a'^{\frac{1}{\alpha}})}\ , \tag{A.24}$$

and

$$s' = \frac{d_{23} + r_2 z_a'^{\frac{1}{\alpha}} + r_3 z_i'^{\frac{1}{\alpha}}}{2}\ . \tag{A.25}$$

At last, in (3.19), the section A_3 is constructed by three arc-shaped areas with the measures of $(r_3 z_i'^{1/\alpha})^2\psi_2 - \frac{1}{2}(r_3 z_i'^{1/\alpha})^2 sin\psi_2$, $(r_2 z_a'^{1/\alpha})^2\psi_3 - \frac{1}{2}(r_2 z_a'^{1/\alpha})^2 sin\psi_3$, and $R^2\psi_1 - \frac{1}{2}R^2 sin\psi_1$, and the triangle with the lengths of a, b, and c, where

$$\psi_1 = cos^{-1}\frac{R^2 + r_2^2 - r_2^2 z_a'^{\frac{2}{\alpha}}}{2Rr_2} + cos^{-1}\frac{R^2 + r_3^2 - r_3^2 z_i'^{\frac{2}{\alpha}}}{2Rr_3} - cos^{-1}\frac{r_2^2 + r_3^2 - d_{23}^2}{2r_2 r_3}\ , \tag{A.26}$$

$$\psi_2 = cos^{-1}\frac{d_{23}^2 + r_3^2 z_i'^{\frac{2}{\alpha}} - r_2^2 z_a'^{\frac{2}{\alpha}}}{2d_{23}(r_3 z_i'^{\frac{1}{\alpha}})} + cos^{-1}\frac{d_{23}^2 + r_3^2 - r_2^2}{2d_{23}r_3} - cos^{-1}\frac{r_3^2 + r_3^2 z_i'^{\frac{2}{\alpha}} - R^2}{2r_3(r_3 z_i'^{\frac{1}{\alpha}})}\ , \tag{A.27}$$

$$\psi_3 = cos^{-1}\frac{d_{23}^2 + r_2^2 z_a'^{\frac{2}{\alpha}} - r_3^2 z_i'^{\frac{2}{\alpha}}}{2d_{23}(r_2 z_a'^{\frac{1}{\alpha}})} + cos^{-1}\frac{d_{23}^2 + r_2^2 - r_3^2}{2d_{23}r_2} - cos^{-1}\frac{r_2^2 + r_2^2 z_a'^{\frac{2}{\alpha}} - R^2}{2r_2(r_2 z_a'^{\frac{1}{\alpha}})}\ , \tag{A.28}$$

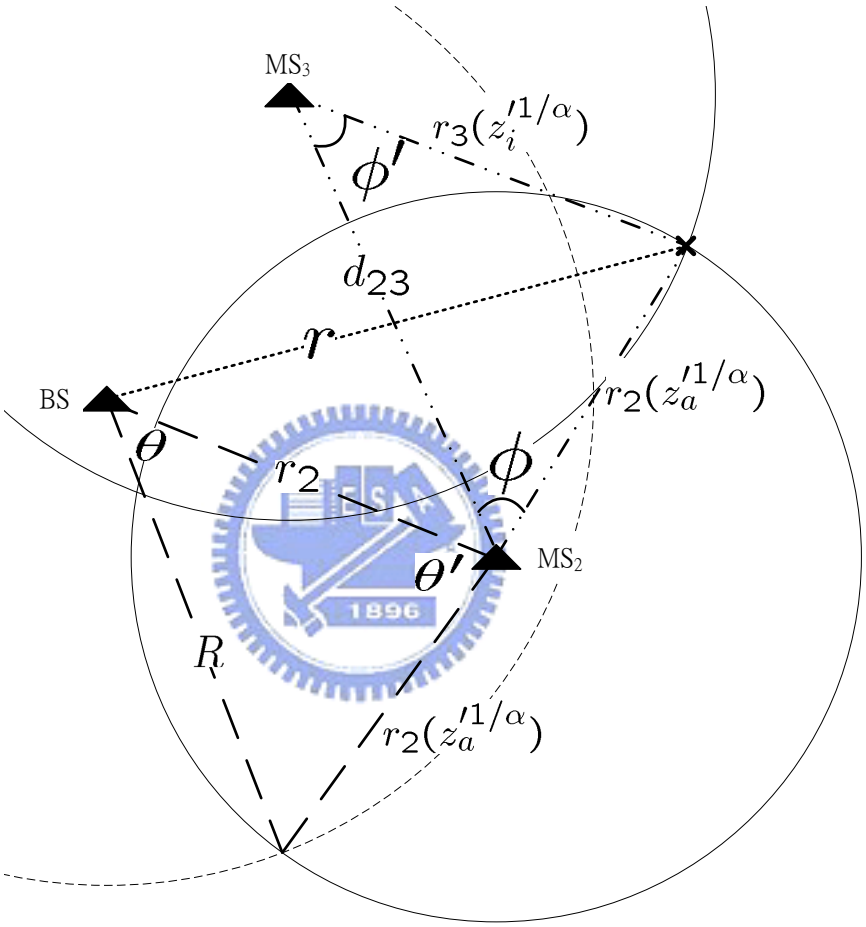

Fig. A.3: Definition of parameters in the calculation of the areas of sections A_1 and A_2 in (3.16) in the infrastructure downlink case when $max(r^+, r^-) > R$.

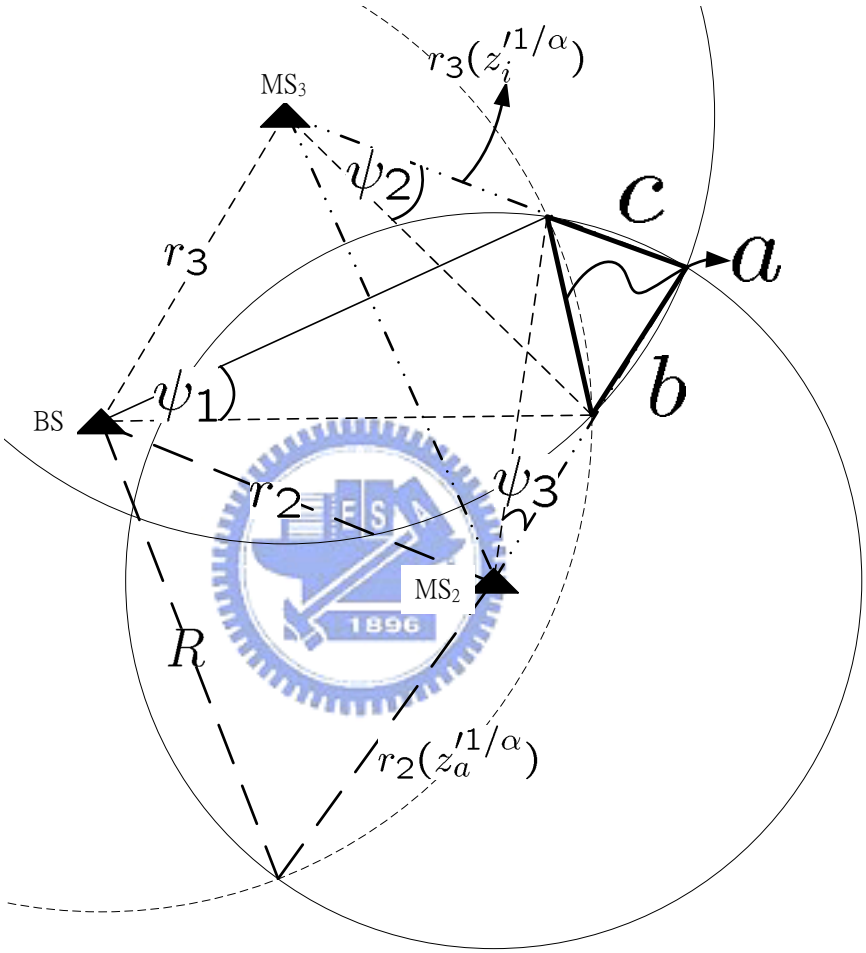

Fig. A.4: Definitions of parameters in the calculation of the area of section A_3 in (3.16) in the infrastructure downlink case when $max(r^+, r^-) > R$.

$$\Delta'' = \sqrt{s''(s''-a)(s''-b)(s''-c)}\ , \tag{A.29}$$

$$s'' = \frac{a+b+c}{2}\ , \tag{A.30}$$

$$a = 2Rsin\frac{\psi_1}{2}\ , \tag{A.31}$$

$$b = 2(r_3 zi'^{\frac{1}{\alpha}})sin\frac{\psi_2}{2}\ , \tag{A.32}$$

and

$$c = 2(r_2 z_a'^{\frac{1}{\alpha}})sin\frac{\psi_3}{2}\ . \tag{A.33}$$

Figure A.4 shows all the parameters in deriving (3.19).

Bibliography

[1] E. M. Noam, "Taking the next step beyond spectrum auctions: open spectrum access," *IEEE Communications Magazine*, vol. 33, pp. 66–73, Dec. 1995.

[2] N. S. Shankar, C. Cordeiro, and K. Challapali, "Spectrum agile radios: Utilization and sensing architectures," *IEEE International Symposium on New Frontiers in Dynamic Spectrum Access Networks*, pp. 160–169, Nov. 2005.

[3] S. M. Mishra, A. Sahai, and R. W. Brodersen, "Cooperative sensing among cognitive radios," *IEEE International Conference on Communications*, vol. 4, pp. 1658–1663, Jun. 2006.

[4] F. C. Commission, *"Notice of Proposed Rule Making and Order," Rep. ET Docket no. 03-108*, Dec. 2003.

[5] The XG Vision. [Online]. Available: http://www.darpa.mil/ato/programs/XG/

[6] T. A. Weiss and F. K. Jondral, "Spectrum pooling: an innovative strategy for the enhancement of spectrum efficiency," *IEEE Communications Magazine*, vol. 42, pp. s8–s14, Mar. 2004.

[7] S. Haykin, "Cognitive radio: brain-empowered wireless communications," *IEEE Journal on Selected Areas in Communication*, vol. 23, no. 2, pp. 201–220, Feb. 2005.

[8] R. W. Thomas, L. A. DaSilva, and A. B. MacKenzie, "Cognitive networks,"

IEEE International Symposium on New Frontiers in Dynamic Spectrum Access Networks, pp. 352–360, Nov. 2005.

[9] I. F. Akyildiz, W. Y. Lee, M. C. Vuran, and S. Mohanty, "NeXt generation/dynamic spectrum access/cognitive radio wireless networks: a survey," *Computer Networks Journal (Elsevier)*, vol. 50, pp. 2127–2159, Sep. 2006.

[10] Q. Zhao, L. Tong, and A. Swami, "A cross-layer approach to cogintive MAC for spectrum agility," *Proceedings of IEEE Asilomar Conference on Signals, Systems, and Computers*, pp. 200–204, Nov. 2005.

[11] S. Krishnamurthy, M. Thoppian, S. Venkatesan, and R. Prakash, "Control channel based MAC-layer configuration, routing and situation awareness for radio networks," *Proceedings of IEEE Military Communications*, pp. 1–6, Oct. 2005.

[12] *IEEE Std. 802.11, "Part 11: Wireless LAN medium access control (MAC) and physical layer (PHY) specification*, Nov. 1999.

[13] J. Mitola and G. Q. Maguire, "Cognitive radio: making software radios more personal," *IEEE Personal Communications*, vol. 6, pp. 13–18, Aug. 1999.

[14] D. Cabric, S. M. Mishra, and R. W. Brodersen, "Implementation issues in spectrum sensing for cognitive radios," *Conference on Signals, Systems, and Computers*, vol. 1, pp. 772–776, Nov. 2004.

[15] H. Tang, "Some physical layer issues of wide-band cognitive radio systems," *IEEE International Symposium on New Frontiers in Dynamic Spectrum Access Networks*, pp. 151–159, Nov. 2005.

[16] Y. Hur, J. Park, W. Woo, K. Lim, C.-H. Lee, H. S. Kim, and J. Laskar, "A wide-band analog multi-resolution spectrum sensing (MRSS) technique for cognitive radio (CR) systems," *Circuits and Systems. Proceedings of IEEE International Symposium on*, pp. 4090–4093, May 2006.

[17] Z. Tian and G. B. Giannakis, "A wavelet approach to wideband spectrum sensing for cognitive radios," *Cognitive Radio Oriented Wireless Networks and Communications, International Conference on*, pp. 1–5, Jun. 2006.

[18] Y. Youn, H. Jeon, H. Jung, and H. Lee, "Discrete wavelet packet transform based energy detector for cognitive radios," *IEEE Vehicular Technology Conference*, pp. 2641–2645, Apr. 2007.

[19] J. G. Proakis, *Digital Communication, 4th edition.* New York: McGraw-Hill, 2001.

[20] W. A. Gardner, "Signal interception: a unifying theoretical framework for feature detection," *IEEE Transactions on Communications*, vol. 36, no. 8, pp. 897–906, Aug. 1988.

[21] K. R. Kolodziejski and J. W. Betz, "Detection of weak random signals in iid non-gaussian noise," *IEEE Transactions on Communications*, vol. 48, no. 2, pp. 222–230, Feb. 2000.

[22] M. Oner and F. Jondral, "Extracting the channel allocation information in a spectrum pooling system using a prefilter delay and multiply nonlinearity," *IEEE Workshop on Statistical Signal Processing*, pp. 46–49, Oct. 2003.

[23] ——, "Extracting the channel allocation information in a spectrum pooling system exploiting cyclostationarity," *IEEE International Symposium on Personal, Indoors, and Mobile Radio Communications*, vol. 1, pp. 551–555, Sep. 2004.

[24] A. Ghasemi and E. S. Sousa, "Collaborative spectrum sensing for opportunistic access in fading environments," *IEEE International Symposium on New Frontiers in Dynamic Spectrum Access Networks*, pp. 131–136, Nov. 2005.

[25] E. Visotsky, S. Kuffner, and R. Peterson, "On collaborative detection of tv transmissions in support of dynamic spectrum sharing," *IEEE International*

Symposium on New Frontiers in Dynamic Spectrum Access Networks, pp. 338–345, Nov. 2005.

[26] Q. Peng, K. Zeng, J. Wang, and S. Li, "A distributed spectrum sensing scheme based on credibility and evidence theory in cognitive radio context," *IEEE International Symposium on Personal, Indoors, and Mobile Radio Communications*, pp. 1–5, Sep. 2006.

[27] M. Gandeeto and C. Regazzoni, "Spectrum sensing: A distributed approach for cognitive terminals," *IEEE Journal on Selected Areas in Communication*, vol. 25, no. 3, pp. 546–557, Apr. 2007.

[28] G. Ganesan and Y. G. Li, "Cooperative spectrum sensing in cognitive radio, part i: Two user networks," *IEEE Transcations on Wireless Communications*, vol. 6, no. 6, pp. 2204–2213, Jun. 2007.

[29] ——, "Cooperative spectrum sensing in cognitive radio, part i: Multiuser networks," *IEEE Transcations on Wireless Communications*, vol. 6, no. 6, pp. 2214–2222, Jun. 2007.

[30] E. Peh and Y.-C. Liang, "Optimization for cooperative sensing in cognitive radio networks," *IEEE Wireless Communications and Networking Conference*, pp. 27–32, Mar. 2007.

[31] R. Chen and J.-M. Park, "Ensuring trustworthy spectrum sensing in cognitive radio networks," *Networking Technologies for Software Defined Radio Networks IEEE Workshop on*, pp. 110–119, Sep. 2006.

[32] T. X. Brown, "An analysis of unlicensed device operation in licensed broadcast service bands," *IEEE International Symposium on New Frontiers in Dynamic Spectrum Access Networks*, pp. 11–29, Nov. 2005.

[33] B. Wild and K. Ramchandran, "Detecting primary receivers for cognitive radio applications," *IEEE International Symposium on New Frontiers in Dynamic Spectrum Access Networks*, pp. 124–130, Nov. 2005.

[34] P. J. Kolodzy, "Interference temperature: a metric for dynamic spectrum utilization," *International Journal of Network Management*, vol. 16, no. 2, pp. 103–113, Mar. 2006.

[35] T. C. Clancy, "Achievable capacity under the interference temperature model," *INFOCOM, IEEE International Conference on Computer Communications*, pp. 794–802, May 2007.

[36] Q. Zhao, L. Tong, and A. Swami, "Decentralized cognitive MAC for dynamic spectrum access," *IEEE International Symposium on New Frontiers in Dynamic Spectrum Access Networks*, pp. 224–232, Nov. 2005.

[37] L. N. Singh and G. R. Dattatreya, "Gaussian mixture parameter estimation for cognitive radio and network surveillance applications," *IEEE Vehicular Technology Conference*, vol. 3, pp. 1993–1997, Sep. 2005.

[38] S. Geirhofer, L. Tong, and B. M. Sadler, "A measurement-based model for dynamic spectrum access in wlan channels," *Proceedings of IEEE Military Communications*, pp. 1–7, Oct. 2006.

[39] L. N. Singh and G. R. Dattatreya, "Channel and data estimation for ad hoc networks and cognitive radio," *International Journal of Wireless Information Networks*, vol. 14, no. 1, pp. 17–31, Mar. 2007.

[40] Q. Zhao, S. Geirhofer, L. Tong, and B. M. Sadler, "Optimal dynamic spectrum access via periodic channel sensing," *IEEE Wireless Communications and Networking Conference*, pp. 33–37, Mar. 2007.

[41] Q. Zhao, L. Tong, A. Swami, and Y. Chen, "Decentralized cognitive MAC for opportunistic spectrum access in ad hoc network: a POMDP framework," *IEEE Journal on Selected Areas in Communication*, vol. 25, no. 3, pp. 589–600, Apr. 2007.

[42] L. Berlemann, G. R. Hiertz, B. H. Walke, and S. Mangold, "Radio resource sharing games: enabling QoS support in unlicensed bands," *IEEE Network*, vol. 19, no. 4, pp. 59–65, Jul./Aug. 2005.

[43] N. Nie and C. Comaniciu, "Adaptive channel allocation spectrum etiquette for cognitive radio networks," *IEEE International Symposium on New Frontiers in Dynamic Spectrum Access Networks*, pp. 269–278, Nov. 2005.

[44] Y. Xing, C. N. Mathur, M. A. Haleem, R. Chandramouli, and K. P. Subbalakshmi, "Dynamic spectrum access with QoS and interference temperature constraints," *IEEE Transcations on Mobile Computing*, vol. 6, no. 4, pp. 423–432, Apr. 2007.

[45] J. E. Suris, L. A. DaSilva, Z. Han, and A. B. MacKenzie, "Cooperative game theory for distributed spectrum sharing," *IEEE International Conference on Communications*, pp. 24–28, Jun. 2007.

[46] W. Wang and X. Liu, "List-coloring based channel allocation for open-spectrum wireless networks," *IEEE Vehicular Technology Conference*, vol. 1, pp. 690–694, Sep. 2005.

[47] M. Thoppian, S. Venkatesan, R. Prakash, and R. Chandrasekaran, "MAC-layer scheduling in cognitive radio based multi-hop wireless networks," *WOWMOM, Proceedings of the International Symposium on on World of Wireless, Mobile and Multimedia Networks*, pp. 191–202, 2006.

[48] S. A. Zekavat and X. Li, "User-central wireless system: ultimate dynamic channel allocation," *IEEE International Symposium on New Frontiers in Dynamic Spectrum Access Networks*, pp. 82–87, Nov. 2005.

[49] N. Choi, M. Patel, and S. Venkatesan, "A full duplex multi-channel MAC protocol for multi-hop cognitive radio networks," *Cognitive Radio Oriented Wireless Networks and Communications, International Conference on*, pp. 1–5, Jun. 2006.

[50] P. A. K. Acharya, S. Singh, and H. Zheng, "Reliable open spectrum communications through proactive spectrum access," *TAPAS: Proceedings of the international workshop on Technology and policy for accessing spectrum*, p. 5, Aug. 2006.

[51] A. C. C. Hsu, D. S. L. Wei, and C. C. J. Kuo, "A cognitive MAC protocol using statistical channel allocation for wireless ad hoc networks," *IEEE Wireless Communications and Networking Conference*, pp. 105–110, Mar. 2007.

[52] G. F. Marias, "Spectrum scheduling and brokering based on QoS demands of competing WISPs," *IEEE International Symposium on New Frontiers in Dynamic Spectrum Access Networks*, pp. 684–687, Nov. 2005.

[53] D. Grandblaise, K. Moessner, G. Vivier, and R. Tafazolli, "Credit token based rental protocol for dynamic channel allocation," pp. 1–5, Jun. 2006.

[54] T. Banerjee, C. Ghosh, and D. P. Agrawal, "Wireless sensor based dynamic channel selection in cellular communication by cognitive radio approach," pp. 1–5, Jun. 2006.

[55] S. Sankaranarayanan, P. Papadimitratos, A. Mishra, and S. Hershey, "A bandwidth sharing approach to improve licensed spectrum utilization," *IEEE International Symposium on New Frontiers in Dynamic Spectrum Access Networks*, pp. 279–288, Nov. 2005.

[56] L. Ma, X. Han, and C.-C. Shen, "Dynamic open spectrum sharing MAC protocol for wireless ad hoc networks," *IEEE International Symposium on New Frontiers in Dynamic Spectrum Access Networks*, pp. 203–213, Nov. 2005.

[57] V. Brik, E. Rozner, S. Banerjee, and P. Bahl, "DSAP: a protocol for coordinated spectrum access."

[58] C. Doerr, M. Neufeld, J. Fifield, T. Weingart, D. C. Sicker, and D. Grunwald, "MultiMAC - an adaptive MAC framework for dynamic radio networking," *IEEE International Symposium on New Frontiers in Dynamic Spectrum Access Networks*, pp. 548–555, Nov. 2005.

[59] D. Zheng and J. Zhang, "Protocol design and throughput analysis of frequency-agile multi-channel medium access control," *IEEE Transcations on Wireless Communications*, vol. 5, no. 10, pp. 2887–2895, Oct. 2006.

[60] C. Cordeiro and K. Challapali, "C-MAC: a cognitive MAC protocol for multi-channel wireless networks," *IEEE International Symposium on New Frontiers in Dynamic Spectrum Access Networks*, pp. 147–157, Apr. 2007.

[61] H. Nan, T.-I. Hyon, and S.-J. Yoo, "Distributed coordinated spectrum sharing MAC protocol for cognitive radio," *IEEE International Symposium on New Frontiers in Dynamic Spectrum Access Networks*, pp. 240–249, Apr. 2007.

[62] G. Auer, H. Haas, and P. Omiyi, "Interference aware medium access for dynamic spectrum sharing," *IEEE International Symposium on New Frontiers in Dynamic Spectrum Access Networks*, pp. 399–402, Apr. 2007.

[63] C. Han, J. Wang, and S. Li, "A spectrum exchange mechanism in cognitive radio contexts," *IEEE International Symposium on Personal, Indoors, and Mobile Radio Communications*, pp. 1–5, Sep. 2006.

[64] X. Zhu, L. Shen, and T.-S. P. Yum, "Analysis of cognitive radio spectrum access with optimal channel reservation," *IEEE Communications Letters*, vol. 11, no. 4, pp. 304–306, Apr. 2007.

[65] D. Willkomm, J. Gross, and A. Wolisz, "Reliable link maintenance in cognitive radio systems," *IEEE International Symposium on New Frontiers in Dynamic Spectrum Access Networks*, pp. 371–378, Nov. 2005.

[66] J. Tian and G. Bi, "A new link maintenance and compensation model for cognitive uwb radio systems," *International Conference on ITS Telecommunications Proceedings*, pp. 254–257, Jun. 2006.

[67] X. Liu and Z. Ding, "ESCAPE: a channel evacuation protocol for spectrum-agile networks," *IEEE International Symposium on New Frontiers in Dynamic Spectrum Access Networks*, pp. 292–302, Apr. 2007.

[68] Q. Shi, D. Taubenheim, S. Kyperountas, P. Gorday, and N. Correal, "Link maintenance protocol for cognitive radio system with OFDM PHY," *IEEE International Symposium on New Frontiers in Dynamic Spectrum Access Networks*, pp. 440–443, Apr. 2007.

[69] G. Bianchi, "Performance analysis of IEEE 802.11 distributed coordination function," *IEEE Journal on Selected Areas in Communication*, vol. 18, no. 3, pp. 535–547, Mar. 2000.

[70] Y. Tay and K. Chua, "A capacity analysis for the IEEE 802.11 MAC protocol," *ACM Wireless Networks*, vol. 7, pp. 159–171, Mar. 2001.

[71] Y. Xiao, "Saturation performance metrics of the IEEE 802.11 MAC," *IEEE Vehicular Technology Conference*, vol. 3, pp. 1453–1457, Oct. 2003.

[72] B.-J. Kwak, N.-O. Song, and L. E. Miller, "Performance analysis of exponential

backoff," *IEEE/ACM Transcations on Networking*, vol. 13, no. 2, pp. 343–355, Apr. 2005.

[73] K. Duffy, D. Malone, and D. J. Leith, "Modeling of 802.11 distributed coordination function in non-satureated condition," *IEEE Communications Letters*, vol. 9, no. 8, pp. 715–717, Aug. 2005.

[74] M. Garetto and C. F. Chiasserini, "Performance analysis of 802.11 WLANs under sporadic traffic," *Networking, Springer*, vol. 3462, pp. 1343–1347, May 2005.

[75] C. H. Foh and J. W. Tantra, "Comments on IEEE 802.11 saturation throughput analysis with freezing of backoff counters," *IEEE Communications Letters*, vol. 9, no. 2, pp. 130–132, Feb. 2005.

[76] P. Chatzimisios, A. Boucouvalas, and V. Vitsas, "IEEE 802.11 packet delay - a finite retry limit analysis," *IEEE Global Telecommunications Conference*, vol. 2, pp. 950–954, Dec. 2003.

[77] Z. Hadzi-Velkov and B. Spasenovski, "Saturation throughput - delay analysis of IEEE 802.11 DCF in fading channel," *IEEE International Conference on Communications*, pp. 121–126, May 2003.

[78] M. Ergen and P. Varaiya, "Throughput analysis and admission control for IEEE 802.11a," *Mobile Networks and Applications, Springer*, vol. 10, no. 5, pp. 705–712, Oct. 2005.

[79] Y. Zheng, K. Lu, D. Wu, and Y. Fang, "Performance analysis of IEEE 802.11 DCF in imperfect channels," *IEEE Transactions on Vehicular Technology*, vol. 55, no. 5, pp. 1648–1656, Sep. 2006.

[80] Z. Hadzi-Velkov and B. Spasenovski, "Capture effect in IEEE 802.11 basic service area under influence of rayleigh fading and near/far effect," *IEEE Inter-*

national Symposium on Personal, Indoors, and Mobile Radio Communications, vol. 1, pp. 172–176, Sep. 2002.

[81] M. M. Carvalho and J. J. Garcia-Luna-Aceves, "A scalable model for channel access protocols in multihop ad hoc networks," *The ACM Annual International Conference on Mobile Computing and Networking*, pp. 330–344, Sep. 2004.

[82] S. Redana, M. Lott, and A. Capone, "Performance evaluation of point-to-multipoint (PMP) and mesh air-interface in IEEE standard 802.16a," *IEEE Vehicular Technology Conference*, vol. 5, pp. 3186–3190, Sep. 2004.

[83] A. E. Xhafa, S. Kangude, and X. Lu, "MAC performance of IEEE 802.16e," *IEEE Vehicular Technology Conference*, vol. 1, pp. 685–689, Sep. 2005.

[84] S. M. Oh and J. H. Kim, "The analysis of the optimal contention period for broadband wireless access network," *IEEE International Conference on Pervasive Computing and Communications Workshops*, pp. 215–219, Mar. 2005.

[85] R. Iyengar, P. Iyer, and B. Sikdar, "Delay analysis of 802.16 based last mile wireless networks," *IEEE Global Telecommunications Conference*, vol. 5, pp. 3123–3127, Dec. 2005.

[86] D. Niculescu and B. Nath, "Ad hoc positioning system (APS)," *INFOCOM, IEEE International Conference on Computer Communications*, vol. 3, pp. 1734–1743, Mar. 2001.

[87] J. Hightower and G. Borriello, "Location systems for ubiquitous computing," *IEEE Computer*, vol. 34, no. 8, pp. 57–66, Aug. 2001.

[88] D. Niculescu and B. Nath, "Ad hoc positioning system (APS) using AOA," *INFOCOM, IEEE International Conference on Computer Communications*, vol. 3, pp. 1734–1743, Mar. 2003.

[89] S. J. Ingram, D. Harmer, and M. Quinlan, "Ultrawideband indoor positioning systems and their use in emergencies," *Position Location and Navigation Symposium*, pp. 706–715, Apr. 2004.

[90] D. Madigan, E. Einahrawy, R. P. Martin, W.-H. Ju, P. Krishnan, and A. S. Krishnakumar, "Bayesian indoor positioning systems," *INFOCOM, IEEE International Conference on Computer Communications*, vol. 2, pp. 1217–1227, Mar. 2005.

[91] G. Sun, J. Chen, W. Guo, and K.-J. R. Liu, "Signal processing techniques in network-aided positioning: a survey of state-of-the-art positioning designs," *IEEE Signal Processing Magazine*, vol. 22, no. 4, pp. 12–23, Jul. 2005.

[92] Y.-C. Tseng, S.-L. Wu, W.-H. Liao, and C.-M. Chao, "Location awareness in ad hoc wireless mobile networks," *IEEE Computer*, vol. 34, no. 6, pp. 46–52, Jun. 2001.

[93] M. Mauve, A. Widmer, and H. Hartenstein, "A survey on position-based routing in mobile ad hoc networks," *IEEE Network*, vol. 15, no. 6, pp. 30–39, Nov./Dec. 2001.

[94] X. Hong, K. Xu, and M. Gerla, "Scalable routing protocols for mobile ad hoc networks," *IEEE Network*, vol. 16, no. 4, pp. 11–21, Jul./Aug. 2002.

[95] T. Park and K. G. Shin, "Optimal tradeoffs for location-based routing in large-scale ad hoc networks," *IEEE/ACM Transcations on Networking*, vol. 13, no. 2, pp. 398–410, Apr. 2005.

[96] H. Celebi and H. Arslan, "Adaptive positioning systems for cognitive radios," *IEEE International Symposium on New Frontiers in Dynamic Spectrum Access Networks*, pp. 78–84, Apr. 2007.

[97] T. S. Rappaport, *Wireless Communications: Principle and Practice, 2nd edition.* New Jersey: Prentice Hall, Inc., 2002.

[98] H. Wu, C. Qiao, S. De, and O. Tonguz, "Integrated cellular and ad hoc relaying systems: iCAR," *IEEE Journal on Selected Areas in Communication*, vol. 19, no. 10, pp. 2105–2115, Oct. 2001.

[99] E. Yanmaz, O. K. Tonguz, S. Mishra, H. Wu, and C. Qiao, "Efficient dynamic load balancing algorithms using icar systems: a generalized framework," *IEEE Vehicular Technology Conference*, vol. 1, pp. 586–590, Sep. 2002.

[100] E. H.-K. Wu, Y.-Z. Huang, and J.-H. Chiang, "Dynamic adaptive routing for heterogeneous wireless network," *IEEE Global Telecommunications Conference*, vol. 6, pp. 3608–3612, Nov. 2001.

[101] Y. D. Lin and Y. C. Hsu, "Multihop cellular: a new architecture for wireless communications," *INFOCOM, IEEE International Conference on Computer Communications*, vol. 3, pp. 26–30, Mar. 2000.

[102] J. Chen, S.-H. G. Chan, J. He, and S. C. Liew, "Mixed-mode WLAN: the integration of ad-hoc mode with wireless LAN infrastructure," *IEEE Global Telecommunications Conference*, vol. 1, pp. 231–235, Dec. 2003.

[103] G. L. Stüber, *Principle of Mobile Communication, 2nd edition.* Boston/Dordrecht/London: Kluwer Academic Pulishers, 2001.

[104] L. C. Wang, S. Y. Huang, and A. Chen, "A cross-layer throughput performance investigation for csma/ca-based wireless local area network with directional antennas and capture effect," *IEEE Wireless Communications and Networking Conference*, vol. 3, pp. 1879–1884, Mar. 2004.

[105] C. Zhu and M. S. Corson, "A five-phase reservation protocol for mobile ad hoc

networks," *INFOCOM, IEEE International Conference on Computer Communications*, vol. 1, pp. 322–331, Mar. 1998.

[106] J. J. Garcia-Luna-Aceves and A. Tzamaloukas, "Receiver-initiated collision avoidance in wireless networks," *ACM Wireless Networks*, vol. 8, no. 2-3, pp. 249–263, Mar.-May 2002.

[107] J. L. Sobrinho and A. S. Krishnakumar, "Quality-of-service in ad hoc carrier sense multiple access networks," *IEEE Journal on Selected Areas in Communication*, vol. 17, no. 8, pp. 1353–1368, Aug. 1999.

[108] A. Lindgren, A. Almquist, and O. Schelen, "Evaluation of quality of service scheme for IEEE 802.11 wireless LANs," *in Proceedings of the 26th Annual IEEE Conference on Local Computer Networks (LCN 2001)*, pp. 384–391, Nov. 2001.

[109] T. Nandagopal, T. E. Kim, X. Gao, and V. Bharghavan, "Achieving MAC layer fairness in wireless packet networks," *The ACM Annual International Conference on Mobile Computing and Networking*, pp. 87–98, Aug. 2000.

[110] N. H. Vaidya, P. Bahl, and S. Gupta, "Distributed fair scheduling in a wireless LAN," *The ACM Annual International Conference on Mobile Computing and Networking*, pp. 167–178, Aug. 2000.

[111] Y. Kwon, Y. Fang, and H. Latchman, "Fast collision resolution (FCR) MAC algorithm for wireless local area network," *IEEE Global Telecommunications Conference*, vol. 3, pp. 2250–2254, Nov. 2002.

[112] *IEEE Std. 802.11e/D3.2, "Wireless LAN Medium Access Control (MAC) and Physical Layer (PHY) Specifications, Medium Access Control(MAC) Enhancement for Quality of Service (QoS)"*, Aug. 2002.

[113] A. Veres, A. T. Campbell, M. Barry, and L. Sun, "Supporting service differentiation in wireless packet networks using distributed control," *IEEE Journal on Selected Areas in Communication*, vol. 19, no. 10, pp. 2081–2093, Oct. 2001.

[114] F. Calì, M. Conti, and E. Gregori, "IEEE 802.11 protocol: design and performance evaluation of an adaptive backoff mechanism," *IEEE Journal on Selected Areas in Communication*, vol. 18, no. 19, pp. 1774–1786, Sep. 2000.

[115] ——, "Dynamic tuning of the IEEE 802.11 protocol to achieve a theoretical throughput limit," *IEEE/ACM Transcations on Networking*, vol. 8, no. 6, pp. 785–799, Dec. 2000.

[116] H. Zhu, M. Li, I. Chlamtac, and B. Prabhakaran, "A survey of quality of service in IEEE 802.11 networks," *IEEE Wireless Communications*, vol. 11, pp. 6–14, Aug. 2004.

[117] D. J. Goodman, R. A. Valenzuela, K. T. Gayliard, and B. Ramamurthi, "Packet reservation multiple access for local wireless communications," *IEEE Transactions on Communications*, vol. 37, no. 8, pp. 885–890, Aug. 1989.

[118] C. R. Lin and M. Gerla, "Asynchronous multimedia multihop wireless networks," *INFOCOM, IEEE International Conference on Computer Communications*, vol. 1, pp. 118–125, Apr. 1997.

[119] S. Elnoubi and A. M. Alsayh, "A packet reservation multiple access (PRMA)-based algorithm for multimedia wireless system," *IEEE Transactions on Vehicular Technology*, vol. 53, no. 1, pp. 215–222, Jan. 2004.

[120] S. T. Sheu and T. F. Sheu, "DBASE: a distributed bandwidth allocation/sharing/extension protocol for multimedia over IEEE 802.11 ad hoc wireless LAN," *INFOCOM, IEEE International Conference on Computer Communications*, vol. 3, pp. 1558–1567, Apr. 2001.

[121] S. Jiang, J. Rao, D. He, X. Ling, and C. C. Ko, "A simple distributed PRMA for MANETs," *IEEE Transactions on Vehicular Technology*, vol. 51, no. 2, pp. 293–304, Mar. 2002.

[122] C. H. Ng, *Queuing Modeling Fundamentals*. New York: John Wiley & Sons, Ltd., 1996.

[123] The Network Simulator- NS2. [Online]. Available: http://www.isi.edu/nsnam/ns

[124] L. Bononi, M. Conti, and L. Donatiello, "Design and performance evaluation of a distributed contention control (DCC) mechanism for IEEE 802.11 wireless local area networks," *WOWMOM, Proceedings of the International Symposium on on World of Wireless, Mobile and Multimedia Networks*, pp. 59–67, Oct. 1998.

[125] X. Yang and N. H. Vaidya, "Explicit and implicit pipelining for wireless medium access control," *IEEE Vehicular Technology Conference*, vol. 3, pp. 1427–1431, Oct. 2003.

[126] J. W. Tantra, C. H. Foh, and B. S. Lee, "An efficient scheduling scheme for high speed IEEE 802.11 WLANs," *IEEE Vehicular Technology Conference*, vol. 4, pp. 2589–2593, Oct. 2003.

[127] Y. Xiao, "Concatenation and piggyback mechanisms for the IEEE 802.11 MAC," *IEEE Vehicular Technology Conference*, vol. 3, pp. 1453–1457, Oct. 2003.

[128] J. H. Kim and J. K. Lee, "Capture effects of wireless CSMA/CA protocols in rayleigh and shadow fading channel," *IEEE Transactions on Vehicular Technology*, vol. 48, no. 4, pp. 1277–1286, July 1999.

[129] N. S. Fahmy, T. D. Todd, and V. Kezys, "Ad hoc networks with smart antennas using IEEE 802.11-based protocols," *IEEE International Conference on Communications*, vol. 5, pp. 3144–3148, Apr. 2002.

[130] J. Yang, J. Li, and M. Sheng, "MAC protocol for mobile ad hoc network with smart antennas," *Electronics Letters*, vol. 39, no. 6, pp. 555–557, Mar. 2003.

[131] A. Nasipuri, S. Ye, J. You, and R. E. Hiromoto, "A MAC protocol for mobile ad hoc networks using directional antennas," *IEEE Wireless Communications and Networking Conference*, vol. 3, pp. 1214–1219, Sep. 2000.

[132] D. Lal, R. Toshniwal, R. Radhakrishnan, D. P. Agrawal, and J. Caffery, Jr., "A novel MAC layer protocol for space division multiple access in wireless ad hoc networks," *Proceedings of 11th International Conference on Computer Communications and Networks*, pp. 614–619, Oct. 2002.

[133] R. R. Choudhury, X. Yang, R. Ramanathan, and N. H. Vaidya, "Using directional antennas for medium access control in ad hoc networks," *The ACM Annual International Conference on Mobile Computing and Networking*, pp. 59–70, Sep. 2002.

[134] M. Takai, J. Martin, A. Ren, and R. Bagrodia, "Directional virtual carrier sensing for directional antennas in mobile ad hoc networks," *Proceedings of ACM international symposium on Mobile ad hoc Networking & Computing*, pp. 183–193, Jun. 2002.

[135] R. Ramanathan, "On the performance of ad hoc networks with beamforming antennas," *Proceedings of ACM international symposium on Mobile ad hoc Networking & Computing*, pp. 95–105, Oct. 2001.

[136] T. ElBatt, T. Anderson, and B. Ryu, "Performance evaluation of multiple access protocols for ad hoc networks using directional antennas," *IEEE Wireless Communications and Networking Conference*, vol. 2, pp. 982–987, Mar. 2003.

[137] K. Kobayashi and M. Nakagawa, "Spatially divided channel scheme using sectored antennas for CSMA/CA - "Directional CSMA/CA"," *IEEE International Symposium on Personal, Indoors, and Mobile Radio Communications*, vol. 1, pp. 227–231, Sep. 2000.

[138] T. Korakis, G. Jakllari, and L. Tassiulas, "A MAC protocol for full exploitation of directional antennas in ad-hoc wireless networks," *Proceedings of ACM international symposium on Mobile ad hoc Networking & Computing*, pp. 98–107, June 2003.

[139] L. Bao and J. J. Garcia-Luna-Aceves, "Transmission scheduling in ad hoc networks with directional antennas," *The ACM Annual International Conference on Mobile Computing and Networking*, pp. 48–58, Sep. 2002.

[140] H. Singh and S. Singh, "DOA-ALOHA: slotted ALOHA for ad hoc networking using smart antennas," *IEEE Vehicular Technology Conference*, vol. 5, pp. 2804–2808, Oct. 2003.

[141] W. T. Chen, M. S. Pan, and J. J. Dai, "An adaptive MAC for wireless ad hoc networks using smart antenna system," *IEEE Vehicular Technology Conference*, vol. 5, pp. 2794–2798, Oct. 2003.

[142] J. P. Linnartz, *Narrowband Land-Mobile Radio Networks.* Boston: London: Artech House, Inc., 1993.

[143] C. T. Lau and C. Leung, "Capture models for mobile packet radio networks," *IEEE Transactions on Communications*, vol. 40, no. 5, pp. 917–925, May 1992.

[144] C. Balanis, *Antenna Theory.* New York: Harper & Row, 1982.

[145] L. C. Wang and K. K. Leung, "A high-capacity wireless network by quad-sector cell and interleaved channel assignment," *IEEE Journal on Selected Areas in Communication*, vol. 18, no. 3, pp. 472–480, Mar. 2000.

[146] M. Zorzi and R. R. Rao, "Capture and retransmission control in mobile radio," *IEEE Journal on Selected Areas in Communication*, vol. 12, no. 8, pp. 1289–1298, Oct. 1994.

[147] M. Zorzi, "Capture probabilities in random-access mobile communications in the presence of rician fading," *IEEE Transactions on Vehicular Technology*, vol. 46, no. 1, pp. 96–101, Feb. 1997.

[148] B. Hajek, A. Krishna, and R. O. LaMaire, "On the capture probability for a large number of stations," *IEEE Transactions on Communications*, vol. 45, no. 2, pp. 254–260, Feb. 1997.

[149] S. Choi, G. H. Hwang, T. Kwon, A. R. Lim, and D. H. Cho, "Fast handover scheme for real-time downlink services in IEEE 802.16e BWA system," *IEEE Vehicular Technology Conference*, vol. 3, pp. 2028–2032, May 2005.

[150] Y. J. Choi, S. Park, and S. Bahk, "Multichannel random access in OFDMA wireless networks," *IEEE Journal on Selected Areas in Communication*, vol. 24, pp. 603–613, Mar. 2006.

[151] X. Fu and H. Minn, "Initial uplink synchronization and power control (ranging process) for OFDMA systems," *IEEE Global Telecommunications Conference*, vol. 6, pp. 3999–4003, Dec. 2004.

[152] H. Minn and X. Fu, "A new ranging method for OFDMA systems," *IEEE Global Telecommunications Conference*, vol. 3, pp. 1435–1440, Dec. 2005.

[153] J. Lee, C. Kim, and J. Kim, "On subcarrier allocation for soft hand-over in OFDMA-based cellular systems," *IEEE Vehicular Technology Conference*, vol. 5, pp. 3087–3091, May 2005.

[154] *IEEE Std. 802.16-2004, "IEEE Standard for Local and metropolitan area*

networks-Part 16: Air Interface for Fixed Broadband Wireless Access Systems", Oct. 2004.

[155] *IEEE Std. 802.16e, "IEEE Standard for Local and metropolitan area networks-Part 16: Air Interface for Fixed and Mobile Broadband Wireless Access Systems Amendment for Physical and Medium Access Control Layers for Combined Fixed and Mobile Operation in Licensed Bands"*, Dec 2005.

[156] Y. Amir, C. Danilov, S. Goose, D. Hedqvist, and A. Terzis, "An overlay architecture for high quality VoIP streams," *IEEE Transactions on Multimedia*, vol. 8, pp. 1250–1262, Dec. 2006.

Vita

Ming Bing Chen (IEEE student member'05) was born in Tainan, Taiwan R.O.C, in 1976. He received the B.S. and M.S. degree in communication engineering from National Chiao Tung University, Hsin-Chu, Taiwan, in 1998 and 1999, respectively. He is currently working toward the Ph.D. degree in communication engineering with the Department of Communication Engineering, National Chiao-Tung University. His current research interests include wireless networks, cross-layer design, and cognitive wireless system. He is the holder of a U.S. patent with three more pendings.

Publication List

Journal Paper (published or accepted)

1. Li-Chun Wang, Anderson Chen and Shi Yen Huang, "A Cross-Layer Investigation for the Throughput Performance of CSMA/CA-Based WLANs With Directional Antennas and Capture Effect," *IEEE Transactions on Vehicular Technology*, vol. 56, no. 5, pp. 2756-2766, Sep. 2007.

Journal Paper (revision)

1. Li-Chun Wang, Anderson Chen, and Kuang-Nan Yen,"Joint Rate and Power Adaptation for Wireless Local Area Networks in Generalized Nakagami Fading Channels," submitted to *IEEE Transactions on Vehicular Technology*, Oct. 2006 (Major revised in Jul. 2007).

2. Li-Chun Wang, Anderson Chen, and David S. L. Wei,"An Enhanced CSMA/CA MAC Protocol With QoS Provisioning for Overlaying Ad Hoc Networks," submitted to *IEEE Transactions on Vehicular Technology*, Dec. 2006 (Major revised in Jul. 2007).

3. Li-Chun Wang and Anderson Chen, "Effects of Location Awareness on Concurrent Transmissions for Cognitive Ad Hoc Networks Overlaying Infrastructure-Based Systems," submitted to *IEEE Transactions on Mobile Computing*, Jan. 2007 (Major revised in Sep. 2007).

4. Li-Chun Wang and Anderson Chen, "Optimal Radio Resource Partition for Joint Contention- and Connection-Oriented Multi-Channel Access in OFDMA Systems," submitted to *IEEE Transactions on Mobile Computing*, Mar. 2007 (Major revised in Sep. 2007).

Journal Paper (to be submitted)

1. Li-Chun Wang and Anderson Chen "On the Performance of Spectrum Handoff for Link Maintenance in Cognitive Radio," to be submitted.

2. Li-Chun Wang, Hung-Hsi Chen and Anderson Chen "Network Selection with Joint Vertical and Horizontal Handoff in the Heterogeneous WLAN and Mobile WiMax System," to be submitted.

3. Li-Chun Wang, Hung-Hsi Chen and Anderson Chen "Optimal Handoff Channel Search Time for Wireless Local Area Networks," to be submitted.

Patent

1. Li-Chun Wang, Ming Bing Chen and et al., "Cross-layer rate adaptation mechanism for WLAN," filed for Taiwan and U.S. patents in Oct. 2005.

2. Li-Chun Wang, Ming Bing Chen, and C. F. Lee, "Method and Device for Cost-Function Based Handoff Determination Using Wavelet Prediction in Vertical Wireless Networks, filed for the U.S. Patent on Jan. 2006.

3. Li-Chun Wang, Ming Bing Chen, Hung-Hsi Chen, and C. F. Lee, "Method for performing a network handoff in a wireless network environment," filed for the U.S. Patent in Feb. 2006

International Conference Paper

1. Li-Chun Wang and Anderson Chen and Hung-Hsi Chen, "Network Selection with Joint Vertical and Horizontal Handoff in Heterogeneous WLAN and Mobile WiMax Systems," *IEEE Vehicular Technology Conference*, pp. 794-798, Apr. 2007.

2. Li-Chun Wang, Anderson Chen, and David S. L. Wei, "A Cognitive MAC Protocol for QoS Provisioning in Overlaying Ad Hoc Networks," *IEEE Consumer Communications and Network Conference, Cognitive Radio Workshop*, pp. 1139-1143, Jan. 2007.

3. Li-Chun Wang and Anderson Chen, "On the Performance of Re-entry Process in OFDMA-based IEEE 802.16 WiMax," appeared in *Wireless Personal Multimedia Conference*, San Diego, Sep. 2006.

4. Li-Chun Wang, Kuang-Nan Yen, Jane-Hwa Huang, Anderson Chen, and Chung-Ju Chang, "Cross-Layer Performance Analysis of Joint Rate and Power Adaptation Schemes with Multuple-User Contention in Nakagami Fading Channels," *ACM International Wireless Communications & Mobile Computing Conference (IWCMC)*, Jul. 2006.

5. Li-Chun Wang and Anderson Chen, "On the Coexistence of Infrastructure-Based and Ad Hoc Connections for a Cognitive Radio System," *IEEE International Conference on Cognitive Radio Oriented Wireless Network and Communications (CROWNCOM)*, pp. 1-5, Jun. 2006.

6. Li-Chun Wang, Hung-Hsi Chen, Anderson Chen and Chung-Ju Chang, "Optimal Channel Search Time for Handoff in the IEEE 802.11 WLANs," *IEEE Vehicular Technology Conference*, pp. 1201-1205, May 2006.

7. Li-Chun Wang, Kaung-Nan Yen, and Anderson Chen, "Joint Rate and Power Adaptation for Wireless Local Area Networks in Nakagami Fading Channel," *IEEE Wireless Communications and Networking Conference*, vol. 3, pp. 1723 -1728, Apr. 2006.

8. Li-Chun Wang, Shi-Yen Huang, and Anderson Chen, "On the Throughput Performance of CSMA-based Wireless Local Area Network with Directional Antennas and Capture Effect: A Cross-layer Analytical Approach," *IEEE Wireless Communications and Networking Conference*, pp. 1879- 1884, Mar. 2004.

9. Anderson Chen and Li-Chun Wang, et. al, "NICER- A Distributed Wireless Medium Access Control Protocol in Mobile Ad Hoc Networks with Multimedia Traffic," *IEEE Vehicular Technology Conference*, pp. 1448-1452, Oct. 2003.

10. Anderson Chen and Li-Chun Wang, et. al, "NICE - a decentralized medium access control using neighborhood information classification and estimation for multimedia applications in ad hoc 802.11 wireless LANSs," *IEEE International Conference on Communications (ICC)*, pp. 208-212, May 2003.

International Conference Paper (submitted)

1. Li-Chun Wang and Anderson Chen "Optimal Radio Resource Partition for Joint Contention- and Connection-Oriented Multi-Channel Access in OFDMA Systems," submitted to *IEEE Infocom* 2008.

2. Li-Chun Wang and Anderson Chen "On the Performance of Spectrum Handoff for Link Maintenance in Cognitive Radio," submitted to *IEEE Wireless Communications and Networking Conference* 2008.